TRANSMISSION LOSS ALLOCATION USING ARTIFICIAL NEURAL NETWORKS

A Thesis

Submitted to the College of Graduate Studies and Research

in Partial Fulfillment of the Requirement

For the Degree of

Master of Science

in the Department of Electrical Engineering

University of Saskatchewan

Saskatoon, Saskatchewan

By

Rezaul Haque

March 2006

PERMISSION TO USE

The author has agreed that the Libraries of University of Saskatchewan may make this thesis freely available for inspection. Moreover, the author further has agreed that permission for extensive copying of this thesis for scholarly purpose may be ranted by the professor or professors who supervised the thesis work recorded herein or, in their absence, by the Head of the Department or the Dean of the College in which the thesis work was done. It is understood that due recognition will be given to the author of this thesis and to the university of Saskatchewan in any use of the material in this thesis. Copying or publication or any other use of the thesis for financial gain without the approval of the University of Saskatchewan and the author's written permission is prohibited.

Requests for permission to copy or to make any other use of the material in this thesis in whole or in part should be addresses to:

Head, Department of Electrical Engineering
University of Saskatchewan
57 Campus Drive
Saskatoon, Saskatchewan
Canada, S7N 5A9

ABSTRACT

The introduction of deregulation and subsequent open access policy in electricity sector has brought competition in energy market. Allocation of transmission loss has become a contentious issue among the electricity producers and consumers. A closed form solution for transmission loss allocation does not exist due to the fact that transmission loss is a highly non-linear function of system states and it is a non-separable quantity. In absence of a closed form solution different utilities use different methods for transmission loss allocation. Most of these techniques involve complex mathematical operations and time consuming computations. A new transmission loss allocation tool based on artificial neural network has been developed and presented in this thesis. The proposed artificial neural network computes loss allocation much faster than other methods. A relatively short execution time of the proposed method makes it a suitable candidate for being a part of a real time decision making process. Most independent system variables can be used as inputs to this neural network which in turn makes the loss allocation procedure responsive to practical situations. Moreover, transmission line status (available or failed) was included in neural network inputs to make the proposed network capable of allocating loss even during the failure of a transmission line. The proposed neural networks were utilized to allocate losses in two types of energy transactions: bilateral contracts and power pool operation. Two loss allocation methods were utilized to develop training and testing patterns; the Incremental Load Flow Approach was utilized for loss allocation in the context of bilateral transaction and the Z-bus allocation was utilized in the context of pool operation. The IEEE 24-bus reliability network was utilized to conduct studies and illustrate numerical examples for bilateral transactions and the IEEE 14-bus network was utilized for pool operation. Techniques were developed to expedite the training of the neural networks and to improve the accuracy of results.

ACKNOWLEDGEMENTS

I wish to express my heartiest gratitude and indebtedness to Dr. Nurul Amin Chowdhury for his guidance, supervision and moral support for the entire period of this research work. His initiatives, encouragement and valuable suggestions are very gratefully acknowledged without which this work would not be possible.

I would like to thank Dr. S.O. Faried and Dr. R. Karki for their valuable suggestions and moral support. I wish to express thanks to the Department of Electrical Engineering for providing me scholarship and other financial assistances that helped me going through the M. Sc. program.

I wish to express my heartiest regards to my parents for their guidance and moral support. I would like to acknowledge the moral support of my wife Sadia Ahmed during this period. Finally, I would like to thank all my friends in Saskatoon for arranging lots of extra-curricular activities that made our stay in Saskatoon enjoyable.

TABLE OF CONTENTS

LIST OF TABLES

LIST OF FIGURES

LIST OF SYMBOLS

$[A_p]$ = coefficient of power loss equation in matrix form

a_i = cost constant

a_{pij} = element of matrix [*Ap*]

$[B_p]$ = coefficient of power loss equation in matrix form

b_i = cost constant

B_{ij} = loss coefficient of George's formula

B_L = Kron's transmission loss constant

B_{L0} = Kron's transmission loss constant

b_{pij} = element of matrix [*Bp*]

$[C]$ = diagonal matrix with elements $\left(\cos \partial_i \big/ |V_i|\right)$

C^{in} = center of the input space

c_i = element of matrix [*C*]

$[D]$ = diagonal matrix with elements $\left(\sin \partial_i \big/ |V_i|\right)$

D_{in} = the maximum possible distance between two points in input space

d_i = element of matrix [*D*]

d_{in} = the distance between two hyperplanes

d_k = target output at layer *k*

E = instantaneous sum of square errors

E_p = Kron's transmission loss constant

E_q = Kron's transmission loss constant

$E(W^2)$ = second moment of weights between input and hidden layer

e_k = difference between the target output and computed output a neuron at layer *k*

$[F]$ = diagonal matrix of f_i

F_i = generation cost of unit *i*

f_i = constant for relationship between real and reactive generation

$[I_B]$ = bus current matrix

I_i = complex bus current at Bus i

$[I_p]$ = matrix of real component of bus currents

I_{pi} = real component of bus current at Bus i

$[I_q]$ = matrix of reactive component of bus currents

I_{qi} = reactive component of bus current at Bus i

$[J]$ = Jacobian matrix

K_{LO} = loss constant

k_{xx} = element of matrix B_L

L_k = real loss allocated to Bus k

$[P]$ = real power injection matrix

$[P_G]$ = real power generation matrix

$[P_D]$ = real power demand matrix

P_{Di} = real power demand at Bus i

P_{dk} = real power demand at Bus k

P_{Gi} = real power generation at Bus i

$P_{gk,}$ = real power generation at Bus k

P_k = real power injection at Bus k

P_{kc} = calculated real power injection at Bus k

P_{ks} = specified real power injection at Bus k

P_L = transmission loss

P_{loss} = real part of transmission loss

P_{max} = maximum real power generation capacity of a generator

P_{min} = minimum real power generation capacity of a generator

p_{gx} = Generation at Bus x

$[Q]$ = reactive power injection matrix

$[Q_D]$ = reactive power demand matrix

Q_{Di} = reactive power demand at Bus i

$[Q_G]$ = reactive power generation matrix

Q_{Gi} = reactive power generation at Bus i

Q_{Gi0} = Kron's loss formula constant

Q_k = reactive power injection at Bus k

Q_{kc} = calculated reactive power injection at Bus k

Q_{ks} = specified reactive power injection at Bus k

Q_{loss} = reactive part of transmission loss

Q_{max} = maximum reactive power generation capacity of a generator

Q_{min} = minimum reactive power generation capacity of a generator

$[R]$ = matrix of real component of bus impedance matrix

$\Re$ = real part of an expression

r_{ij} = element of matrix $[R]$

S_i = complex power injection at Bus i

S_L = total power loss

S_{Lij} = power loss in the line between Bus i & Bus j

u_x = element of matrix B_{L0}

Vi = bus voltage of Bus i

v_j = sum of the weights to the neuron at layer j

v_k = sum of the weights to the neuron at layer k

w_{ji} = synaptic weight between layer j and layer i neurons

w_{ki} = synaptic weight between layer j and layer k neurons

$[X]$ = imaginary part of bus impedance matrix element

$[Y]$ = admittance matrix

Y_{kn} = element of bus admittance matrix between buses k and n

y_j = output of a neuron at layer j

y_k = output of a neuron at layer k

$[Z_B]$ = bus impedance matrix

α = momentum factor

β = market clearing price, \$/MW-hr

γ = step size for updating weights

γ_k = ratio of power generation and difference between generation and demand at Bus k

ΔP_k =mismatch between calculated and specified real power at Bus k

ΔQ_k = mismatch between calculated and specified reactive power at Bus k

$\Delta\eta$ = incremental learning rate

Δw_{ji} = incremental change in synaptic weight

θ_{kn} = angle associated with Y_{kn}

δ_i = phase angle of bus voltage at Bus i

δ_k = local gradient for layer k

η = learning rate

θ_{kn} = angle associated with Y_{kn}

λ = incremental running cost of a generator

λ_{sys} = incremental running cost of whole power system

Σ = summation

$\varphi(.)$ = activation function

$\varphi'(.)$ = derivative of activation function

CHAPTER 1: INTRODUCTION

1.1 Emergence of Electric Power Systems

Electricity, one of the most widely used form of energy, has been discovered little more than a century ago. After the discovery of Edison's electric bulb, electricity has been commercially produced and marketed in USA. Thomas Alva Edison, regarded as the pioneer of electric power system, first established "The Pearl Street Power Station" in New York, USA in 1882 [1]. Later more companies were established. In early days there was no regulation in electric power industries. Small companies operated small generators in municipal areas and sold power to industries and other users in that area. These companies were somewhat inefficient and redundant in the services they provided. Separate companies provided electricity for different needs such as street illumination, industrial power, residential lighting and street car service. They frequently operated under nonexclusive franchises, often in competition with one another. In 1896, Westinghouse pioneered the use of alternating current to deliver electricity over a long distance from its hydroelectric plant at Niagara Falls. This generating and delivery system was far more efficient and quickly became the national standard. This development quickly led to the formation of large "public utility" companies. Today, electric power systems have become common entities all over the world. Thousands of electric utility and companies are supplying power to billions of consumers. People cannot imagine living without electricity. It has become an essential commodity in our every day life and billions of equipment and accessories are being used in the world today that are solely dependent on electric power.

1.2 The Evolution of The Natural Monopoly

Early leaders recognized that electric companies suffered from high fixed costs as a result of heavy investment needed to finance central generating plants and transmitting system. Utilities frequently found that it was difficult to maintain investor confidence and attract adequate capital. This was attributable to both the dubious franchise process, which made operation of the utility over the long term an uncertain prospect, and the

low returns investors received. Early industry leaders began to think that if the franchise granting process and the rates charged by utilities were overseen by a nonpartisan state agency instead of a city council, financing might be easier and cheaper to obtain.

In 1898, in an address before the National Electric Light Association (the forerunner of Edison Electric Institute), Samuel Insull proposed that electric companies be regulated by state agencies which would establish rates and set service standards [1]. The idea became increasingly appealing to investor-owned companies in the face of public enthusiasm for the growth of municipal electric systems. Privately-owned companies surmised that the public might be more supportive if their companies were regulated so that customer interest would be protected. By 1916, 33 states had regulatory agencies. Early regulation of the industry proved beneficial to both the electric companies and their customers, who got reliable, reasonably priced service without the uncertainties caused by duplicate services and inefficient operations. Later electric industry was developed as regulated industry all over the world.

1.3 Traditional Electric Power

Starting from very small utility networks, electric utilities have grown billion times larger. Now, electric power systems became widespread and complex in nature. From its birth to present, power system networks and utilities have gone through various stages of evolution. For the last one hundred years electric power systems operated as regulated monopolies. In a regulated monopoly, an electric power system can be divided into four main functional zones; generation, transmission, distribution and retail service.

- Generation – generation is the conversion of electric energy from other forms of energy like chemical (gas, coal, hydrogen), nuclear, solar, hydro energy, geothermal energy, wind and wave energy.
- Transmission – transmission is the transfer of bulk electric energy from one place to another through some transmission network. It connects the generator network and distribution network.

- Distribution – distribution is the process of delivering electric power from the local network to the consumers.
- Retail Service – retail service can broadly called retail customer service. Its main function is measuring and billing customers for the power delivered.

In a regulated monopoly, these four functional blocks are controlled by one single entity. As today's power system networks are very large in production volume and geographical area, their operation became a complex phenomenon which does not only depend on the state of technology but also on complex issues like economy, social advancement, environmental impact and political decisions. In traditional monopoly, one company is allowed to generate, transmits and distribute electrical power to the consumers in one jurisdiction. The service area is primarily determined by political map and jurisdiction. In some cases, distribution is divided among two or more electric utilities, e.g. city corporation or other private distribution companies. Price of electricity is determined by the same utility which is justified by cost of generation, transmission and distribution. The schematic diagram of a traditional power industry is shown in Figure 1.1.

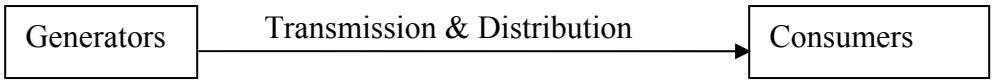

Fig. 1.1: Schematic diagram of traditional power industry

1.3.1 The traditional regulated power industry structure – Traditional power industry may be categorized by the functions they perform. Many utilities performed all four functions of power industry described above, others perform one or two. Depending upon the functions they perform, they can be categorized as:

a) **Vertically integrated electric utilities:** They own facilities and manage all the functions of producing, transmitting, delivering and selling of electric power. Vertically integrated means that all the functions needed were intertwined into one system and company. Almost all electric utilities prior to 1990s fall into these category. They were granted a monopoly franchise by the state or government, which granted them exclusive rights to produce and sell electric

power. In return they were obliged to provide power to all customers who wanted it.

b) **Generation and transmission (G &T) utilities:** These utilities produce electricity and move energy in bulk to various locations, where they sell in bulk quantities to other utilities. For example, Tri-State G&T Association Inc, Denver, CO, serve G&T functions for 34 rural electric and public power districts in Colorado, Nebraska and Wyoming.

c) **Local distribution companies:** These are local electric utilities that own and operate only a distribution system. They also provide retail sales and services. Many municipal organizations have local distribution companies.

d) **Independent power producer (IPP) and non-utility generators (NUG):** Independent power producers are companies that owns and operate generators outside the control of traditional power utility. IIPs sell power to other utilities. Non-utility generators are owned by manufacturers or processes who use their generators to produce power for their own use and sell any surplus energy to utilities.

1.3.2 Functional divisions of traditional vertically integrated utility: The following functional divisions exist in a vertically integrated power system:

a) Generation division: Generation division is responsible for building, operation and maintenance of power plants.

b) T&D division: The Transmission and Distribution division designs, installs and maintains transmission lines, substations and other equipment.

c) Operation division: This division operates the entire power system. It coordinates the functions of all units of power system starting from generation to bulk distribution. It performs system operation that includes monitoring and control of generation and dispatch. It is responsible for voltage stability and system security.

d) Marketing and customer service division: The function of marketing and customer service encompasses marketing, sales, billing, customer service and public relation.

1.4 Deregulation

Electric power systems in the early days were developed on the concept of natural monopoly. Natural monopoly occurs if the production costs decrease as the output grows larger. Before 1990s, all power systems in the world were running as vertically integrated monopoly system. Later it was realized that the electric power industry was not necessarily a natural monopoly at least when it came to generating electricity. It was proven that open access and competition in business lowers the unit price. The same is believed to happen in electric power industry. Therefore, bringing competition in power sector in generation and retail consumer level became essential. The regulatory process and lack of competition gave electric utility no incentive to improve on yesterday's performance or to take risk on new ideas that might increase customer value. The main argument used to support deregulation is that a free market promotes efficiency. In a regulated environment, for example, wholesale and retail electricity power prices are calculated based on a utility's costs. If a utility invests in what turns out to be an uneconomical project, it can still add the costs of the investment to the price it charges for electricity. Thus, the risks and economic consequences of a poor investment are passed to the electricity customer. Competition will encourage new technologies for generating electricity with better efficiency and inefficient generating plants will die out.

In many of the countries where electric utility deregulation first occurred e.g. Argentina, England, the government was privatizing the industry. By deregulating i.e. by privatizing the power sector, government can withdraw huge amount of money. It has also been proved in many cases that a private organization can serve better than a government organization. Competitions also increase customer focus. Another reason for deregulation is to give customer a meaningful choice to select their supplier, although the term 'customer' is confined only to bulk or retail buyer.

Deregulation and re-structuring of electric power industry is occurring in most part of the world. Some are rapidly progressing towards full deregulation while others are re-structuring their power industry to allow some types of deregulation. Although the reasons for these changes are not always the same, their expected impacts are the same.

1.5 Deregulated Electric Utility Structure

Contrary to traditional vertically integrated power system, monopoly is fully removed from generation and distribution (including retail service) sectors in a deregulated power system. As a result, generation and distribution are competitive, with many different companies vying for those businesses. On the other hand, most governments and regulators realized that it is best to have only one transmission system. Therefore, in most cases transmission sector remained regulated. Brazil is trying to deregulate transmission sector, not by creating many transmission lines, but by leasing sections of the transmission lines to different companies. Basic features of a deregulated power system are discussed below.

a) ***Independent system operator*** - An independent system operator (ISO) plays the role of a supervisor for system operation, planning and security. It has operational control authority over the whole power system and normally operates and maintains the transmission lines. An ISO normally performs the following functions:

- provides open and comparable access to similarly situated customers to the transmission facilities
- operates exclusively the ISO Controlled Grid in an efficient and reliable manner
- adopts, safeguards and monitors compliance with inspection, maintenance, repair and replacement standards for the ISO Controlled Grid so as to provide high quality, safe and reliable electric service including during periods of emergency and disaster;
- provides or obtains adequate ancillary services for the ISO Controlled Grid and to dispatch such services as necessary;

- schedules transmission service for all transactions on the ISO Controlled Grid;
- redispatches available resources to relieve transmission congestion;
- develops and submits (i) transmission service rate methodologies and (ii) rates for such transmission services and ancillary services and to recover administrative costs;
- establishes operating rules and protocols for the reliable operation and for participation in the ancillary services market;
- maintains the reliability of operations of the ISO Controlled Grid
- provides open market pricing information for the transmission services and ancillary services markets;
- secures generating and transmission resources as necessary for achievement of planning and operating reserve criteria
- promotes the development of, and enter into, agreements for power buying and selling including bilateral contracts
- allocates and manages transmission losses to participating parties
- keeps track of all transactions and calculate the transmission usage for each generator and IPP
- also works as a spot market for buying and selling power (in absence of "power exchange")

In some states or countries where there is no "power exchange" for trading energy, ISO does the job of energy trading as well.

b) **Power exchange** – An organization, some what like a stock exchange, that permits buyers and sellers of wholesale electricity to buy and sell electric power as a commodity. It trades electricity between buyers and sellers electronically.

c) **Competitive power generations** – An open access in generation sector, in which any entity that is qualified, competent, solvent, able to meet standards can get licensed and can produce and sell power. Usually many independent power

producers (IPP) and non-utility generators (NUG) compete with each others to produce and sell electric power on a wholesale market.

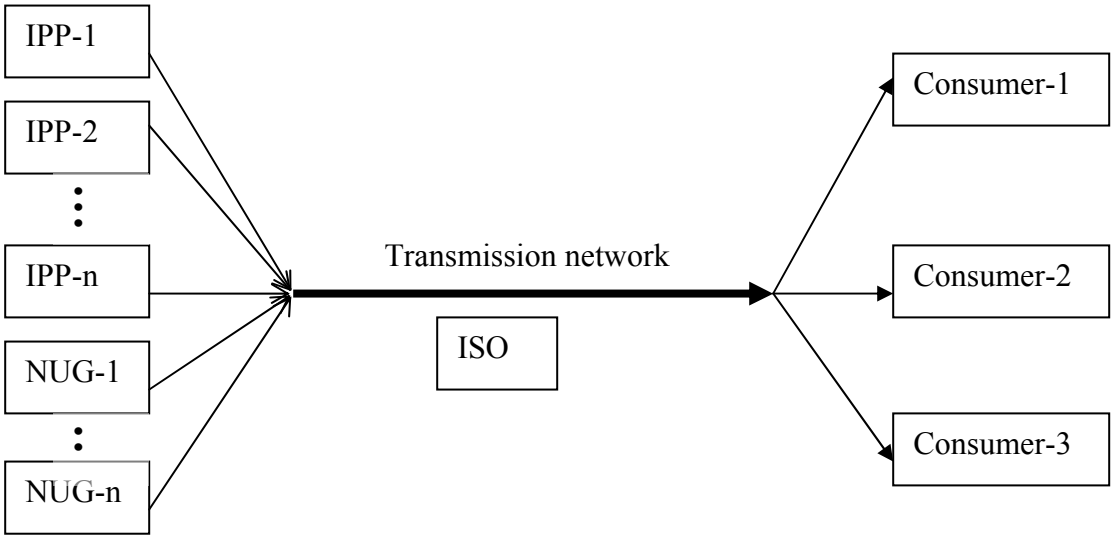

Fig. 1.2: Schematic diagram of a deregulated power network with ISO

d) **Competitive distributors** – Competitive distributors buy power in bulk at the wholesale level and sell it to the consumers. They bid for buying power at "power exchange" or ISO (in absence of power exchange") similarly as IPPs or NUGs bid for selling power. Distributors supply power to individual home, business or other entity. They charge individuals for the energy they consumed at a rate fixed by state or governments or at a rate set by "act of electricity deregulation" in that jurisdiction. Distributors can choose their suppliers. Any distributor or bulk power consumer may buy power from a generator through a bilateral contract as well.

e) **Bilateral contracts**- Many bulk power consumers enter into bilateral contracts with power producers or suppliers to avoid price fluctuations of energy market in a deregulated environment. The seller arranges the transportation of the contracted power over a third party's transmission network. These are individual contracts and would not affect any other contracts which are already in place. The concept of bilateral contracts allows the customers and generating plants to work according to their policy and does not make them dependent on everyday bid like in a power pool system. The price fixation and other services and particulars of the

contract would be determined by the two parties involved in the contract. This would give them more freedom and flexibility of choice. Bilateral contracts enable customers to make their best price deals for power supply with whoever in the competitive market is most effective to meet their demands. Allowing power producers to contract directly with customers, marketers, or retailers creates competition on both sides of the transaction. Generators compete among themselves to supply this demand. This gives customers and their representatives a full range of choices among suppliers. Suppliers may charge any price the market will bear and may choose to compete not only by price but by duration of contract, payments options, type of generation, and quality of electric service. Thus, bilateral contracts provide a wide range of choices to meet various customer needs. Many electric utilities which are not deregulated yet, allows bilateral contracts as a first step towards deregulation. Customers in bilateral contracts, on the other hand, have broad choices of various types of suppliers. Large customers can deal with a power producer directly or purchase energy through the marketers, power brokers or energy service company. Smaller customers can form load aggregators and purchase energy in a similar manner

f) **Power pool**- A deregulated power pool is the most common form of market at present due to its simple structure. Generating utilities or IPPs and customers both bid for selling and buying power at the power pool. A power pool conducts different types of auctions like day ahead market, hour ahead market, real time market etc. to buy power necessary for its customers. In a pool system, generating utilities do not have any target for any specific customer rather than they bid for getting access to the grid. A generating utility would be out of the competitive market if its price is too high. Similarly, a customer would not get any power if its offer is too low. Thus pool fixes a single price for every hour which is determined by basic supply-demand relationship of economics. All parties involved in the market have equal right to access the information regarding price and demand. A power pool system uses the existing economic dispatch procedures.

   In addition to the day-ahead market and hour-ahead market, a power pool also operates its spot market. A spot market of electricity is somewhat different from

other commodity. Electric power is generally a non-elastic item and must be consumed when it is generated. For this reason, a spot market operates ahead of real time. A spot market can update its bids every 10 minutes or 30 minutes or at any convenient time

g) **Market clearing price** – An independent system operator is responsible to maintain a balance between the supply and demand of power. An ideal electric power system must have sufficient power in order to meet the customer's demands. Market clearing price is the price at which suppliers and buyers agree to sell and buy power to a specified amount that is set by this price. A system operator determines the market clearing price from the supply and demand relation in such a way that all power demand would be satisfied. The companies who bid higher than the market clearing price will not be able to sell any power. All companies who bid less than the market clearing price are considered as successful bidders and will be supplying the demand. All successful bidders will get paid at the market clearing price irrespective of their bidding prices.

   The competition among the suppliers of electric power is at the core of deregulation. If a supplier's bid is higher than the market clearing price, then its energy will not be included in the load dispatch schedule. This fact will force the supplier out of business. The fear of getting out of business encourages the supplier to bid the most competitive price to stay in wholesale market place.

   In many power pool e.g. in Alberta power pool, electricity is purchased on a centralized basis. Generators bid on an hourly basis to supply energy. Power pool determines the market clearing price from the supply curve of power and from the total load demand. Demand side bidding is not considered. Figure 1.3 shows how the power pool determines market clearing price for a particular hour [2].

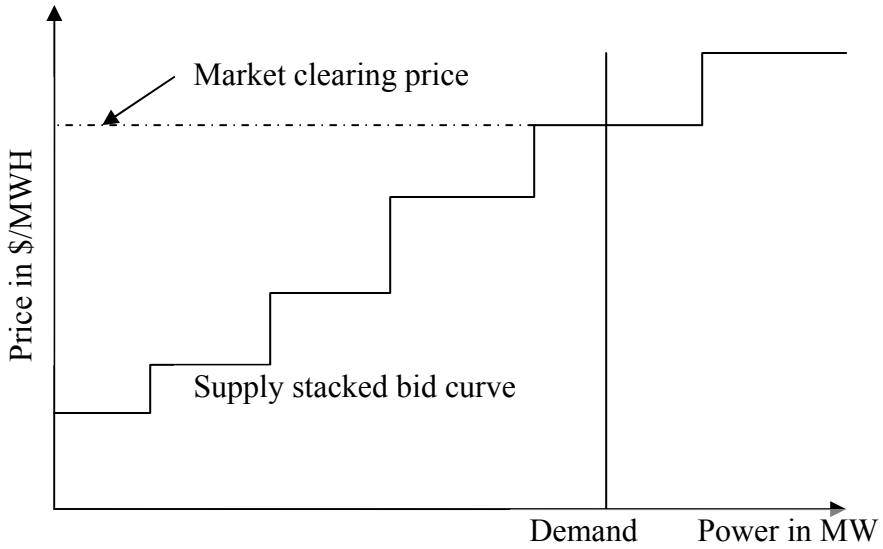

Fig. 1.3: Determination of market clearing price (In Alberta Power Pool)

In Ontario and New England, the system operators set the limits of upper and lower boundaries of energy price [3]. Generating utilities offer their selling price in between them and market clearing price is set in the same way as Alberta power pool.

In some jurisdictions, market clearing price is set in different ways. For example, in Norway, Nordic energy sellers as well as energy buyers submit their bids for selling and buying power respectively. Participants offer their bids for next-day power delivery. Nordic Power Exchange collects bids and prepares two curves: an aggregate demand curve and an aggregate supply curve. Demand decreases as the price goes up, on the other hand, supply increase with increase in price. The market clearing price is set by the intersection of these two curves. Figure 1.4 shows the supply and demand curves and market clearing price of Nordic power market [4].

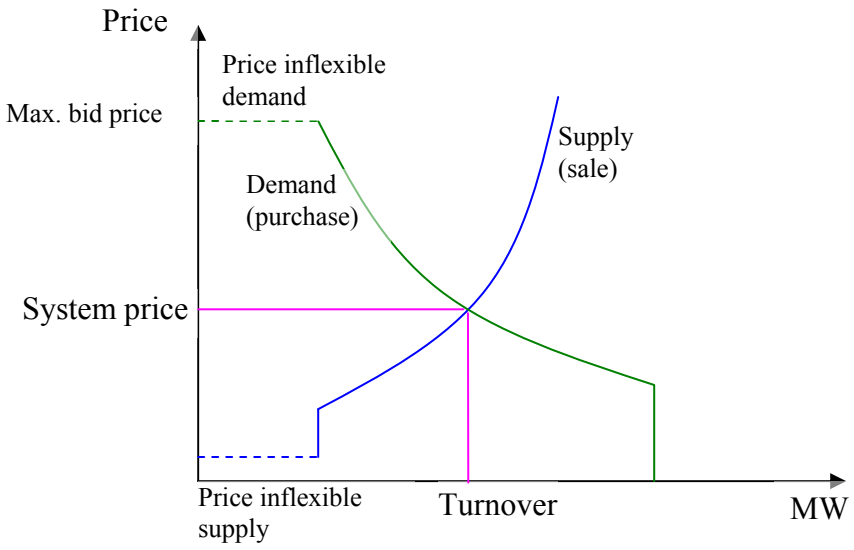

Fig. 1.4: Market clearing price in Nordic Power Pool

1.6 Effect of Deregulation on Operation And Planning

In a traditional power industry, control is much simpler -a system is run in a way that minimizes the overall cost. Daily, weekly and monthly load forecasts are done by the utility. Load flow study, cost analysis and economic scheduling of generation are done accordingly well ahead of time. Since all generations and distributions are under one umbrella, planners are not accountable to individual generators or distributors. They are accountable to owners or governments only. In real time operation, generator scheduling and load dispatch are done in an almost pre-planned way. Very seldom they have to use spinning reserve to meet actual demand or to meet emergency situation. System operators take all decisions to keep the system secure and reliable according to some set criteria. Transmission congestion can be easily avoided by proper generation scheduling.

The operation and planning activities in a deregulated power system is much more complex than that of a traditional one. One of the complexities arises due to the fact that electric energy has to be generated and consumed at the same moment. When there is an increased load demand, either generation has to be increased to fulfill the load or load has to be curtailed. Loads in a network vary every hour, to be more specific vary every moment. Since loads are controlled by distributors, load forecast becomes very difficult.

Buying of power from the grid depends on the retailers not on the system operator. In most cases, long time planning like weekly or monthly planning becomes very difficult or inaccurate. Many decisions are to be taken on real time basis or just few minutes ahead of the situation. Transmission planning becomes difficult due to spot selling of power. Most distributors want to buy power from the cheapest supplier which sometimes causes transmission congestion. Congestion management becomes a big contentious issue in a deregulated system. Transmission loss allocation is another contentious issue. Estimation of total transmission loss is not enough; it has to be allocated to individual generations.

1.7 Transmission Loss

Transmission loss in electric power system is a natural phenomenon. Electric power has to be moved from generation place to the consumer's place through some wires for consumption. All wires have some resistance, which consume some power. The power consumed in this way is referred to as "loss". Most of this loss is attributable to the heating of the power lines by the electrical current flowing through them. The loss (i^2R) is then lost to the surrounding of the power lines. Transmission loss represents about 5% to 10% of total generation, a quantity worth millions of dollar per year. In Alberta alone, total transmission loss costs about 200 million dollars per year.

Power loss in a Transmission and Distribution network is influenced by a number of factors such as:

- the location of generating plant and load connection points and the energy associated with each;
- types of connected loads;
- network configuration;
- voltage levels and voltage unbalance;
- dynamic factors associated with the operation of large alternating current networks (e.g. power factor, harmonics and the control of active and reactive power);

- the length of the lines - this is an almost linear relationship (e.g. doubling the line length would double the line loss);
- the current in the line - this is a square law relationship where doubling the line current would quadruple the line loss;
- the design of lines, particularly the size, material and type of cables; and
- the types of transformers and their loadings.

In a traditional power system, total transmission loss is optimized while keeping the running cost at the minimum. In a deregulated power system, due to the competition in the generation sector, transmission loss has to be allocated to individual generators.

1.8 Transmission Loss Allocation in A Deregulated Power System

In a deregulated power system transmission loss has to be allocated to individual suppliers, generators and contracts. Loss allocation does not affect generation levels or power flows, however it does modify the distribution of revenues and payments at the network buses among suppliers and consumers. In a deregulated power system, every supplier has to supply the power they want to sell plus the transmission loss corresponding to that transaction. Therefore, system operator has to allocate losses to every individual generation and load. Depending on the contract, a supplier may supply the contracted load and the corresponding loss or supply the load and pay for the loss. In later case, the loss may be supplied by a contracted generator or ISO may buy the power to meet the loss from a spot market. Depending upon who will supply the loss, the allocation will vary to some extent.

1.9 Present Problems in Transmission Loss Allocation

Transmission loss allocation became a contentious issue as it corresponds to a huge amount of money. It is mentioned earlier that transmission loss depends on a number of factors of the power system. Transmission loss is a highly non-linear function of these factors. The main problem associated with loss allocation is the fact that transmission loss is a non-separable entity. Any attempt to separate it is further complicated by its non-linear nature. The challenge facing by a typical power pool and an ISO is how to

allocate the transmission loss and what should be the criterion for charging other utilities. Utilities in general, look for locational signal, consistency, simplicity, accuracy and predictability in a loss allocation method. It is an extremely hard task to accommodate all these considerations in a complex phenomenon like transmission loss allocation. In a deregulated environment, the economic and market related factors are as important as technical factors. Not only accurate calculations are necessary, but fair and equitable allocation of the losses to all the stakeholders is also important. Although no ideal or standard loss allocation method exists, some methods have been reported in literature [2, 5-14]. But all these methods require time consuming and complex mathematical computations and, therefore found limited acceptance by the industry.

1.10 Review of Current Methods

In recent years, some methods of transmission loss allocation have been reported in literature. In absence of an ideal or unanimous transmission loss allocation method, utilities around the world are using some of these methods. Prior to deregulation, wheeling of power through transmission line was allowed in many jurisdictions. H. H. Happ introduced some methods for calculating cost of power wheeling [5]. Conejo et al [6] have discussed the Pro Rata (PR) procedure, a technique used in Mainland Spain for allocation of transmission loss, where losses are globally assigned to generators and consumers, and then a proportional allocation rule is used. The loss allocated to a generator or consumer is proportional to its level of energy generation. PR procedure ignores the network and, therefore, is not consistent with solved power flow. Conejo et al [6] have also discussed two other methods called 'Marginal Procedure' and 'Proportional Sharing'. In 'Marginal Procedure', losses are assigned to generators and consumers through so-called incremental transmission loss co-efficient (ITL). Normalization has to be performed after allocation, since this method results in over recovery. The standard marginal procedure based on ITL coefficients depends on the selection of the slack bus because ITL coefficients do depend on the slack bus. The ITL coefficient of the slack bus is zero by definition, thus the slack bus is allocated no losses. This is a drastic limitation for this method that requires that pool agents agree beforehand on the selection of the slack bus. 'Proportional sharing' procedure requires the assumption of proportional sharing principle. According to this law "in flows to a

bus are proportional to outflows from that bus" which could neither be proved nor disproved.

Conejo et al [7] proposed a loss allocation method called "Z-bus allocation". It is based on the exact network equations as defined by the complex impedance matrix and the complex nodal injections. All calculations are based on the sparse admittance matrix. It uses complex current flows instead of power flow. Power flow solution required to get injected bus current and power has to be converted to current.

Strbac et al [8] have proposed a transmission loss allocation method by tracing the generator and load contributions to line flows. This method traces the contributions of each generator and of each load to the line flows instead of marginal contributions. Since the allocation method had been proposed on the basis of maximum flows in the lines, it does not reflect the actual load condition. Bialek et al [9] had proposed another method of loss allocation in which power flows in the lines are traced and a proportional sharing principle is used.

Cheng et al [10] addressed different challenges associated with bilateral contracts in a deregulated power system network. The authors described modeling of bilateral contracts using a transaction matrix. A two-dimensional matrix that includes power generators and load demands is termed as a transaction matrix.

Anderson and Yang [11] proposed a structure to determine the use of transmission system. Instead of proportional sharing, a power flow comparison is used to determine the use of transmission line. Power flow comparison method uses load flow study to find a generator's contribution by superimposing the generator on the base load. The difference obtained from the two load flows are attributed to generator's account. This method goes in sequence for each generator to calculate its effect on load flow studies. Loss allocation depends on the sequence of generator used. Results vary widely for different sequences.

Fand and David [12] discussed power dispatch issue in a power network structure dominated by bilateral and multilateral transmission contracts. A framework of price-based operation under deregulated structure was developed and a solution to optimal transmission dispatch is proposed. This paper particularly concentrates on dispatch curtail challenges with bilateral and multilateral contracts in a power system.

Expósito et al [13] have proposed a method based on unbundling of branch flows. The method presented in this paper is modified incremental loss factor method and is applicable on a nodal basis. The authors proposed four methods for splitting branch flows; proportional allocation, quadratic allocation, geometric allocation and fast geometric allocation.

Bhuiya and Chowdhury [14] have proposed two methods of loss allocation namely, *Incremental Load Flow Approach* (ILFA) and *Marginal Transmission Loss Approach (MTLA)*. The former uses a modified load flow technique to assess transmission loss. In this method, at each load bus, load is increased in a discrete step while the loads at the other buses are kept constant. The resulting differential transmission loss is attributed to the corresponding generator. The loads are incremented in an alternate sequence, in discrete steps, from zero to their respective levels. This method is consistent with solved load flow and rewards counter flow in the system but it requires a high computation time. The later method is based on Kron's transmission loss expression and results in an iterative process. To reflect the effect of bilateral contracts, Kron's loss expression is modified and expressed in terms of loads instead of generations. In MTLA, a generator's share of transmission loss can be found by making an incremental change in the generator's active power demand, while keeping all other loads fixed. This method requires many complex mathematical analyses and operations.

1.11 Objective And Scope of This Research

The main objective of this research work is to develop an artificial neural network that can be utilized to assess transmission loss allocation in a deregulated system.

Power flow in a transmission network varies from one moment to another depending upon the changes in load and generation schedule. A fast loss allocation tool / technique is required to account for the variation in power flows. Moreover, a transmission network is subjected to line failures for various reasons. Sometimes transmission lines are taken out for preventive maintenance as well. The loss allocation, therefore, will change with a change in the line configuration in the system. Also, loss allocation depends on the underlying allocation principle that the stakeholders would agree. Based on these practical considerations the intended ANN should meet the following criteria.

1) Provide loss allocation results in a relatively fast manner.
2) Be flexible enough to accommodate line failures.
3) Be retrained and adapted to implement different loss allocation principles with relative ease.

1.12 Outline of The Thesis

This thesis is organized in seven chapters. Chapter 1 and 2 deal with the basic concepts of power system and transmission loss. Power systems around the world are going through great changes in recent years. From vertically integrated monopoly business, it is moving towards fully deregulated competitive business. Chapter 1 describes in brief about the components of power systems and their operation. It also describes the evolution of power systems, recent changes in deregulated power industry structure and the effect of deregulation on operation and planning. It explains transmission loss and the issues associated with loss allocation in a deregulated system. A literature review on loss allocation also is presented in this chapter.

Transmission loss, its assessment and the principles of traditional system operation are discussed in Chapter 2. The basic configuration and features of an artificial neural network are described in Chapter 3. The working principles including learning and testing of an ANN are also discussed in this chapter.

An artificial neural network needs some known input-output patterns for training. Incremental Load Flow Approach (ILFA) was used to derive these patterns. Chapter 4 explains in detail the ILFA method of loss allocation with examples. Selection of inputs, proposed architecture of neural network, and its training is described in detail in this chapter. Loss allocation in the IEEE 24 bus system utilizing the proposed ANN is presented in this chapter. Allocation results obtained from the ANN are compared with those obtained from the ILFA.

Transmission line failures and their effects on loss allocation are discussed in Chapter 5. The change in architecture to include line failures and the corresponding training and testing details are also discussed in this chapter.

Loss allocation in a deregulated power pool is different than loss allocation for bilateral contracts. Loss allocation in a deregulated power pool utilizing the proposed ANN is discussed in Chapter 6. *Z-bus allocation* has been utilized to derive the input-output vector to train the proposed neural network. The effects of transmission line failures on loss allocation is discussed in details in this chapter. Development of the proposed ANN, its architecture, selection of inputs and training issues are discussed as well. Allocation results obtained from the ANN are compared with that of *Z-bus allocation*.

The concluding remarks and the scope of future work are presented in Chapter 7.

CHAPTER 2: TRANSMISSION LOSS & ECONOMIC POWER SYSTEM OPERATION

2.1 Transmission Loss in Power System Operation

A power system consists of three essential functional areas, namely generation, transmission and distribution. The combination of these three entities and their optimized utilization is the goal of power system operation. The generation may consist of different types of power plants e.g. thermal, hydro, nuclear, wind, solar, geothermal. Start up time of these plants varies from few minutes to few days. Some responds to load variation quickly while others takes a lot of time to respond. Fuel cost of these plants also varies greatly. System operators usually want to use the available generating units in an optimized and efficient way. Loads in a network vary throughout the day and also during various seasons. Power system operators take all these factors in consideration and operate their systems at lowest possible cost.

Loads in a network follow some patterns and go high and low at different times of the day. Load forecast predicts the nature of the load from patterns and events from previous records with good accuracy. From these predictions, system operator determines the required number of generating unit to meet the demand; an essential activity of power system operation, generally known as unit commitment. Unit commitment dictates the number of generating units to be in spinning condition to meet the demand for 24 hours. It also states the order of the units to be engaged in production according to the production cost of the units and starting time of the units. Production costs of these units depend on working principle and fuel used. For example, production cost of hydro units is far less than those of gas and steam turbines.

Whatever fact lies with the production cost and working principles of the generating units, transmission loss plays a vital role in the decision making of how the units are committed and loaded. Transmission loss cannot be avoided due to fact that all transmission and distribution lines offer resistance to flow of current through them.

Some power loss occurs (i^2R) during transmission of power which depends on distance, size of line, voltage level and flow of current (power) i.e. total system load. Sometimes a distant hydro power plant becomes costlier than a gas turbine near load center. Therefore, after predicting load for an hour, a tentative generating schedule is prepared. Optimum schedule is done after assessing transmission loss and considering other factors like voltage level, water level in hydro plants and some other factors like starting time and response time of the generating units. However, assessing transmission loss is essential to the efficient operation of a power system.

Transmission loss consists of two components: real and reactive. Real part cost money, millions of dollars per year and reactive part costs voltage stability. Both of them need to be assessed properly for power system security and stability. AC load flow technique, transmission loss expressions, Kron's formula etc are used to assess transmission loss. Out of these techniques, AC load flow technique is the most popular and powerful, since it gives all power flows, line losses and voltage level of all buses in a system.

2.2 Transmission Loss Calculation from Load Flow Analysis

Load flow analysis forms the heart of power system analysis. In general, load flow analysis solves for any unknown bus voltage and unspecified generation and finally for complex power flow in the network components for a given power system network, with known loads and some set of specifications or restrictions on power generation and voltages. A load flow analysis can be utilized to determine total transmission loss in a system as well as losses in individual components e.g. in transformers or in lines. A load flow analysis provides real and reactive powers at different buses. Total transmission loss can be calculated from the algebraic sum of powers injected at all buses.

2.2.1 AC load flow technique- Two methods of load flow analysis are mostly used in power system operation. They are Gauss-Seidal and Newton-Raphson methods [15]. Both need some input parameters for performing analysis. Network parameters e.g. Y-bus or Z-bus is required to be calculated before proceeding a solution. Buses in a network are divided into three categories: swing bus, generator or PV bus and load or

PQ bus. Each bus is associated with four parameters: voltage magnitude, phase angle, real and reactive power.

Swing bus – it is a generator bus whose voltage and angle have been specified for load flow analysis. The real and reactive powers are calculated to match the generation, load and losses.

Generator bus – Generators are connected in these buses. The bus voltage and real power generation are specified and reactive power and phase angle are determined.

Load bus – generally loads are connected in these buses. Real and reactive load of these buses are known and bus voltage and phase angle are calculated.

The load flow technique actually solves a set of simultaneous non-linear equations in an iterative process. Gauss-Seidal method is easy to use but takes lot of iterations to give a solution with a specified accuracy. Newton-Raphson method converges faster than Gauss-Seidal method but needs matrix calculations. Due to easy calculation of matrices in computer, Newton-Raphson method is widely used in load flow analysis. Since Newton-Raphson method has been used in this research work, only this method will be explained here. The following simultaneous equations are required for a solution of load flow by Newton-Raphson method.

$$P_k = \sum_{n=1}^{N} |V_k V_n Y_{kn}| \cos(\theta_{kn} + \delta_n - \delta_k) \quad \ldots \quad \ldots \quad \ldots \quad (2.1)$$

$$Q_k = -\sum_{n=1}^{N} |V_k V_n Y_{kn}| \sin(\theta_{kn} + \delta_n - \delta_k) \quad \ldots \quad \ldots \quad \ldots \quad (2.2)$$

where,

P_k = real power at Bus k

Q_k = reactive power at Bus k

V_k = voltage magnitude at Bus k

V_n = voltage magnitude at Bus n

Y_{kn} = element of bus admittance matrix between buses k and n

θ_{kn} = angle associated with Y_{kn}

δ_k = phase angle of Bus k

δ_n = phase angle of Bus n

For every bus, there will be two such equations and two unknowns to be solved. The unknowns are real and reactive generations for swing bus; phase angle and reactive generation for *PV* bus and voltage magnitude and phase angle for load bus. The method starts with some initial values for the specified parameters, P and Q for every bus except the swing bus. Estimated values of V and δ for each bus except the swing bus are used to calculate the same parameters. The mismatch in power calculation originating from specified and calculated values are determined for each bus. For Bus k,

$$\Delta P_k^{(0)} = P_{ks} - P_{kc}^{(0)} \quad \ldots \quad \ldots \quad \ldots \quad \ldots \quad (2.3)$$

$$\Delta Q_k^{(0)} = Q_{ks} - Q_{kc}^{(0)} \quad \ldots \quad \ldots \quad \ldots \quad (2.4)$$

where the subscript k is bus number, subscripts s and c represent specified and calculated values respectively and the superscript represents the iteration number. From equations of all buses, Jacobian J is determined in following manner;

$$\begin{bmatrix} \Delta P_1^{(0)} \\ \ldots \\ \Delta P_{N-1}^{(0)} \\ \Delta Q_1^{(0)} \\ \ldots \\ \Delta Q_{N-1}^{(0)} \end{bmatrix} = \begin{bmatrix} \frac{\partial P_1}{\partial |\delta_1|} \ldots \frac{\partial P_1}{\partial |\delta_{N-1}|} & \frac{\partial P_1}{\partial |V_1|} \ldots \frac{\partial P_1}{\partial |V_{N-1}|} \\ \vdots \quad \ddots \quad \vdots & \vdots \quad \ddots \quad \vdots \\ \frac{\partial P_{N-1}}{\partial |\delta_1|} \ldots \frac{\partial P_{N-1}}{\partial |\delta_{N-1}|} & \frac{\partial P_{N-1}}{\partial |V_1|} \ldots \frac{\partial P_{N-1}}{\partial |V_{N-1}|} \\ \frac{\partial Q_1}{\partial |\delta_1|} \ldots \frac{\partial Q_1}{\partial |\delta_{N-1}|} & \frac{\partial Q_1}{\partial |V_1|} \ldots \frac{\partial Q_1}{\partial |V_{N-1}|} \\ \vdots \quad \ddots \quad \vdots & \vdots \quad \ddots \quad \ldots \vdots \\ \frac{\partial Q_{N-1}}{\partial |\delta_1|} \ldots \frac{\partial Q_{N-1}}{\partial |\delta_{N-1}|} & \frac{\partial Q_{N-1}}{\partial |V_1|} \ldots \frac{\partial Q_{N-1}}{\partial |V_{N-1}|} \end{bmatrix} \begin{bmatrix} \Delta \delta_1^{(0)} \\ \ldots \\ \Delta \delta_{N-1}^{(0)} \\ \Delta |V_1^{(0)}| \\ \ldots \\ \Delta \left| V_{N-1}^{(0)} \right| \end{bmatrix} \quad \ldots\ldots \ldots \ldots \quad (2.5)$$

Equation (2.5) can be written as

$$\begin{bmatrix} \Delta P^k \\ \Delta Q^k \end{bmatrix} = \begin{bmatrix} J_1 & J_2 \\ J_3 & J_4 \end{bmatrix} \begin{bmatrix} \Delta \delta^k \\ \Delta |V^k| \end{bmatrix} \quad \ldots \quad \ldots \quad \ldots \quad \ldots \quad \ldots \quad (2.6)$$

The diagonal and off-diagonal elements of J_1 are

$$\frac{\partial P_i}{\partial \delta_i} = \sum_{j \neq i} |V_i||V_j||Y_{ij}|\sin(\theta_{ij} - \delta_i + \delta_j) \quad \ldots \quad \ldots \quad \ldots \quad \ldots \quad (2.7)$$

$$\frac{\partial P_i}{\partial \delta_j} = -|V_i||V_j||Y_{ij}|\sin(\theta_{ij} - \delta_i + \delta_j), \quad j \neq i \quad \ldots \quad \ldots \quad \ldots \quad (2.8)$$

The diagonal and off-diagonal elements of J_2 are

$$\frac{\partial P_i}{\partial |V_i|} = 2|V_i||Y_{ii}|\cos(\theta_{ii}) + \sum_{j \neq i} |V_j||Y_{ij}|\cos(\theta_{ij} - \delta_i + \delta_j) \quad \ldots \quad \ldots \quad (2.9)$$

$$\frac{\partial P_i}{\partial |V_j|} = |V_i||Y_{ij}|\cos(\theta_{ij} - \delta_i + \delta_j) \quad j \neq i \quad \ldots \quad \ldots \quad \ldots \quad (2.10)$$

The diagonal and off-diagonal elements of J_3 are

$$\frac{\partial Q_i}{\partial \delta_i} = \sum_{j \neq i} |V_i||V_j||Y_{ij}|\cos(\theta_{ij} - \delta_i + \delta_j) \quad \ldots \quad \ldots \quad \ldots \quad \ldots \quad (2.11)$$

$$\frac{\partial Q_i}{\partial \delta_j} = -|V_i||V_j||Y_{ij}|\cos(\theta_{ij} - \delta_i + \delta_j), \quad j \neq i \quad \ldots \quad \ldots \quad \ldots \quad (2.12)$$

The diagonal and off-diagonal elements of J_4 are

$$\frac{\partial Q_i}{\partial |V_i|} = -2|V_i||Y_{ii}|\sin(\theta_{ii}) - \sum_{j \neq i} |V_j||Y_{ij}|\sin(\theta_{ij} - \delta_i + \delta_j) \quad \ldots \quad \ldots \quad (2.13)$$

$$\frac{\partial Q_i}{\partial |V_j|} = -|V_i||Y_{ij}|\sin(\theta_{ij} - \delta_i + \delta_j) \quad j \neq i \quad \ldots \quad \ldots \quad (2.14)$$

Equation (2.6) can also be written in the following way

$$\begin{bmatrix} \Delta \delta^k \\ \Delta |V^k| \end{bmatrix} = [J]^{-1} \begin{bmatrix} \Delta P^k \\ \Delta Q^k \end{bmatrix} \quad \ldots. \quad \ldots. \quad \ldots. \quad \ldots. \quad \ldots. \quad (2.15)$$

Equation (2.15) is solved and errors in voltages and angles are calculated. New values of V and δ are estimated by subtracting these errors from the respective parameters. These new voltage and angles are used to calculate new bus powers using Equations (2.3) and (2.4). This process is repeated until mismatch at each bus goes below the tolerance limit.

2.2.2 Example of load flow analysis

A small 3-bus network is shown in Figure 2.1 to illustrate Newton-Raphson load flow technique. There are two generators in Buses 1 and 2 and two loads in Buses 2 and 3. Buses 1, 2 and 3 are defined as swing bus, voltage control bus and load bus respectively. Line parameters and generator data are shown in Tables 2.1 and 2.2 respectively. Real and reactive load at Bus 2 are 120 MW and 50 MVAR and at Bus 3 are 250 MW and 80 MVAR. The base values used for this load flow analysis are 100 MVA and 138 kV.

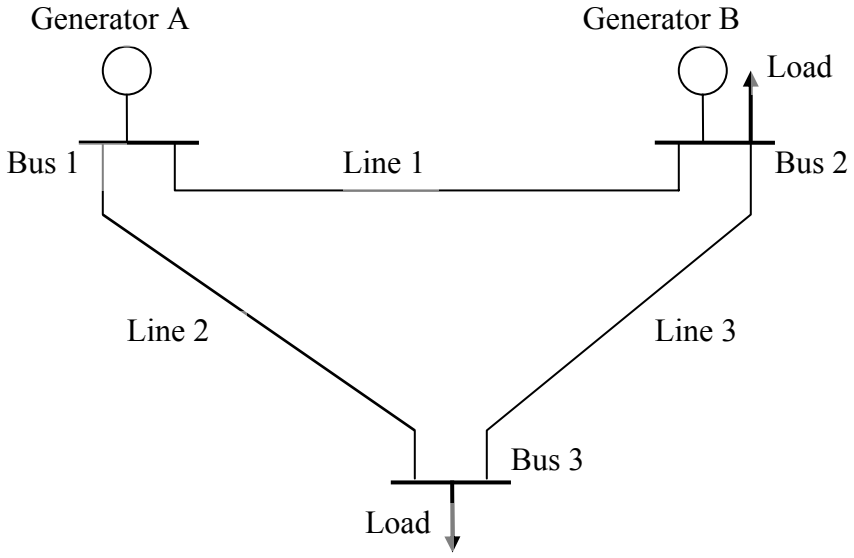

Fig. 2.1: A 3-bus power system network.

Table 2.1: Line parameters for the system shown in Figure 2.1.

Line No.	From Bus	To Bus	Resistance (p.u.)	Reactance (p.u.)
1	1	2	0.0200	0.0400
2	1	3	0.0100	0.0300
3	2	3	0.0125	0.0250

Table 2.2: Generator data

Generating unit	Maximum output (MW)	Minimum output (MW)
Generator A	450	90
Generator B	250	30

Before starting a flow analysis, voltage magnitude and phase angle of swing bus and voltage magnitude of voltage control buses have to be defined. Let us assume voltage magnitudes of Buses 1 and 2 are 1.05 p.u. and 1.04 p.u respectively and phase angle of Bus 1 (swing bus) is 0. To check the convergence of iteration, we will use a value for tolerance of 0.0001

From line parameters, we get the line admittances y_{12}=10-j20, y_{13}=10-j30, and y_{23}=16-j32. This results in the following bus admittance matrix,

$$[Y_{bus}] = \begin{bmatrix} 20 - j50 & -10 + j20 & -10 + j30 \\ -10 + j20 & 26 - j52 & -16 + j32 \\ -10 + j30 & -16 + j32 & 26 - j62 \end{bmatrix}$$

Converting the bus admittance matrix to polar form with angles in radian,

$$[Y_{bus}] = \begin{bmatrix} 53.8517\angle -1.9029 & 22.3607\angle 2.0344 & 31.6228\angle 1.8925 \\ 22.3607\angle 2.0344 & 58.1378\angle -1.1071 & 35.7771\angle 2.0344 \\ 31.6228\angle 1.8925 & 35.7771\angle 2.0344 & 67.2310\angle -1.1737 \end{bmatrix}$$

From Equations (1) and (2), the expressions for real power at Buses 2 and 3 and the reactive power at Bus 3 are:

$$P_2 = |V_2||V_1||Y_{21}|\cos(\theta_{21} - \delta_2 + \delta_1) + |V_2^2||Y_{22}|\cos(\theta_{22}) + |V_2||V_3||Y_{23}|\cos(\theta_{23} - \delta_2 + \delta_3)$$

$$P_3 = |V_3||V_1||Y_{31}|\cos(\theta_{31} - \delta_3 + \delta_1) + |V_3||V_2||Y_{32}|\cos(\theta_{32} - \delta_2 + \delta_3) + |V_3^2||Y_{33}|\cos(\theta_{33})$$

$$Q_3 = -|V_3||V_1||Y_{31}|\sin(\theta_{31} - \delta_3 + \delta_1) - |V_3||V_2||Y_{32}|\sin(\theta_{32} - \delta_2 + \delta_3) - |V_3^2||Y_{33}|\sin(\theta_{33})$$

Initial values of bus voltages for Bus 1,2 and 3 are $1.05\angle 0, 1.04\angle 0$ and $1.0\angle 0$. With these initial values P_2, P_3 and Q_3 in per unit quantities are:

$$P_2^{(0)} = 0.5616$$

$$P_3^{(0)} = -1.14$$

$$Q_3^{(0)} = -2.78$$

Loads and generations expressed in per units are

$$P_2^{sch} = \frac{100 - 120}{100} = -0.20 \text{ p.u}$$

$$P_3^{sch} = \frac{0-250}{100} = -2.50$$

$$Q_3^{sch} = \frac{0-80}{100} = -0.80$$

From Equations (2.3) and (2.4) we get

$$\Delta P_2^{(0)} = P_2^{sch} - P_2^{(0)} = -0.2 - 0.5616 = -0.7616$$

$$\Delta P_3^{(0)} = P_3^{sch} - P_3^{(0)} = -2.5 - (-1.14) = -1.3600$$

$$\Delta Q_3^{(0)} = Q_3^{sch} - Q_3^{(0)} = -0.8 - (-2.78) = 1.9800$$

Therefore, matrix $\begin{bmatrix} \Delta P \\ \Delta Q \end{bmatrix}$ of Equation (2.15) is $\begin{bmatrix} -0.7616 \\ -1.3600 \\ 1.9800 \end{bmatrix}$. Using Equations (2.7)-(2.14)

we get the Jacobian J = $\begin{bmatrix} 55.1200 & -33.2800 & -16.6400 \\ -33.2800 & 64.7800 & 24.8600 \\ 16.6400 & -27.1400 & 59.2200 \end{bmatrix}$

Using Equation (2.15), we get

$$\begin{bmatrix} \Delta\delta_2 \\ \Delta\delta_3 \\ \Delta V_3 \end{bmatrix} = \begin{bmatrix} 55.1200 & -33.2800 & -16.6400 \\ -33.2800 & 64.7800 & 24.8600 \\ 16.6400 & -27.1400 & 59.2200 \end{bmatrix}^{-1} \begin{bmatrix} -0.7616 \\ -1.3600 \\ 1.9800 \end{bmatrix} = \begin{bmatrix} -0.0362 \\ -0.0479 \\ 0.0217 \end{bmatrix}$$

The corrected values are

$$\delta_2^{(1)} = 0 + (-0.0362) = -0.0362$$

$$\delta_3^{(1)} = 0 + (-0.0479) = -0.0479$$

$$V_3^{(1)} = 1 + 0.0217 = 1.0217$$

With these values of voltage magnitude and phase angle, $\begin{bmatrix} \Delta P_2 \\ \Delta P_3 \\ \Delta Q_3 \end{bmatrix} = \begin{bmatrix} -0.0169 \\ 0.0148 \\ -0.0832 \end{bmatrix}$

Jacobian J= $\begin{bmatrix} 55.6277 & -34.1972 & -16.2495 \\ -33.7994 & 65.4309 & 24.1015 \\ 17.3970 & -29.6530 & 62.6409 \end{bmatrix}$

In the next iteration Equation (2.15) becomes

$$\begin{bmatrix}\Delta\delta_2\\ \Delta\delta_3\\ \Delta V_3\end{bmatrix}=\begin{bmatrix}55.6277 & -34.1972 & -16.2495\\ -33.7994 & 65.4309 & 24.1015\\ 17.3970 & -29.6530 & 62.6409\end{bmatrix}^{-1}\begin{bmatrix}-0.0169\\ 0.0148\\ -0.0832\end{bmatrix}=\begin{bmatrix}-0.0003\\ 0.0004\\ -0.0010\end{bmatrix}$$

Now the corrected values are

$$\delta_2^{(2)}=-0.0362+(-0.0003)=-0.0365$$
$$\delta_3^{(2)}=-0.0479+0.0004=-0.0475$$
$$V_3^{(2)}=1.0217+(-0.0010)=1.0207$$

and

$$\begin{bmatrix}\Delta P_2\\ \Delta P_3\\ \Delta Q_3\end{bmatrix}=\begin{bmatrix}-0.3219x10^{-4}\\ 0.0612x10^{-4}\\ -0.9761x10^{-4}\end{bmatrix},\qquad \text{J=}\begin{bmatrix}55.5764 & -34.1499 & -16.2753\\ -33.7787 & 65.3836 & 24.0867\\ 17.3534 & -29.5835 & 62.4949\end{bmatrix}$$

After the 3rd iteration,

$$\begin{bmatrix}\Delta\delta_2\\ \Delta\delta_3\\ \Delta V_3\end{bmatrix}=\begin{bmatrix}55.5764 & -34.1499 & -16.2753\\ -33.7787 & 65.3836 & 24.0867\\ 17.3534 & -29.5835 & 62.4949\end{bmatrix}^{-1}\begin{bmatrix}-0.3219x10^{-4}\\ 0.0612x10^{-4}\\ -0.9761x10^{-4}\end{bmatrix}=\begin{bmatrix}-0.0888x10^{-5}\\ 0.0102x10^{-5}\\ -0.1267x10^{-5}\end{bmatrix}$$

Now since the maximum error is less than the tolerance, the solution converged in three iterations. New values are:

$$\delta_2^{(3)}=-0.0365+(-0.000000888)=-0.03650089\ radian=-2.0913^o$$
$$\delta_3^{(3)}=-0.0475+0.000000102=-0.0474999\ radian=-2.7215^o$$
$$V_3^{(3)}=1.0207+(-0.000001267)=1.020698$$

P_1=2.75637 p.u.

Q_1=0.27866 p.u

Q_2=0.66681 p.u

The load flow solution is shown in Table 2.3.

Table 2.3: Load flow solution using Newton-Raphson method

Bus	Voltage magnitude (p.u.)	Phase Angle (degree)	Generation		Load	
			Real (MW)	Reactive (MVAR)	Real (MW)	Reactive (MVAR)
1	1.0500	0.0000	275.637	27.866	0.000	0.000
2	1.0400	-2.0913	100.000	116.681	120.000	50.000
3	1.0207	-2.7215	0.000	0.0000	250.000	80.000
Total			375.637	144.546	370.000	130.000

2.2.3 Calculation of transmission loss from load flow analysis– Transmission loss can be calculated from the solved load flow analysis mentioned in Section 2.2.1. Solved load flow analysis gives voltage magnitude and phase angle of all buses. From these values current though all lines can be calculated. Current from Bus *i* to Bus *j* can be calculated using following equation

$I_{ij}=Y_{ij}(V_i-V_j)$ … … … …. … … (2.16)

where Y_{ij} is the admittance of the transmission line between Bus *i* and Bus *j*.

From known values of bus voltage and current injected in each line, power injection can be calculated. Line loss is the sum of power injection in a line from both sides of it. Power injection in a line can be determined from the following equations.

$S_{ij}=V_iI_{ij}^*$ ... ... (2.17)

$S_{ji}=V_jI_{ji}^*$ ... ... (2.18)

$S_{Lij}=S_{ij}+S_{ji}$ ... ... (2.19)

where,

S_{ij} = power injection from Bus *i* to the line between Bus *i* & Bus *j*

S_{ji} = power injection from Bus *j* to the line between Bus *i* & Bus *j*

S_{Lij} =power loss in the line between Bus *i* & Bus *j*

I_{ij}^* =complex conjugate of current I_{ij}

Thus power loss in all lines can be calculated. Total transmission loss is the sum of losses in all lines.

Using Equation (2.16) all line currents can be obtained. Utilizing Equations (2.17)-(2.19), line losses can be calculated. Table 2.4 shows the line loss for the system shown in Figure 2.1

Table 2.4: Line flows and losses in the network shown in Figure 2.1

Line	From Bus	To Bus	Real power (MW)	Reactive power (MAVR)	Line loss	
					Real (MW)	Reactive (MVAR)
1	1	2	91.023	-17.439	1.559	3.116
	2	1	-89.464	20.555		
2	1	3	184.617	45.307	3.278	9.832
	3	1	-181.339	-35.475		
3	2	3	69.464	46.133	0.803	1.607
	3	2	-68.661	-44.525		
Total transmission loss					5.640	14.555

Transmission loss calculated from a load flow analysis is more accurate than any other method. Electrical utilities have been calculating transmission loss using load flow analyses for more than hundred years. Before the deregulation of electric sector, load flow analyses were sufficient for estimating transmission loss. After the introduction of deregulation, it became necessary to compute transmission loss due to individual power transaction i.e. from a particular generator to a particular load. Load flow analyses in their current forms cannot be utilized to compute this type of loss.

2.3 Transmission Loss Expressions

A transmission loss expression is often used to compute total transmission loss in a system. A transmission loss expression can be derived from the relation of bus voltage, power and line current. Complex power S_i in any Bus i is

$$S_i = V_i I_i^* \quad \ldots \quad \ldots \quad \ldots \quad \ldots \quad \ldots \quad \ldots \quad (2.20)$$

where,

V_i = voltage at Bus i

I_i* = complex conjugate of injected current at Bus i

Transmission loss is the sum of injected power at all buses. So,

$$S_L = P_L + jQ_L = \sum_i S_i \quad \ldots \quad \ldots \quad \ldots \quad \ldots \quad (2.21)$$

where,

S_L = total complex power loss

P_L = total real power loss

Q_L = total reactive power loss

S_i = injected complex power at Bus i

Equation (2.21) can be written as

$$S_L = [V_B]^T [I_B]^* \quad \ldots \quad \ldots \quad \ldots \quad \ldots \quad \ldots \quad (2.22)$$

where,

$[V_B] = [Z_B][I_B]$

$[Z_B] = [R]+[jX]$

$[I_B] = [I_p]+[jI_q]$

$[Z_B]$ = bus impedance matrix

$[R]$ = real part of bus impedance matrix element

$[X]$ = imaginary part of bus impedance matrix element

$[I_p]$ = real component of injected bus current

$[I_q]$ = reactive component of injected bus current

Replacing V_B and I_B by their real and imaginary parts in equation (2.22),

$S_L = [I_B]^T[Z_B][I_B]^*$

$= ([I_p]+[jI_q]^T([R]+[jX])([I_p]+[jI_q])^*$

Separating real and imaginary parts,

$$P_L = [I_p]^T [R][I_p] + [I_q]^T [R][I_q] \quad \ldots \quad \ldots \quad \ldots \quad \ldots \quad \ldots \quad (2.23)$$

$$Q_L = [I_p]^T [X][I_p] + [I_q]^T [X][I_q] \quad \ldots \quad \ldots \quad \ldots \quad \ldots \quad (2.24)$$

Injected power at any Bus *i* is given by,

$$P_i + jQ_i = V_i I_i^*$$

where,

$V_i = |V_i|(\cos\delta_i + j\sin\delta_i)$

$I_i = I_{pi} + jI_{qi}$, I_{pi} is the real part and I_{qi} is the imaginary part of the injected bus current

Therefore,

$$P_i + jQ_i = |V_i|(\cos\delta_i + j\sin\delta_i)(I_{pi} + jI_{qi}) \quad \ldots \quad \ldots \quad \ldots \quad \ldots \quad (2.25)$$

Equating the real and imaginary parts,

$$P_i = |V_i| I_{pi} \cos\delta_i + |V_i| I_{qi} \sin\delta_i \quad \ldots \quad \ldots \quad \ldots \quad \ldots \quad \ldots \quad (2.26)$$

$$Q_i = |V_i| I_{pi} \sin\delta_i - |V_i| I_{qi} \cos\delta_i \quad \ldots \quad \ldots \quad \ldots \quad \ldots \quad \ldots \quad (2.27)$$

Solving Equations (2.26) & (2.27) for I_{pi} and I_{qi},

$$I_{pi} = \frac{P_i \cos\delta_i + Q_i \sin\delta_i}{|V_i|}$$

$$I_{qi} = \frac{P_i \sin\delta_i - Q_i \cos\delta_i}{|V_i|}$$

The above two equations can be written in vector form as below,

$$[I_p] = [C][P] + [D][Q] \quad \ldots \quad \ldots \quad \ldots \quad \ldots \quad \ldots \quad (2.28)$$

$$[I_q] = [D][P] - [C][Q] \quad \ldots \quad \ldots \quad \ldots \quad \ldots \quad \ldots \quad (2.29)$$

where,

$[C]$ = diagonal matrix with elements $(\cos \delta_i / |V_i|)$

$[D]$ = diagonal matrix with elements $(\sin \delta_i / |V_i|)$

Now putting the values of I_p and I_q in Equation (2.23), it becomes,

$$P_L = [I_p]^T [R][I_p] + [I_q]^T [R][I_q]$$

$$= ([C][P] + [D][Q])^T [R]([C][P] + [D][Q]) + ([D][P] - [C][Q])^T [R]([D][P] - [C][Q])$$

Or,

$$P_L = [P]^T ([C]^T [R][C] + [D]^T [R][D])[P] - [P]^T ([D]^T [R][C] + [C]^T [R][D])[Q]$$
$$+ [Q]^T ([D]^T [R][C] - [C]^T [R][D])[P] + [Q]^T ([C]^T [R][C] + [D]^T [R][D])[Q]$$

which can be written in the following matrix form,

$$P_L = \begin{bmatrix} [P]^T & [Q]^T \end{bmatrix} \begin{bmatrix} [A_p] & -[B_p] \\ [B_p] & [A_p] \end{bmatrix} \begin{bmatrix} [P] \\ [Q] \end{bmatrix} \quad \ldots \quad \ldots \quad \ldots \quad (2.30)$$

where,

$$[A_p] = [C]^T [R][C] + [D]^T [R][D]$$

$$[B_p] = [D]^T [R][[C] - [C]^T [R][D]$$

Again,

$$[C]^T [R][C] = \begin{bmatrix} c_1 & 0 & 0 & 0 \ldots 0 \\ 0 & c_2 & 0 & 0 \ldots 0 \\ \vdots & & & \\ 0 & 0 & 0 & 0 \ldots c_n \end{bmatrix} \begin{bmatrix} r_{11} & r_{12} \cdots r_{1n} \\ r_{21} & r_{22} \cdots r_{2n} \\ \vdots & \\ r_{n1} & r_{n2} \cdots r_{nn} \end{bmatrix} \begin{bmatrix} c_1 & 0 & 0 & 0 \ldots 0 \\ 0 & c_2 & 0 & 0 \ldots 0 \\ \vdots & & & \\ 0 & 0 & 0 & 0 \ldots c_n \end{bmatrix}$$

$$= \begin{bmatrix} c_1 r_{11} c_1 & c_1 r_{12} c_2 & \cdots c_1 r_{1n} c_n \\ c_2 r_{21} c_1 & c_2 r_{22} c_2 & \cdots c_2 r_{2n} c_n \\ \vdots & & \\ c_n r_{n1} c_1 & c_n r_{n2} c_2 & \cdots c_n r_{nn} c_n \end{bmatrix}$$

The elements of $[A_p]$ are

$$a_{pij} = c_i r_{ij} c_j + d_i r_{ij} d_j$$

$$= \frac{\cos\delta_i \cos\delta_j}{|V_i||V_j|} r_{ij} + \frac{\sin\delta_i \sin\delta_j}{|V_i||V_j|} r_{ij}$$

$$= \frac{r_{ij}}{|V_i||V_j|} \cos(\delta_i - \delta_j) \quad \ldots \quad \ldots \quad \ldots \quad \ldots \quad \ldots \quad (2.31)$$

The elements of $[B_p]$ are

$$[B_p] = [D]^T [R][C] - [C]^T [R][D]$$

$$b_{pij} = d_i r_{ij} c_j - c_i r_{ij} d_j$$

$$= \frac{r_{ij}}{|V_i||V_j|} \sin(\delta_i - \delta_j) \quad \ldots \quad \ldots \quad \ldots \quad \ldots \quad \ldots \quad (2.32)$$

Equation (2.30) can be written as

$$P_L = [P]^T [A_p][P] - [P]^T [B_p][Q] + [Q]^T [B_p][P] + [Q]^T [A_p][Q] \quad \ldots \quad (2.33)$$

Real and reactive power injection at any Bus *i* can be written as

$$P_i = P_{Gi} - P_{Di} \quad \ldots \quad \ldots \quad \ldots \quad \ldots \quad \ldots \quad \ldots \quad \ldots \quad (2.34)$$

$$Q_i = Q_{Gi} - Q_{Di} \quad \ldots \quad \ldots \quad \ldots \quad \ldots \quad \ldots \quad \ldots \quad \ldots \quad (2.35)$$

where,

P_i = real power injection at Bus *i*

Q_i = reactive power injection at Bus *i*

P_{Gi} = power generation at Bus *i*

P_{Di} = power demand at Bus *i*

Q_{Gi} = reactive power generation at Bus *i*

Q_{Di} =reactive power demand at Bus *i*

From Equations (2.33), (2.34) & (2.35)

$$
\begin{aligned}
P_L &= (P_G{}^T - P_D{}^T)A_p(P_G - P_D) - (P_G{}^T - P_D{}^T)B_p(Q^T - Q_D{}^T)A_p(P_G - P_D) \\
&\quad + (Q_G{}^T - Q_D{}^T)A_p(Q_G - Q_D) \\
&= P_G{}^T A_p P_G - P_D{}^T A_p P_G - P_G{}^T A_p P_D + P_D{}^T A_p P_D - P_G{}^T B_p Q_G + P_D{}^T B_p Q_G \\
&\quad + P_G{}^T B_p Q_D - P_D B_p Q_D + Q_G{}^T B_p P_G - Q_D{}^T B_p P_G - Q_G B_p P_D + Q_D{}^T B_p P_D \\
&\quad + Q_G{}^T A_p Q_G - Q_D{}^T A_p Q_G - Q_G{}^T A_p Q_D + Q_D{}^T A_p Q_D \qquad \cdots \qquad \cdots \qquad (2.36)
\end{aligned}
$$

This is a standard transmission loss expression in terms of generation and demand. Similarly, expression for reactive power can also be obtained. In Equation (2.36) P_G, P_D, Q_G, Q_D, A_p, B_p are expressed in matrix form.

2.4 Approximate Loss Formula

In many applications approximate loss expressions are used instead of Equation (2.36). A widely known approximate loss expression, known as Kron's loss formula is derived with the help of the following assumptions.

a. linear relationship between reactive and real power of all generators, which can be defined by

$$Q_{Gi} = Q_{Gi0} + f_i P_{Gi}$$

b. constant generator angular position δ_i

c. voltage magnitude of generator-bus is constant &

d. a fixed demand pattern defined by the following matrices,

$$[Q_{G0}] = col[Q_{Gi0}]$$

$$[F] = daig(f_i)$$

where, f_i is a constant.

Using these assumptions, Equation (2.36) can be written as,

$$P_L = [P_G^T][B_L][P_G] + [B_{L0}^T] + K_{L0} \qquad \cdots \qquad \cdots \qquad \cdots \qquad \cdots \qquad (2.37)$$

where,

$$[B_L] = [A_p] - [B_p][F] + [F]^T[B_p] + [F]^T[A_p][F]$$

$$[B_{L0}]^T = [E_p] + [E_q][F] + 2[Q_{G0}]^T \{[A_p][F] + [B_p]\}$$

$$K_{L0} = \begin{bmatrix}[P_D]^T & [Q_D]^T\end{bmatrix}\begin{bmatrix}[A_p] & -[B_p] \\ [B_p] & [A_p]\end{bmatrix}\begin{bmatrix}[P_D] \\ [Q_D]\end{bmatrix} + [Q_{G0}]^T[A_p][Q_{G0}] + [E_q][Q_{G0}]$$

$$[E_p] = 2\left(-[P_D]^T[A_p] - [Q_D]^T[B_p]\right)$$

$$[E_q] = 2\left([P_D]^T[B_p] - [Q_D]^T[A_p]\right)$$

Equation (2.37) is known as Kron's transmission loss equation. Derivation of Equation (2.37) from Equation (2.36) is shown in Appendix B. $B_L, B_{L0}^T \,\&\, K_{L0}$ are taken as constants. These values, however, do not remain constant for the entire production range of the generators. In spite of this, Kron's formula can assess transmission loss with a fair accuracy. This formula has been used in finding the economic load dispatch for 24 hour generations for weekdays and weekends later in this chapter.

An even simpler form of transmission loss expression, known as George's loss formula is often used where only an approximate estimate of the transmission loss is required. George's loss formula is expressed as

$$P_L = \sum_i \sum_j P_i B_{ij} P_j \qquad \ldots \quad \ldots \quad \ldots \quad \ldots \quad \ldots \qquad (2.38)$$

where $B_{ij}'s$ are known as loss coefficients. Use of this formula is limited due to its inaccuracy. Since this formula is not used in this research, it will not be discussed in detail.

2.5 Economic Power Flow Solution

A modern power system is a very complex entity. Power system engineers face the challenging task of planning and operating the system in an efficient way. Economic dispatch ranks high among the major functions in a power industry. Economic dispatch is the distribution of total required power generation among the available sources for optimal system economy with due consideration of generation cost, transmission loss, and several recognized constraints imposed by the requirements of reliable service and

equipment limitations. Conventional economic dispatch is a static optimization procedure to dispatch pre-selected generating units. When excess generation capacity is available in a system such that an economic choice of units can be made, the set of units to be dispatched is normally determined by a unit commitment program. The hydro-thermal generation economic schedule is different from the all-thermal one. The former involves the planning of the usage of a limited resource over a period of time. The resource is the water available for hydro generation. However, in this research we have assumed that the power system is deregulated and power pool buys power at a fixed cost in every hour. It eliminates the problem of hydro-thermal case. In this case, a power pool does not base its decision on the source of power rather concentrates on the cost of power.

Economic power flow solution is an optimization problem. The target is to operate the system at the minimum cost. Most thermal generation cost can be described by the following equation [16],

$$F_i = a_i P_{Gi}^{\ 2} + b_i P_{Gi} + c_i$$

where,

F_i=running cost of unit i

P_{Gi}=power generation in MW

a_i, b_i, c_i are constant for generator I, generally known as cost parameters.

In a deregulated power system, power producers do not supply the cost parameter information to the system operator. In most cases, price of power is determined by market clearing price which remain fixed for a specified period of time usually an hour. So, cost function becomes,

$$F_i = \beta P_{Gi} \qquad \ldots \quad \ldots \quad \ldots \quad \ldots \qquad (2.39)$$

where,

F_i= cost of energy for unit i

β = market clearing price, \$/MW-hr

P_{Gi} = energy in MW-hr (produced by unit *i*)

Let transmission loss is defined by P_{loss}. Then penalty factor PF_i for unit *i* can be expressed as:

$$PF_i = \frac{1}{1 - \frac{\partial P_L}{\partial P_{Gi}}} \quad \ldots \quad \ldots \quad \ldots \quad \ldots \quad (2.40)$$

Differentiating Equation (2.39) with respect to power P_{Gi}, we get

$$\frac{\partial F_i}{\partial P_{Gi}} = \beta \quad \ldots \quad \ldots \quad \ldots \quad \ldots \quad (2.41)$$

For economic load scheduling,

$$\frac{\partial F_i}{\partial P_{Gi}} PF_i = \lambda_{sys} \quad \ldots \quad \ldots \quad \ldots \quad \ldots \quad (2.42)$$

where, λ_{sys} is the incremental running cost of the system.

2.6 Example of Economic Power Flow Solution

For economic power flow solution for an n-bus system, Kron's transmission loss formula and penalty factor Equation (2.40) have to be generalized. Let us consider a 4-bus system as shown in Figure 2.2. To calculate [Y_{bus}] and [Z_{bus}], let us consider Bus 4 as reference. Therefore, [Y_{bus}] is,

$$[Y_{bus}] = \begin{bmatrix} y_{11} & -y_{12} & -y_{13} \\ -y_{21} & y_{22} & -y_{23} \\ -y_{31} & -y_{32} & y_{33} \end{bmatrix}$$

and $[Z_{bus}] = [Y_{bus}]^{-1}$

Therefore, A_p & B_p become 3x3 matrices which can be determined using Equations (2.31) & (2.32).

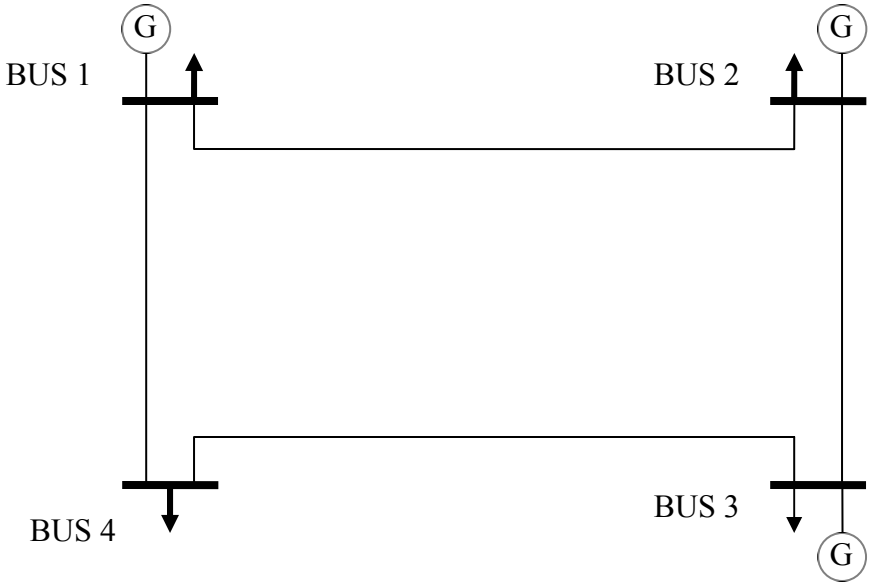

Fig. 2.2: 4-bus test network

Now we can rewrite the equation (2.37) for 4-bus network as

$$P_L = \begin{bmatrix} p_{g1} & p_{g2} & p_{g3} \end{bmatrix} \begin{bmatrix} k_{11} & k_{12} & k_{13} \\ k_{21} & k_{22} & k_{23} \\ k_{31} & k_{32} & k_{33} \end{bmatrix} \begin{bmatrix} p_{g1} \\ p_{g2} \\ p_{g3} \end{bmatrix} + \begin{bmatrix} u_1 & u_2 & u_3 \end{bmatrix} \begin{bmatrix} p_{g1} \\ p_{g2} \\ p_{g3} \end{bmatrix} + K_{LO} \quad (2.43)$$

where k_{xx} and u_x are elements of matrices [B_L]and [B_{LO}] respectively and p_{gx} are generations at different buses.

Expanding the matrices in Equation (2.43) we get

$$P_L = k_{11} {p_{g1}}^2 + k_{22} p_{g2}^2 + k_{33} p_{g3}^2 + k_{12} p_{g1} p_{g2} + k_{13} p_{g1} p_{g3} + k_{21} p_{g1} p_{g2} + k_{23} p_{g2} p_{g3} + k_{32} p_{g2} p_{g3} + k_{31} p_{g1} p_{g3} + u_1 p_{g1} + u_2 p_{g2} + u_3 p_{g3} + K_{LO}$$

$$P_L = \sum_{i=1}^{3} k_{ii} p_{gi}^2 + \sum_{i=1}^{3} \sum_{\substack{j=1 \\ i \neq j}}^{3} k_{ij} p_{gi} p_{gj} + \sum_{i=1}^{3} u_i p_{gi} + K_{LO} \quad \ldots \quad .. \quad (2.44)$$

For an n-bus system Equation (2.44) can be written as

$$P_L = \sum_{x=1}^{n-1} k_{xx} p_{gx}^2 + \sum_{x=1}^{n-1} \sum_{\substack{j=1 \\ x \neq j}}^{n-1} k_{xj} p_{gx} p_{gj} + \sum_{x=1}^{n-1} u_x p_{gx} + K_{LO} \quad \ldots\ldots \quad \ldots \quad (2.45)$$

Differentiating Equation (2.45) with respect to $p_{gx,}$

$$\frac{\partial P_L}{\partial p_{gx}} = 2k_{xx} p_{gx} + 2\sum_{\substack{j=1 \\ j \neq x}}^{n-1} k_{xj} p_{gj} + u_x \quad \text{[Since } k_{1n}=k_{n1} \text{ and so]} \ldots \quad \ldots \quad (2.46)$$

Putting these values in Equation (2.42),

$$\frac{\partial F_x}{\partial p_{gx}} \frac{1}{1 - \dfrac{\partial P_L}{\partial p_{gx}}} = \lambda_{sys}$$

Or, $\beta \dfrac{1}{1 - \dfrac{\partial P_L}{\partial p_{gx}}} = \lambda_{sys}$

Or, $\dfrac{\partial P_L}{\partial p_{gx}} = \dfrac{\lambda - \beta}{\lambda}$

Or, $2k_{xx} p_{gx} + 2\sum_{\substack{j=1 \\ j \neq x}}^{n-1} k_{xj} p_{gj} + u_x = \dfrac{\lambda - \beta}{\lambda}$

Or, $k_{xx} p_{gx} + \sum_{\substack{j=1 \\ j \neq x}}^{n-1} k_{xj} p_{gj} = \dfrac{\lambda - \beta}{2\lambda} - \dfrac{u_x}{2} \quad \ldots\ldots \quad \ldots \quad \ldots \quad (2.47)$

Equation (2.47) can be written as,

$$\left.\begin{aligned}
&k_{11} p_{g1} + k_{12} p_{g2} + k_{13} p_{g3} \ldots + k_{1n-1} p_{gn-1} = \frac{\lambda - \beta}{2\lambda} - \frac{u_1}{2} \\
&k_{21} p_{g1} + k_{22} p_{g2} + k_{23} p_{g3} \ldots + k_{21n-1} p_{gn-1} = \frac{\lambda - \beta}{2\lambda} - \frac{u_2}{2} \\
&k_{31} p_{g1} + k_{32} p_{g2} + k_{33} p_{g3} \ldots + k_{3n-1} p_{gn-1} = \frac{\lambda - \beta}{2\lambda} - \frac{u_3}{2} \\
&\vdots \\
&k_{n-1,1} p_{g1} + k_{n-1,2} p_{g2} + k_{n-1,3} p_{g3} \ldots + k_{n-1n-1} p_{gn-1} = \frac{\lambda - \beta}{2\lambda} - \frac{u_{n-1}}{2}
\end{aligned}\right\} \quad (2.48)$$

The sets of Equation (2.48) can be expressed in matrix form as:

$$\begin{bmatrix} k_{11} & k_{12} & k_{13}\cdots k_{1,n-1} \\ k_{21} & k_{22} & k_{23}\cdots k_{2,n-1} \\ k_{31} & k_{32} & k_{33}\cdots k_{3,n-1} \\ \vdots & & \\ k_{n-1,1} & k_{n-1,2} & k_{n-1,3}..k_{n-1,m-1} \end{bmatrix} \begin{bmatrix} p_{g1} \\ p_{g2} \\ p_{g3} \\ \vdots \\ p_{gn-1} \end{bmatrix} = \begin{bmatrix} \frac{\lambda-\beta}{2\lambda} - \frac{u_1}{2} \\ \frac{\lambda-\beta}{2\lambda} - \frac{u_2}{2} \\ \vdots \\ \frac{\lambda-\beta}{2\lambda} - \frac{u_{n-1}}{2} \end{bmatrix} \quad \ldots \quad (2.49)$$

Or, $[B_L][P_G] = [U]$

Or, $[P_G] = [B_L]^{-1}[U]$ … … … … … … (2.50)

A particular value of λ will satisfy the condition of power balance i.e. total generation will be equal to total load plus losses. These values of generation will be the optimum for the least cost operation of a power system.

2.7 Test System

In this research the IEEE 24-bus system [17] shown in Figure 2.3 was used as an example system for study. It is assumed that the system is run as a pool operation. Its economic power flow solution was obtained using the method mentioned in Section 2.6. An example of economic load flow solution for the peak hour is illustrated here.

There are 10 generator buses and 15 load buses in this system. Line, generator & load parameters are shown in Tables 2.5 & 2.6. Matrices [Q_{G0}] and [F] have been determined using the load flow data of two consecutive hours. Transmission losses obtained from Kron's formula and load flow analysis are very close, which proves the accuracy of the formulation of Kron's formula. Matrices [F] and [Q_{G0}]are given in appendix A.

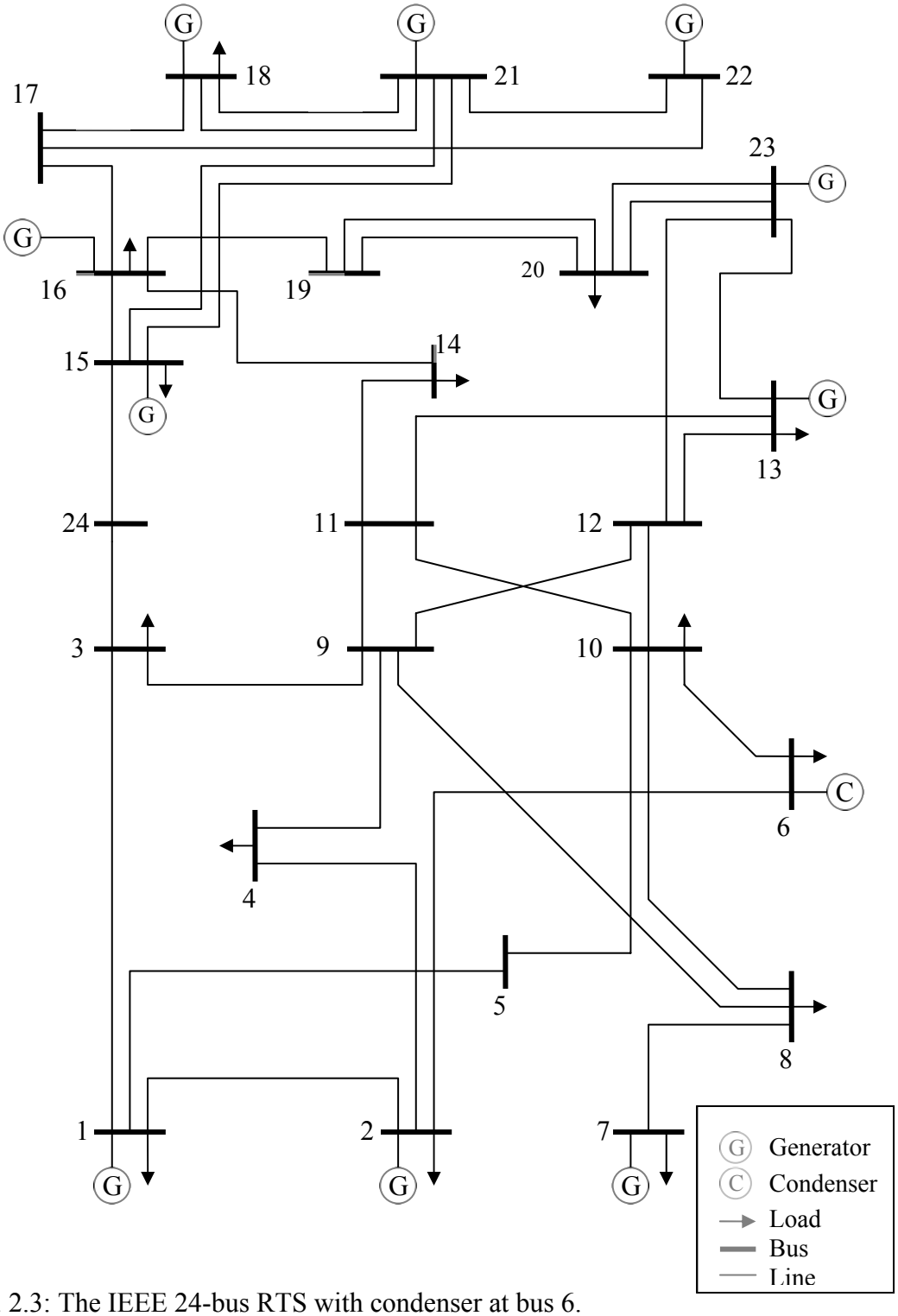

Fig. 2.3: The IEEE 24-bus RTS with condenser at bus 6.

Table 2.5: Line parameters of the test system

Line no.	From Bus	To Bus	Resistance (R) (p.u.)	Reactance (X) (p.u.)
1	1	2	0.0026	0.0139
2	1	3	0.0546	0.2112
3	1	5	0.0218	0.0845
4	2	4	0.0328	0.1267
5	2	6	0.0497	0.1920
6	3	9	0.0308	0.1190
7	3	24	0.0023	0.0839
8	4	9	0.0268	0.1037
9	5	10	0.0228	0.0883
10	6	10	0.0139	0.0605
11	7	8	0.0159	0.0614
12	8	9	0.0427	0.1651
13	8	10	0.0427	0.1651
14	9	11	0.0023	0.0839
15	9	12	0.0023	0.0839
16	10	11	0.0023	0.0839
17	10	12	0.0023	0.0839
18	11	13	0.0061	0.0476
19	11	14	0.0054	0.0418
20	12	13	0.0061	0.0476
21	12	23	0.0124	0.0966
22	13	23	0.0111	0.0865
23	14	16	0.0050	0.0389
24	15	16	0.0022	0.0173
25	15	21	0.0063	0.0490
26	15	21	0.0063	0.0490
27	15	24	0.0067	0.0519
28	16	17	0.0033	0.0259
29	16	19	0.0030	0.0231

Table 2.5 (continued)

30	17	18	0.0018	0.0144
31	17	22	0.0135	0.1053
32	18	21	0.0033	0.0259
33	18	21	0.0033	0.0259
34	19	20	0.0051	0.0396
35	19	20	0.0051	0.0396
36	20	23	0.0028	0.0216
37	20	23	0.0028	0.0216
38	21	22	0.0087	0.0678

Table 2.6: Bus data for the test system

Bus no.	Bus Type	Bus Voltage	Bus Angle	Real load (P)	Reactive load (Q)
1	0	1.03	0.00	1.08	0.22
2	2	1.03	0.00	0.97	0.20
3	1	0.00	0.00	1.80	0.37
4	1	0.00	0.00	0.74	0.15
5	1	0.00	0.00	0.71	0.14
6	1	0.00	0.00	1.36	0.28
7	2	1.02	0.00	1.25	0.25
1	1	0.00	0.00	1.71	0.35
9	1	0.00	0.00	1.75	0.36
10	1	0.00	0.00	1.5	0.40
11	1	0.00	0.00	0.00	0.00
12	1	0.00	0.00	0.00	0.00
13	2	1.03	0.00	2.65	0.54
14	1	0.00	0.00	1.94	0.39
15	2	1.03	0.00	3.17	0.64
16	2	1.03	0.00	1.00	0.2
17	1	0.00	0.00	0.00	0.00
18	2	1.02	0.00	3.33	0.68

Table 2.6 (continued)

Bus no.	Bus Type	Bus Voltage	Bus Angle	Real load (P)	Reactive load (Q)
19	1	0.00	0.00	1.81	0.37
20	1	0.00	0.00	1.28	0.26
21	2	1.03	0.00	0.00	0.00
22	2	1.03	0.00	0.00	0.00
23	2	1002	0.00	0.00	0.00
24	1	0.00	0.00	0.00	0.00

Table 2.7: Generation data for the test system

Bus no.	P_{Gmax}	Q_{Gmin}	Q_{Gmin}	V_{max}	V_{min}
1	1.92	1.20	-0.75	1.05	0.95
2	1.92	1.20	-0.75	1.05	0.95
7	3.00	2.70	0.00	1.05	0.95
13	5.91	3.60	0.00	1.05	0.95
15	2.15	1.65	-0.75	1.05	0.95
16	1.55	1.20	-0.75	1.05	0.95
18	4.00	3.00	-0.75	1.05	0.95
21	4.00	3.00	-0.75	1.05	0.95
22	3.00	1.45	-0.90	1.05	0.95
23	6.60	4.50	-0.75	1.05	0.95

With the bus data shown in Table 2.6, load flow studies have been performed using Newton-Raphson method. Detailed results of the load flow study are shown in Table A9 in Appendix A. From the load flow study, the total transmission loss is calculated as 51.3 MW and 422.3 KVAR. Using Equation (2.50) economic loading of generators is obtained which is shown in Table 2.8. With the optimum loading of generators as shown in Table 2.8, a load flow study shows that the total transmission loss is reduced to 36.4 MW and 271.7 MVAR. Details of this load flow study is shown in Table A10 in Appendix A.

Table 2.8: Economic loading of generators

Generator at Bus no.	Real power generation (p.u.)
1	4.018
2	0.483
7	1.007
13	5.327
15	1.439
16	2.797
18	3.904
21	3.813
22	0.451
23	4.006

Typical 24-hour load variation in the test system were considered which is shown in Tables A1-A8 in Appendix A. An extensive load flow studies have been performed and economical load dispatch were obtained using Equation (2.50). Market clearing price was used to find the cost of generation for every hour. Transmission loss was calculated using both Kron's loss formula and load flow studies for 24 hour load conditions and economical load dispatches were obtained. Figure 2.4 shows reduction in transmission loss due to economical load dispatches for 24 hour load conditions as obtained by Kron's loss formula and the load flow studies. It was assumed that the operator of the test system always use economical load dispatch for pool operation.

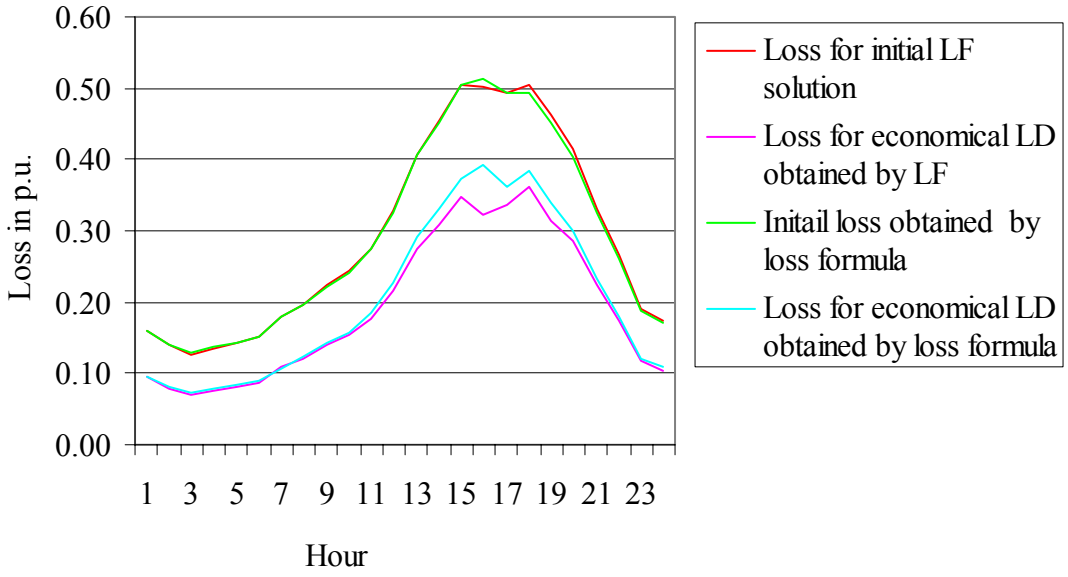

Fig. 2.4: Transmission loss for initial and economical load dispatch.

2.8 Summary

Transmission loss in electric power system has been discussed in this chapter. Load flow study and transmission loss calculations were illustrated with examples. Transmission loss expressions were derived. Economic power flow solutions were discussed. The IEEE 24-bus RTS network was utilized to illustrate economic power flow solution with various loading conditions.

CHAPTER 3: ARTIFICIAL NEURAL NETWORK

3.1 Introduction

Artificial neural networks, commonly referred to as "Neural Networks" are a different paradigm for computing. The motivation behind the development of neural network was right from the recognition that brain works in an entirely different way from the conventional digital computer. Although today's computers are very fast and gained tremendous speed in information processing, still they are well behind the capability of a biological brain. For example, the sonar echo location system, of a bat. In addition to providing information about how far a target (i.e. a flying insect) is, a bat's sonar system conveys information about the relative velocity of the target, the size and various features, the azimuth and elevation of the target. These complex neural computations needed to extract all these information from the target echo occur within a brain of the size of a palm. Indeed, an echo-locating bat can pursue and capture its target with a success rate that would be the envy of a radar or sonar engineer. To understand the functions of an artificial neural network, we need to know how human brain works.

3.2 Biological Neural Network

A brain is the central processing unit (CPU) of a biological neural network. The struggle to understand how a brain works, owes much to the pioneering work of Ramón Y Cajal, who first introduced the idea of neurons as structural constituents of a brain [18]. Human brain consists of 10 billion neurons. Figure 3.1 shows the structure of a brain neuron [19]. Neurons are wired up in a 3-dimensional pattern. There are about 60 trillion synapses or interconnections between them. Much is still unknown about how the brain trains itself to process information, so theories abound. In the human brain, a typical neuron collects signals from others through a host of fine structures called *dendrites*. The neuron sends out spikes of electrical activity through a long, thin stand

known as an *axon*, which splits into thousands of branches. At the end of each branch, a structure called a *synapse* converts the activity from the axon into electrical effects that inhibit or excite activity from the axon into electrical effects that inhibit or excite activity in the connected neurons. When a neuron receives excitatory input that is sufficiently large compared with its inhibitory input, it sends a spike of electrical activity down its axon. Learning occurs by changing the effectiveness of the synapses so that the influence of one neuron on another changes. During early stages of development, about one million synapses are formed per second.

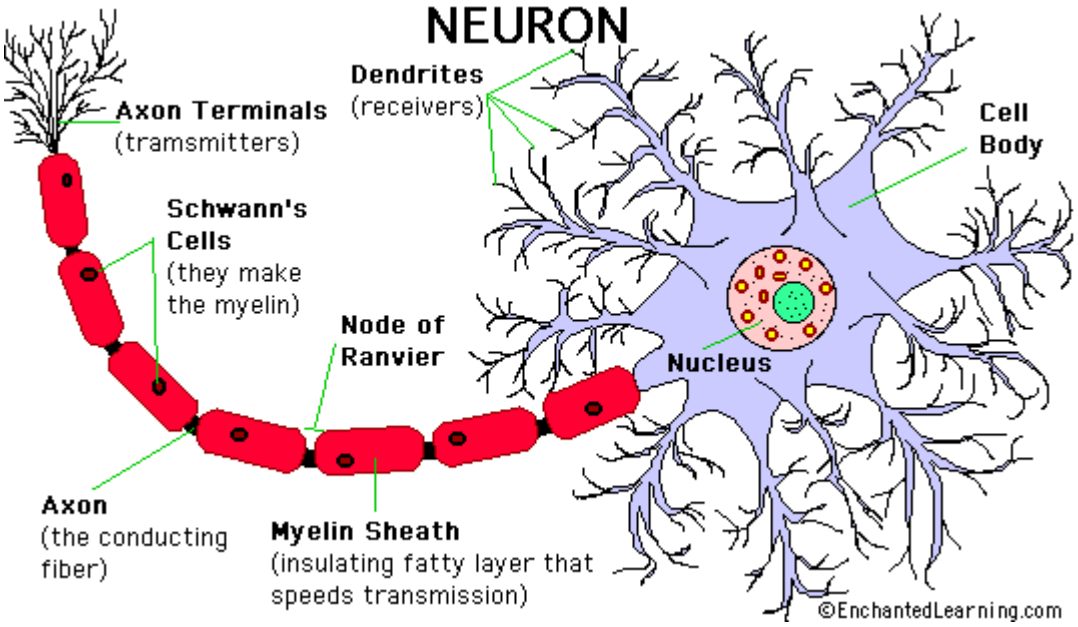

Fig. 3.1: Biological neuron [19].

A brain is a highly complex, nonlinear, and parallel computer. It has the capability of organizing neurons so as to perform certain computations (e.g. pattern recognition, perception, and motor control) many times faster than the fastest digital computer in existence today. Energetic efficiency of brain is also much better that any efficient computer. Brain takes only 10^{-16} joules per operation per second whereas the corresponding value for the best computers in use during 1994 was about 10^{-6} joules per operation [20]. A biological neuron may have as many as 10,000 different inputs, and may send its output to many other neurons [21]. It can learn from experience, and from the senses taken by any sensory organs. Real brains, however, many times more complex than any artificial neural network so far considered.

3.3 Mathematical Model of A Neuron

A nerve cell, which is the building block of human nervous system including brain, is called a neuron. In nature, the biological neurons are involved in various complex sensory, control and cognitive aspects of mathematical processing and in decision making processes. Similarly an artificial neural network consists of many identical neurons. Figure 3.2 shows mathematical model of a neuron [22].

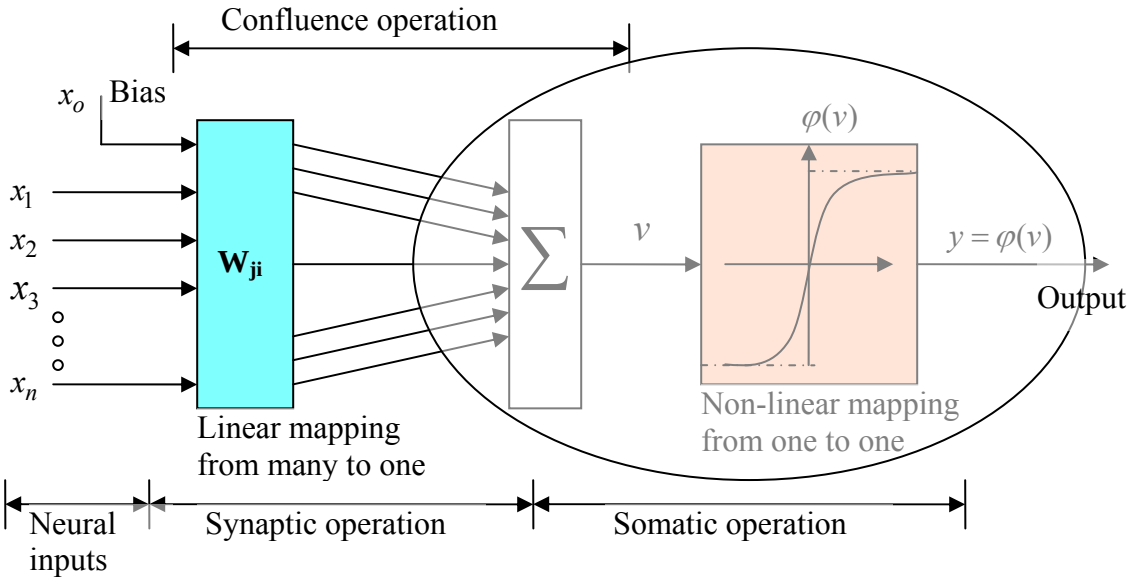

Fig.3.2: A mathematical model of a neuron

3.4 Evolution of Artificial Neural Networks

Neural network simulations appear to be a recent development. However, this field was established before the advent of computers. It started with the modeling the functions of a human brain by McCulloch and Pitts in 1943, who published a paper that describes the logical calculus of neural networks. The major development of neural networks came in 1949 with the publication of Hebb's book *The Organization of Behavior*, in which an explicit statement of a physiological learning rule for synaptic modification was presented for the first time. Hebb's book has been a source of inspiration for the development of computational models of *learning and adaptive system*. In 1954, Minsky wrote a thesis on "neural network" in his Ph.D study. In 1961, he wrote a paper on artificial intelligence entitled *Steps Towards Artificial Intelligence*. In 1954, Gabor,

the early pioneer of communication proposed the idea of *nonlinear adaptive filter*. He tried to build a machine, in which learning was accomplished by feeding samples of a stochastic process into the machine, together with the target function that the machine was expected to produce. In 1958, Rosenbatt proposed a new approach to pattern recognition problem. The crowning achievements of Rosenbatt's work was called perceptron convergence theorem. In 1960, Widrow and Hoff introduced least *mean-square algorithm* (LMS). One of the earliest trainable layered neural networks with multiple adaptive elements was the Madaline (multiple-adaline) structure proposed by Widrow (1962). In 1965, Nilsson's book, *Learning Machines*, was published, which is still the source for the best-written exposition of linearly separable patterns in hyper surfaces.

The major problem in early research on neural network was in part technological and in part financial. In absence of today's personal computer or workstations, neural network design and training had to be done on analog circuits. For example, Gabor developed his nonlinear filter, which took his research team further six years to build the filter with analog devices. There was not enough finance in early days to carry out research. However, in 1980s, with the development of personal computers, there was a resurgence of interests in neural networks.

In the 1980s, major contributions to the theory and design of neural networks were made on several fronts. Grossberg (1980) established a new principle of self-organization that combines bottom-up adaptive filtering and contrast enhancement in short-term memory with top-down template matching and stabilization of code of learning. Given such capability, if the input pattern and learned feedback match, a dynamic state called *adaptive resonance* takes place. This phenomenon provides the basis of new class of neural networks known as *adaptive resonance theory* (ART). In 1982, Hopefield used the idea of energy function to formulate a new way of understanding the computation performed by recurrent networks with symmetric synaptic connections. He developed a new class of neural network with feedback, which is well known as *Hopefield Networks*. Another important development in 1982 was made by Kohonen. He developed a self-organizing map using one or two lattice structure. In 1983, Kirpatrick, Gallat and Vecchi described a new procedure called

simulated annealing, for solving combinational optimization problem. In 1985, Hinton and Sejnowski developed a learning algorithm called Boltzmann learning which uses Boltzmann distribution.

In 1986, Rumelhart, Hinton and Williams developed a learning algorithm called *Back Propagation Algorithm.* Their publications "*Parallel Distributed Processing*" & "*Explorations in the Microstructures of Cognition*" had been a major influence in the use of back-propagation learning, which had emerged as the most popular learning algorithm for the training of multilayer perceptron. Later, back-propagation algorithm was modified by many researchers to increase the speed of training. Broomhead and Lowe, in 1988, described a procedure for the designing of layered feed forward networks using radial basis functions, which provides an alternative to multilayer perceptrons.

Neural networks have certainly come a long way from the early days of McCulloch and Pitts. The 1982 paper by Hopefield and the two volume book by Rumelhart and McLelland were the most influential publications responsible for the resurgence of interest in neural network in the 1980s. Today, neural networks have established themselves as an interdisciplinary subject with deep roots in neuroscience, psychology, mathematics, physical science and engineering. Today, neural networks have been successfully used to solve many complicated real world problem. Current resurgence of interest in neural network will keep them growing in theory and applications.

3.5 Architecture of Neural Networks

There are wide variety of neural networks and their architectures. Types of neural networks range from simple Boolean networks (perceptions) to complex self-organizing networks (Kohonen networks). There are also many other types of networks like Hopefield networks, Pulse networks, Radial-Basis Function networks, Boltzmann machine. Although architecture of neural networks cannot be bound by definite set rules, there are some standard network architectures as described below.

3.5.1 Single-Layer feedforward networks: It is the simplest type of network which consists of an input layer of source nodes that projects directly onto neurons of output

layer. There is no hidden layer in this architecture. It is strictly of feedforward type, as there is no feedback from output layer. Figure 3.3 shows a Single-Layer Feedforward network.

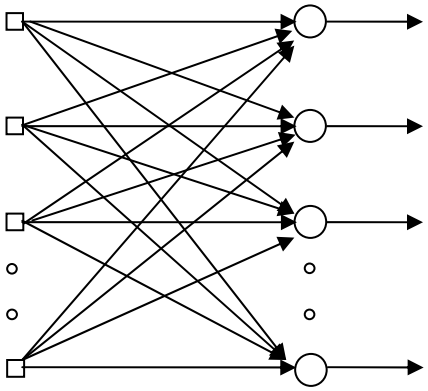

Fig.3.3: Single-layer feedforward network

3.5.2 Multilayer feedforward networks: A multilayer feedforward network, often known as Multilayer Perceptron (MLP) distinguishes itself by the presence of one or more hidden layers. Hidden neurons in hidden layers intervene between external input and the network outputs. The addition of hidden layers in MLP increases its capability of extracting higher-order statistics. This feature of MLP increases its capability to deal with high degree on non-linearity and complex situations. MLPs can be fully connected or partially connected. In fully connected multilayer feedforward networks, every neuron in each layer is connected to every other neuron in the adjacent forward layer. Figure 3.4 shows a fully connected multilayer feedforward network. If some synaptic connections between the neurons are missing, the network is termed as partially connected feedforward network. Figure 3.5 shows a partially connected feedforward network.

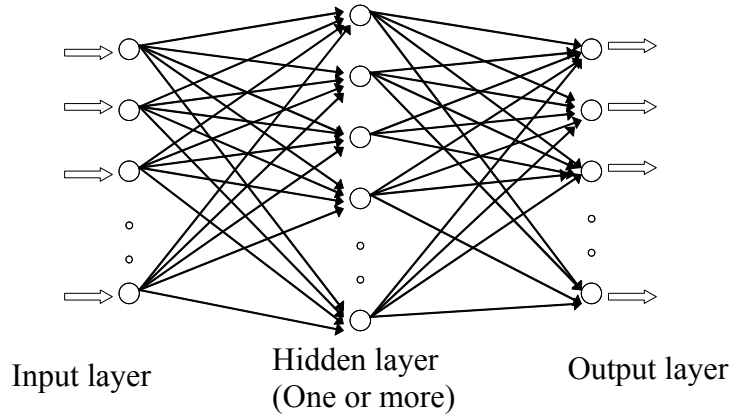

Fig 3.4: Fully connected network

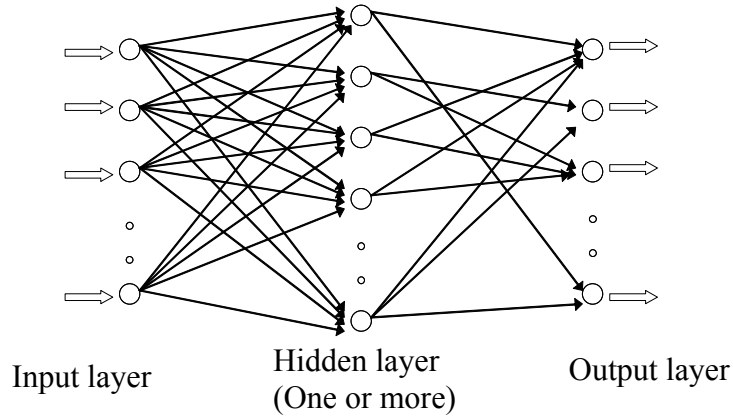

Fig 3.5: Partially connected feedforward network

3.5.3 Recurrent networks: Unlike a feedforward network, in a recurrent network there must be at least one feedback loop. One or more outputs of output layer are fed back to the input or hidden layer. It can be made up of any number of layers. If any output is fed back to its own input, the network is termed as recurrent network with self-feedback. The feedback loops involve the use of unit delay elements, which results in non-linear dynamic behavior. Unit delay elements are denoted by z^{-1}. The presence of feed back loops in recurrent network has profound impact in learning and performance. Figure 3.6 shows a recurrent network.

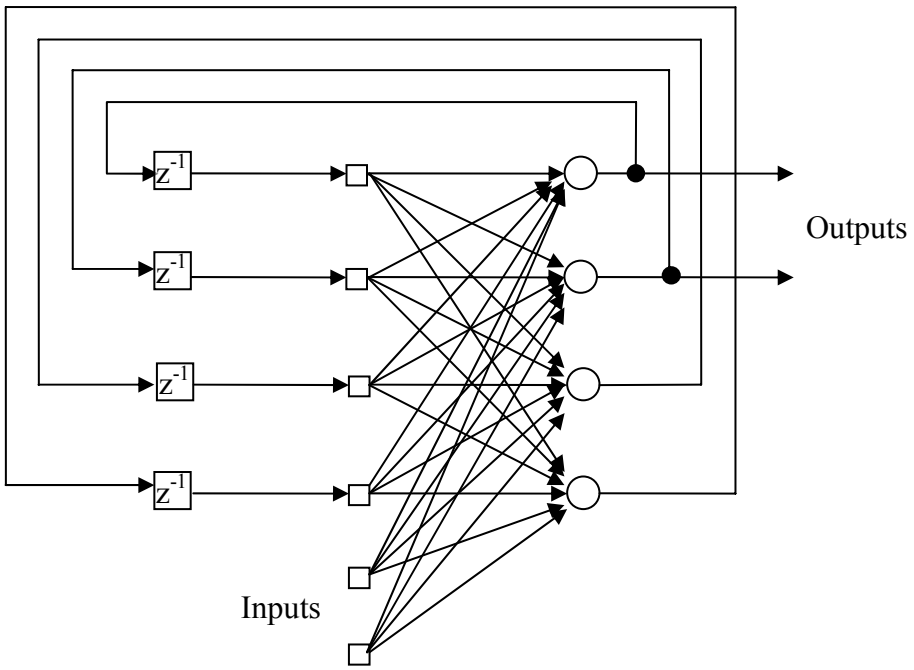

Fig 3.6: Recurrent network with hidden neurons

3.5.4 Lattice Structures: A lattice structure is different from other types of architecture of neural networks by its arrangements of neurons and their connections. It consists of a one-dimensional, two-dimensional or higher-dimensional array of neurons with corresponding set of source nodes that supply the input signals to the array. Figure 3.7 depicts a two-dimensional lattice of 3-by-3 neurons fed from an input layer of three source nodes. It is similar to feedforward network with the output neurons arranged in rows and columns.

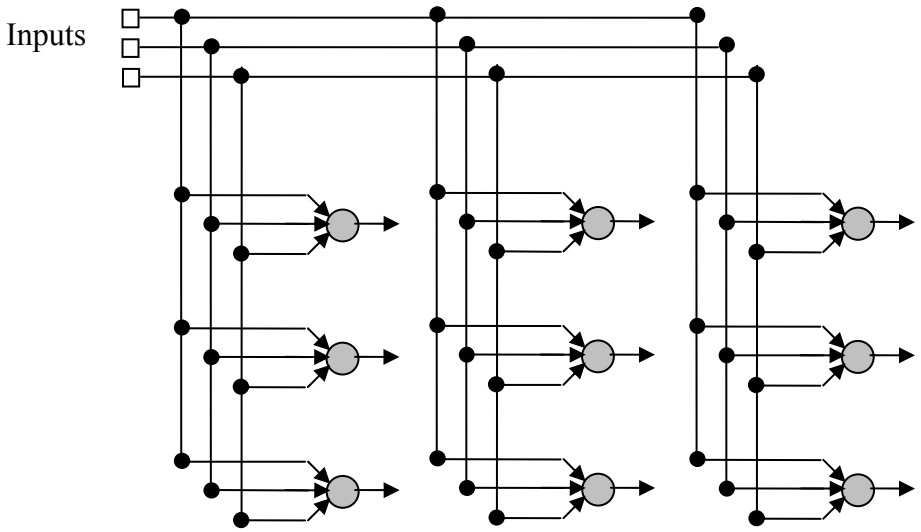

Fig.3.7: Two-dimensional lattice structure of 3-by-3 neurons

3.6 Learning of Artificial Neural Networks

The most significant property of a neural network is that it can learn from environment, and can improve its performance through learning. Learning is a process by which the free parameters of a neural network i.e. synaptic weights and thresholds are adapted through a continuous process of stimulation by the environment in which the network is embedded. The network becomes more knowledgeable about environment after each iteration of learning process. There are three types of learning paradigms namely, supervised learning, reinforced learning and self-organized or unsupervised learning. In supervised learning, an external teacher, having the knowledge of the environment, represents a set of input-output examples for the neural network which may not have any prior knowledge about that environment. When the teacher and the neural network are both exposed to a training vector drawn from environment, by virtue of built-in knowledge, the teacher is able to provide the neural network with a desired response for that training vector. The network adjusts its weights and thresholds until the actual response of the network is very close to the desired response. Figure 3.8 shows a diagram of supervised learning.

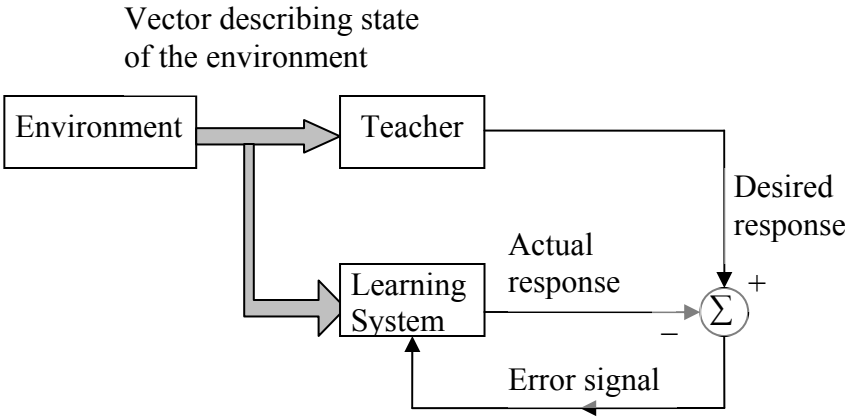

Fig.3.8: Block diagram of supervised learning

Reinforcement learning system consists of three elements: learning element, knowledge base and performance element. A critic is used instead of a teacher, which produces heuristic reinforce signal for the learning element. State input vector goes to critic, learning element and performance element at the same time. With the state vector and primary reinforce signal from the environment as inputs, the critic (predictor) estimates the evaluation function. By virtue of inputs received from the environment and the knowledge base, the performance element determines the input-output mapping. Figure 3.9 shows the block diagram of reinforcement learning.

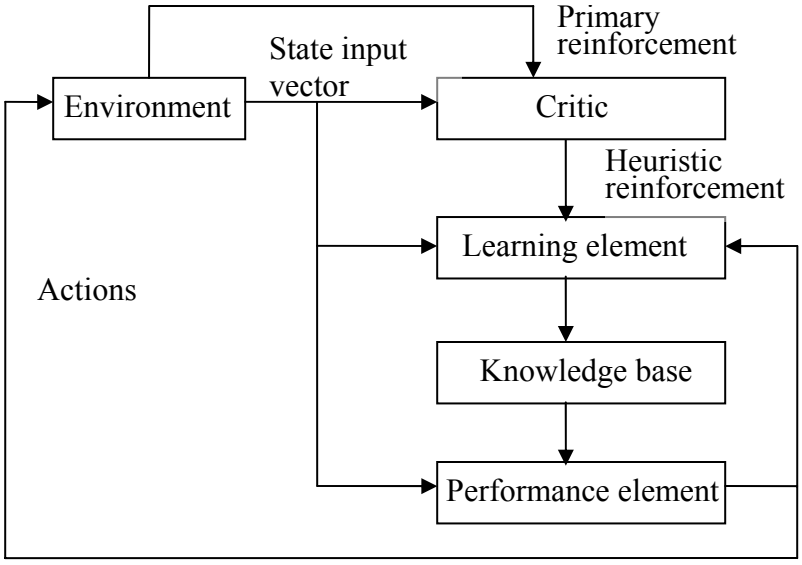

Fig.3.9: Block diagram of reinforcement learning system

In unsupervised or self-organized learning there is no external teacher or critic to oversee the learning process. The network representation and free parameters are optimized to become tuned to statistical regularities of the input data to develop the ability to form internal representation for encoding input data and thereby gather knowledge about the environment.

There are many different kinds of learning algorithm for example, error correction learning, Boltzmann learning, Thorndike's law of effect, Hebbian learning and competitive learning. In competitive learning the outputs of a neural network compete among themselves for being the one to be active whereas in Hebbian learning several output neurons may be active at the same time. Some other learning algorithms are: back propagation algorithm, conjugate gradient descent, Quasi-Newton, Levenberg-Marquardt, quick propagation, Delta-bar-Delta, and Kohonen training. Back propagation algorithm is the mostly used algorithm for feedforward neural network. It is a supervised learning algorithm which requires a set of training data with known input and output vector. It uses steepest gradient descent of error which propagates backwards for updating the synaptic weights and thresholds. The advantage of this algorithm is the simplicity of calculation during weight updates. Although widely used, the back propagation algorithm suffers from slow rate of convergence and hence requires long training time for large network with large number of training patterns. However, some methods have been developed to overcome the slow rate of learning, for example, optimization of initial weights [23], adaptation of learning rate using delta-bar-delta learning rule [24], use of multiple activation functions [25]. Also adding a momentum factor, it can learn faster and can overcome local minima [26].

Conjugate gradient descent works by constructing a series of line searches across the error surface. It first works out the direction of steepest descent, just as back propagation would do. However, instead of taking a step proportional to a learning rate, conjugate gradient descent projects a straight line in that direction and then locates a minimum along this line, a process that is quite fast as it only involves searching in one dimension. Subsequently, further line searches are conducted. The directions of the line searches (the conjugate directions) are chosen to try to ensure that the directions that

have already been minimized stay minimized. Quasi-Newton is the most popular algorithm in nonlinear optimization, with a reputation for fast convergence. It works by exploiting the observation that, on a quadratic error surface, one can step directly to the minimum using the Newton step - a calculation involving the Hessian matrix. Main draw backs of this algorithm is that the Hessian matrix is difficult and expensive to calculate and Newton step would be wrong if the error surface is non-quadratic. It requires a huge memory and therefore it is not advised to use it for large networks.

3.7. Working Principles of Artificial Neural Networks

Artificial neural network solutions are very attractive due to their simplicity and relative speed. Although an ANN can solve highly non-linear complex problem, its working principle is very simple. Working process of a fully connected multilayer feedforward network, shown Figure 3.10, is described here.

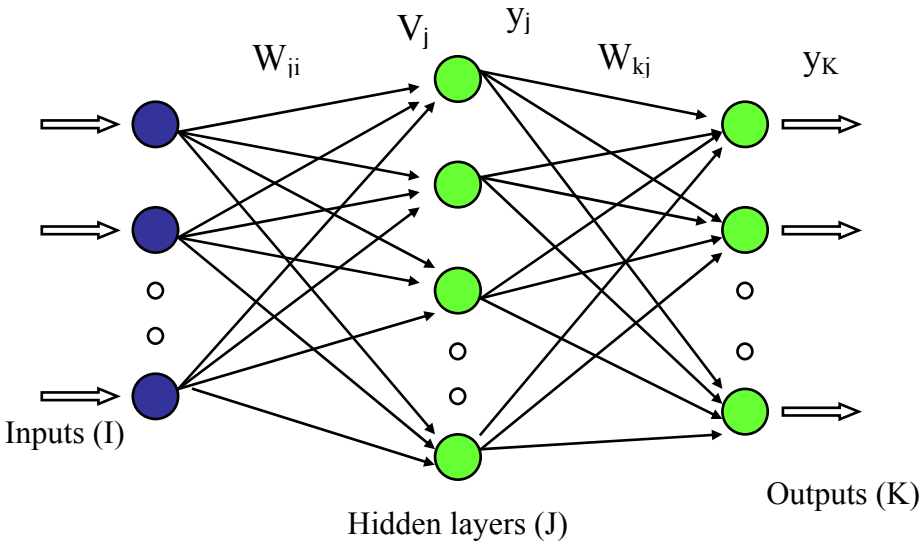

Fig.3.10: A multilayer feedforward neural network

The input layer is connected to an adjacent layer, typically known as a hidden layer, by some synaptic weights. Input neurons are activated by external input signals and these signals passes through the synaptic weights to the next layer. While passing through the synaptic weights, input signals are multiplied by the corresponding weights (W_{ji}). All

signals that reach a neuron of a hidden layer are summed, described by the Equation (3.1), and converted to the output of that neuron by some activation functions.

$$v_j(n) = \sum_{i=1}^{n} w_{ji}(n) y_i(n) \quad \ldots \quad \ldots \quad \ldots \quad \ldots \quad (3.1)$$

Various transfer functions such as sigmoid, Gaussian, hyperbolic tangent, hyperbolic secant etc. are used as activation functions in neural networks. Sigmoid functions are very popular among them. A typical sigmoid function is described by Equation (3.2) and shown in Figure 3.11.

$$y_j = \frac{1}{1 + e^{-vj + vj0}} \quad \ldots \quad \ldots \quad \ldots \quad \ldots \quad (3.2)$$

where v_{j0} is a threshold value, which is independent of input signal.

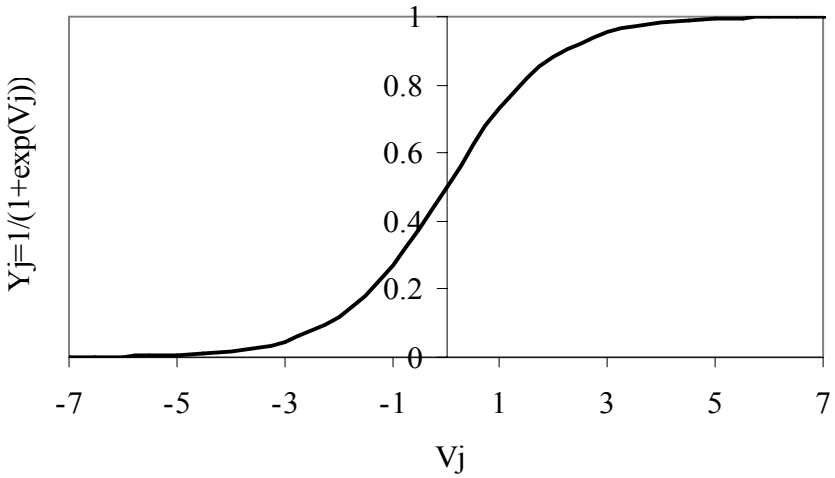

Fig.3.11. Sigmoidal transfer function

Another widely used activation function is hyperbolic tangent function which is described by Equation (3.3) and shown in Figure 3.12. Outputs of a hidden layer pass to the next hidden layer or output layer in a similar way. The method is very fast in speed because of the fact that all inputs activate the input neurons at the same time (in parallel) and signal passes to the output layer with some manipulations by weights and activation functions, and output is obtained in one pass of the signals. Therefore, whatever complex relation exist between input and output, however large the network is, a trained neural network can give output in fractions of a second.

$$y_j(n) = a \tanh(b * v_j(n)) \quad \ldots \quad \ldots \quad \ldots \quad \ldots \quad (3.3)$$

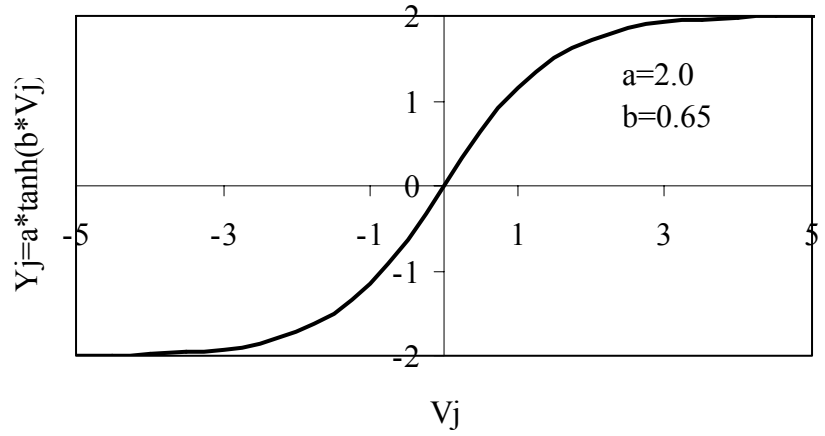

Fig.3.12. Hyperbolic tangent function

3.8 Testing of Artificial Neural Networks

After design and training of an artificial neural network to solve a particular problem, the network should be tested to check its performance. To do this job, test patterns i.e. an input vector describing all possible situation of the environment is created and the teacher (conventional method) calculates the corresponding output vector. This input vector is utilized to obtain corresponding output vector using the trained neural network, and the output vector is compared with the actual output vector created by the teacher. For a properly designed and trained neural network the error i.e. the difference between these two output vectors will be smaller than the tolerance. The smaller the error, the better the performance.

3.9 Applications

Although research on artificial neural networks had started in early 1900s, the development and application were very limited before the advent of personal computers. Remarkable development and application of neural networks were made in last two decades. Today, artificial neural networks have been used in a wide variety of real world problems. Many complex problems that require time consuming computations have been solved by artificial neural networks in a simpler and faster way. Neural networks proved to have promising application in image processing, for example, identifying hand-written characters; matching a photograph of a person's face

with a different photo in a database; performing data compression on an image with minimal loss of content. Other applications are: voice recognition; language translation, RADAR signature analysis; stock market prediction, weather forecasting, electrical load forecasting, process modeling and control, machine diagnostics, portfolio management, target recognition, medical diagnosis, credit rating, targeted marketing, financial forecasting, quality control, intelligent searching, fraud detection. All of these problems involve large amounts of data, and complex relationships between the different parameters. Now a days, it has been used in control systems, protection systems and in many military applications. Neuro-fuzzy network proved to be promising in its use in control systems and robotic applications. People are trying to build artificial intelligence with the capacity of a human brain using neural networks. Another promising use of neural networks can be assisting doctors with their diagnosis by analyzing reported symptoms, test data, image data such as MRI, X-rays. The goal of this research is to develop a neural network as a tool to allocate transmission loss in a deregulated power system.

CHAPTER 4: ARTIFICIAL NEURAL NETWORK BASED TRANSMISSION LOSS ALLOCATION

4.1 Introduction

After the introduction of deregulation in electric power industry in early 90s, many power systems in the world started moving from century old vertically integrated regulated monopoly business to open access competitive market. The present era can be called a transition period for power system deregulation. In a deregulated power system it is necessary to assess transmission loss originating from individual transactions. Many energy users sign bilateral contacts with energy suppliers to avoid price fluctuations of an open market. In this circumstance, transmission loss has to be allocated to each bilateral transaction. In many cases power producers form an energy pool to run their operation as a single entity. In a pool operation, loss is shared by all participating suppliers according to a previously agreed rule or algorithm. In some pool systems both suppliers and consumers share loss. In this chapter the loss allocation for bilateral contract will be discussed. Many techniques have been reported in the literature and mentioned in Chapter 1 that can assess transmission loss allocation for bilateral contracts. Most of these loss allocation procedures involves complex mathematical expressions and requires time consuming computations. Incremental Load Flow Approach (ILFA) has almost all the desired properties of loss allocation but it requires time consuming computations which increase with an increase in system size. Artificial neural networks (ANN) have been developed and utilized in this research to allocate transmission loss to individual transactions. The ILFA has been used as an external teacher to create a set of input and output vector for loss allocation. An ANN has been designed and trained with those input and output vectors, and it was observed that it can produce results similar to those produced by the ILFA.

4.2 Incremental Load Flow Approach (ILFA)

Incremental load flow approach (ILFA) uses conventional load flow study repeatedly. In the ILFA, a load flow program is run from load level zero to their given level for each load under a bilateral contract in a sequential manner. Loads are incremented by a small value in each iteration. Each generator is assumed to have a fixed consumer or load in the system and supposed to produce the power to meet the load demand of its customer and the associated loss. When a certain load is increased by a pre-specified increment, the increment in total transmission loss is calculated by load flow study and, the corresponding increase in transmission loss is assigned to the generator that is in contract with this particular consumer. When two bilateral contracts are considered, the load for each contract is incremented in an alternate manner and the corresponding loss is calculated and assigned to respective generator. For multiple contracts, the load of each contract is incremented in a sequential manner.

4.2.1 Example System

A small hypothetical system has been considered in this section for the purpose of numerical examples related to the allocation of transmission loss.

The hypothetical system consists of six buses with three generators, two loads under normal pool operation and two contracted loads. The load under normal pool operation will be termed as ‘base load’ hereafter. Figure 4.1 shows the diagram of the example system. Generators A, B, and C are connected to Bus 1, Bus 4 and Bus 3 respectively. Base loads are connected to Bus 2 and Bus 5. Two contracted loads, Load A and Load B are connected to Bus 5 and Bus 6 respectively. Contract A exists between Generator A and Load A and Contract B exists between Generator B and Load B. The details of base and contracted loads are shown in Table 4.1 and the generation capacity of each generator is shown in Table 4.2.

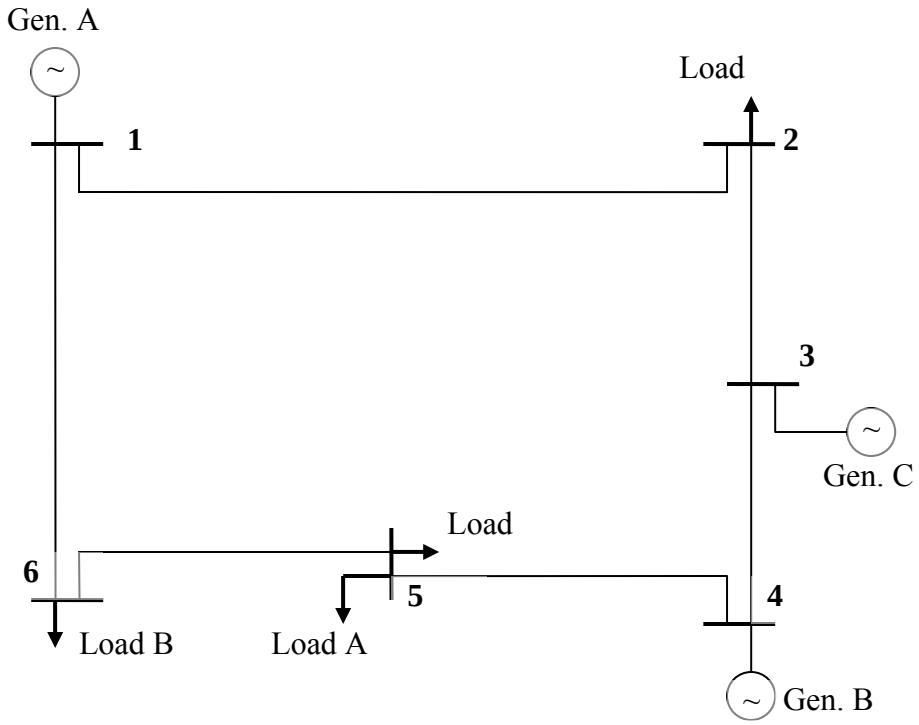

Fig.4.1: Six bus test system with two bilateral contracts

Table 4.1: Load for test system

Load Type	Bus	Real Load (MW)	Reactive load (MVAR)
System	2	110	70
	5	120	60
Contract	5	80	35
	6	100	50

Table 4.2: Generation Capacity of the system

Generator	P_{min}(MW)	P_{max}(MW)
A	60	270
B	70	220
C	40	150

It should be noted that besides the contracted loads, Generator A and Generator B produce energy for pool operation as well. The assumed share of Generator A & B for base load is shown in Table 4.3. Line parameters for the example system are shown in Table 4.4.

Table 4.3: Share of generation for base load

Generator	Real power generation (MW)	Reactive power generation (MVAR)
A	70	40
B	80	35
C	Remaining load plus losses	

Table 4.4: Line data

From Bus	To Bus	R(ohm)	X(ohm)
1	2	2.0	10
1	6	3.0	11
2	3	0.5	4
2	5	2.0	8
3	4	0.5	3
4	5	2.0	8
5	6	1.5	6

The contracted generators are bound to supply their contracted loads and the corresponding share of transmission loss. The unknown at this point is the share of loss that an individual generator is responsible for. First, the generation and transmission loss will be determined by load flow analysis for the base case. The bilateral contracts are then imposed using the ILFA on top of the base load conditions. The contracted generators will be responsible for the incremental transmission loss.

4.3 Loss Allocation Using the ILFA

In order to allocate transmission loss to a generator involved in a bilateral contract, total loss for pool operation with base load has been assessed using conventional load flow analysis. The base parameters are 200 MVA and 138 KV. Voltage magnitude of voltage control buses are: 1.02, 1.01 & 1.01 for Bus 1, 3 & 4 respectively. For the data shown in Tables 4.1 to 4.4, load flow solution for normal pool operation is as follows:

Load Flow solution for system without contract is:

Bus	Bus-	Voltage	Angle	------ Generation ----		------ Load --------	
no.	type	Mag.	degree	MW	MAVR	MW	MVAR
1	2	1.0200	-0.1085	70.000	54.619	0.000	0.000
2	0	1.0002	-1.0405	0.000	0.000	110.000	50.000
3	1	1.0100	0.0000	81.486	38.088	0.000	0.000
4	2	1.0100	0.0946	80.000	24.410	0.000	0.000
5	0	0.9922	-1.4202	0.000	0.000	120.000	60.000
6	0	1.0018	-0.9430	0.000	0.000	0.000	0.000

Total MW Generation = 231.4858

Total MVAR generation = 117.1158

Total real load MW = 230.0000

Total reactive load MVAR = 110.0000

Total real loss MW = 1.4858

Total reactive loss MVAR = 7.1158

When the contracted loads are added to the system the corresponding load flow solution shows that the total real loss is 6.0914 MW and the total reactive loss is 26.1049 MVAR. The additional real loss of 4.6056 MW and reactive loss of 18.9891 MVAR have to be allotted to the contracted Generators A & B. To do this an incremental amount of contracted load for Contract A (or B) is first added to the system and transmission loss is calculated using load flow technique. From the load flow solutions, incremental loss is calculated and assigned to the corresponding generator. Then the load for Contract B (or A) is increased by an incremental amount and the incremental loss is assigned to that generator. In this way the total contracted loads are applied and

the shares of loss are calculated. A problem appears at this stage is how to select a swing bus in a load flow study. It was shown in reference [2] that loss allocation varies depending on the selection of a swing bus.

To resolve the issue of swing bus each contracted generator bus has been utilized as a swing bus in an alternate manner. When Load A is increased, the bus connecting Generator A is used as a swing bus. Similarly, the bus connected to Generator B is used as a swing bus when Load B is increased. Table 4.5 shows loss allocation using the alternate swing bus concept.

Table 4.5: Loss allocation using alternate swing bus

	Contracted Load A (MW /MVAR)	Contracted Load B (MW /MVAR)	Share of Generator A (MW / MVAR)	Share of Generator B (MW/MVAR)	Additional Loss for contracts (MW /MVAR)
Real	80	100	2.1300	2.4756	4.6056
Reactive	35	50	8.3952	10.5938	18.9890

4.4 Test System

The 24-bus IEEE RTS have been utilized as a test system in this chapter. It has been assumed that two bilateral transactions take place in the system. The transactions are governed by two contracts: Contract A and Contract B. Location of contracted loads and generators are shown in Figure 4.2. Contract A exists between Generator A at Bus 7 and Load A at Bus 9. Contract B exists between Load B at Bus 19 and Generator B at Bus 23. The line parameters of the test system are shown in Table 2.5 and the bus data for the peak hour is shown in Table 2.6.

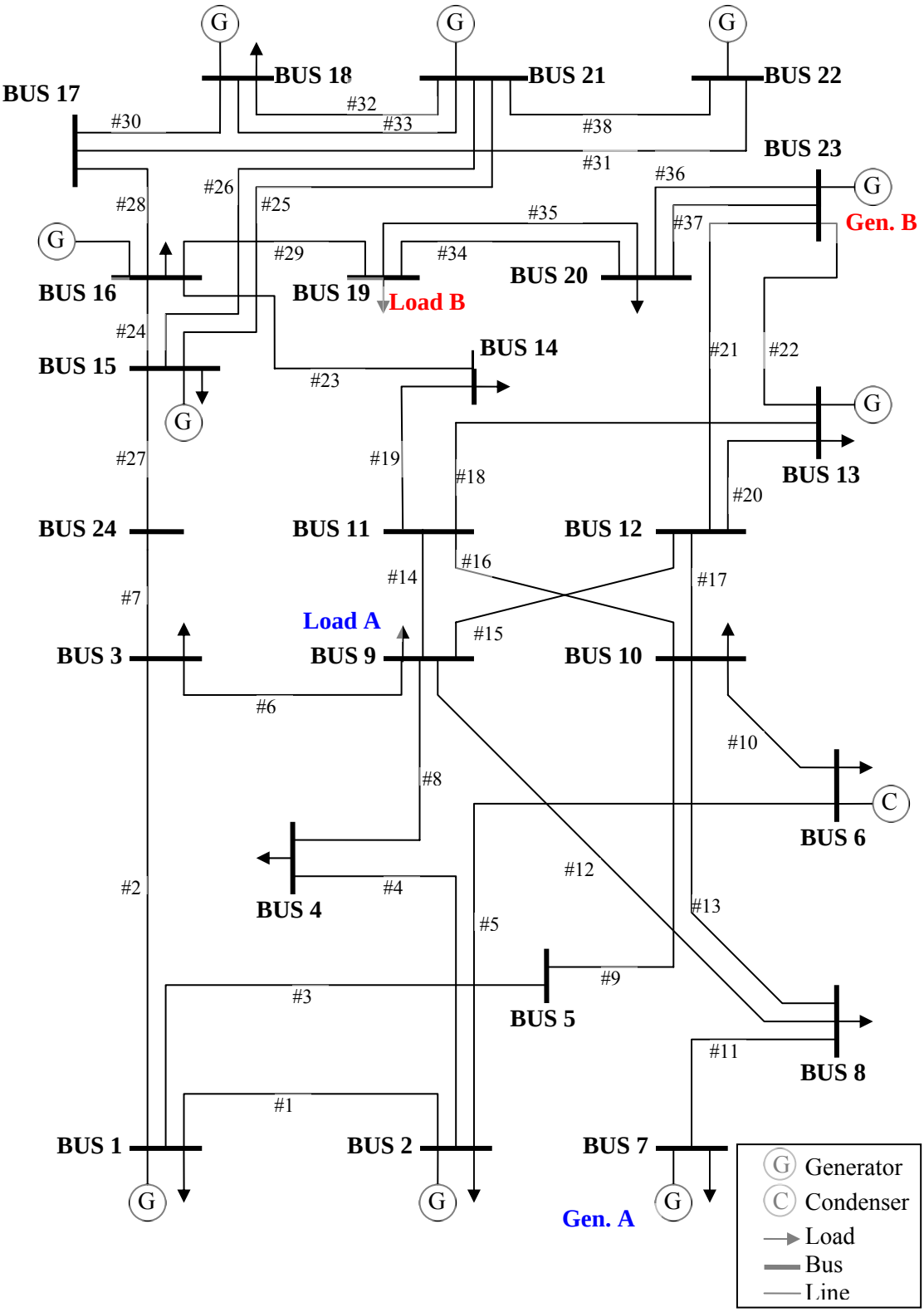

Fig. 4.2: The IEEE 24-bus RTS with two bilateral contracts.

In this study, the IEEE 24-bus test system was slightly modified by moving the synchronous condenser from Bus 14 to Bus 6. This modification was necessary to increase the voltage stability during bilateral transactions. Load flow study showed that voltage at Bus 6 goes below tolerance limit (± 5%) for a small load of Contract A. With the addition of a synchronous condenser at Bus 6, it was possible to increase the contracted load up to 185 MW while maintaining the voltage stability. Loss allocation was studied at various loading conditions. The system has a peak load of 2494 MW. The load profile of California ISO [10] was utilized to produce 24-hour loads during the weekdays and weekends. Figure 4.3 and Figure 4.4 show the 24-hour real and reactive loads at various buses for a weekday. Fig. 4.5 shows the corresponding generation at various generation buses. 24 hour real and reactive loads of the system for weekdays and weekends are shown in Table A1 to Table A8 in Appendix A.

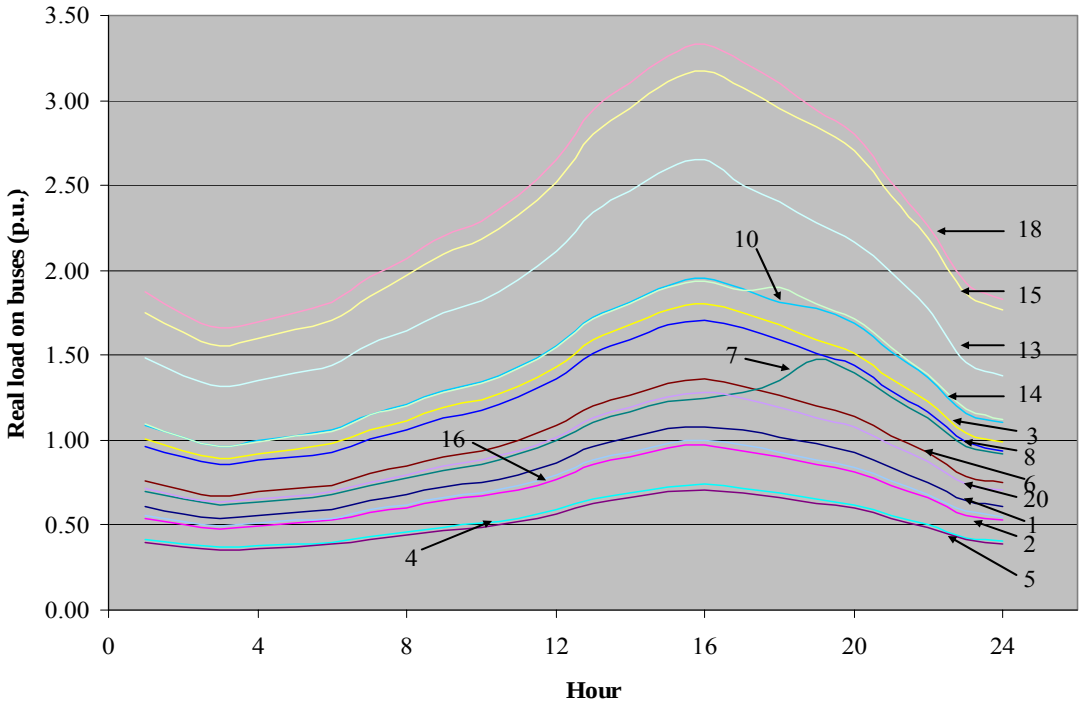

Fig. 4.3: 24 hour real load at various buses on weekdays

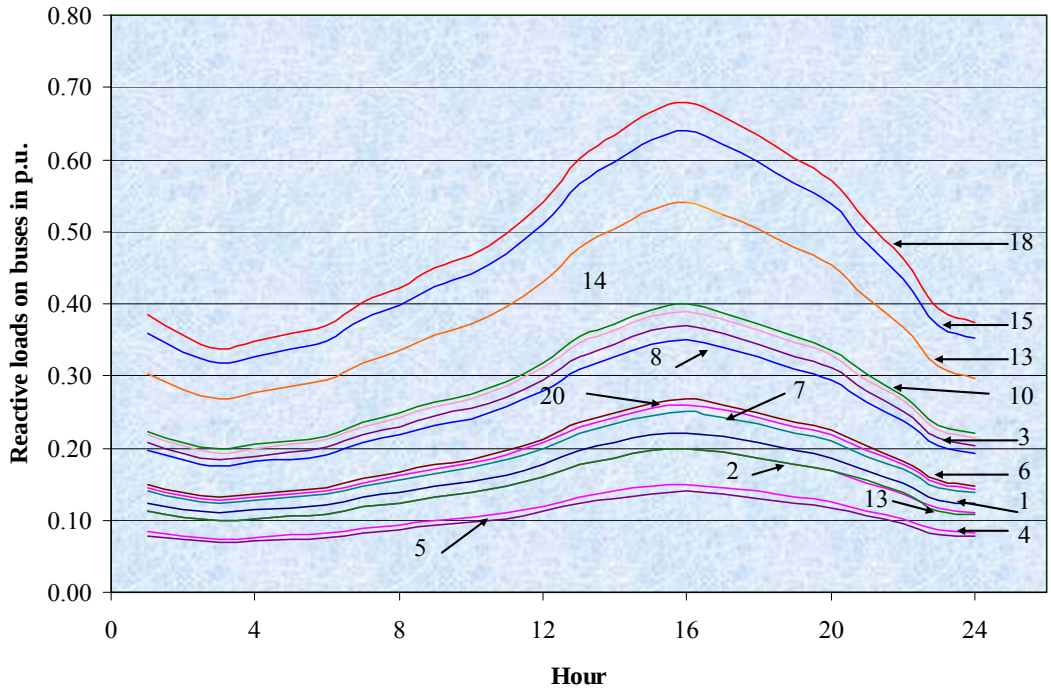

Fig. 4.4: 24 hour reactive load at various buses on weekdays

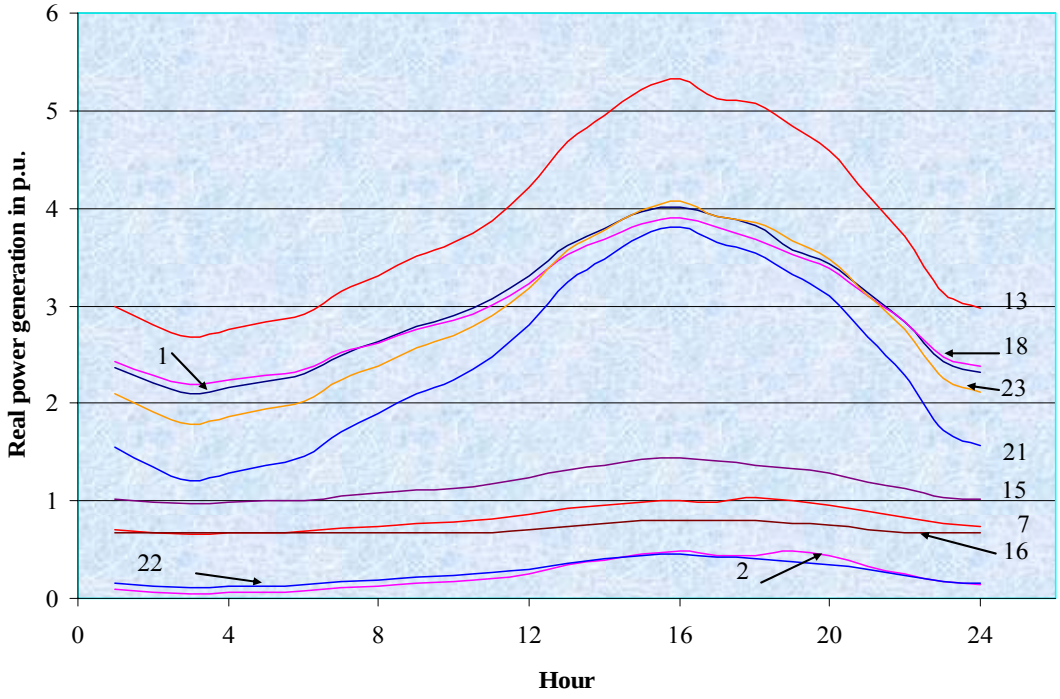

Fig.4.5: 24 hour real power generation at various buses on weekdays

4.5 Proposed Neural Network

Many types of neural networks had been developed so far for various purposes. Some of these neural networks have been described in Chapter 3. All artificial neural networks are based on the concept of neurons, connections and transfer functions, and there is a similarity between the different structures or architectures or neural networks. There is no limitation for their applications but some of them showed better performance in specific applications. Basically, most applications of neural networks fall into five categories: prediction/ estimation, classification, data association, data conceptualization and data filtering. Feedforward and Self-organizing Back Propagation networks are suitable for estimation or prediction, Learning Vector Quantization and Probabilistic Neural networks for classification, Hopfield and Boltzmann Machine for data association, Self-organizing Map for data conceptualization and Recurring networks for data filtering [27]. Feed Forward Multilayer Neural networks are the most popular among all types of networks due to their effectiveness and ease of learning using back propagation algorithm. One of the significant advantages of a feed forward multilayer neural network is its ability to provide solutions for highly non-linear systems and also for systems with ill-defined problems. Transmission loss is a non-linear function of system parameters and states. Due to this non-linearity a multilayer feed forward neural network structure has been utilized in this research.

A multilayer feedforward neural network has been developed for loss allocation for the bilateral contracts. Inputs and outputs of the network were selected carefully so that the proposed network represents all possible practical situations in a power system network. Most independent system variables have been used as inputs to this neural network which in turn makes the loss allocation process responsive to practical situations. There are four outputs of the network which are real loss and reactive loss for contracts A and B. The inputs and outputs of the network are described in Table 4.6.

Table:4.6: Description of inputs and outputs of ANN

Layer	Neurons	Description
Inputs	I_1-I_2	Real load for Contracts A & B (p.u.)
	I_3-I_4	Reactive load for contracts A & B (p.u.)
	I_5-I_{19}	Real loads on buses (p.u.)
	I_{20}-I_{34}	Reactive loads on buses (p.u.)
	I_{35}-I_{44}	Generations on buses (p.u.)
	I_{45}-I_{54}	Bus voltages (p.u.)
Output	O_1-O_2	Real loss for Contracts A & B (p.u.) respectively
	O_3-O_4	Reactive loss for contracts A & B (p.u.) respectively

To find the most suitable architecture for loss allocation, number of hidden layers and number of neurons in the hidden layers have to be optimized. For a single hidden layer, the number of hidden neurons was varied from 10 to 55 and convergence characteristics and performance for various test patterns were observed. To speed up learning, some measures were taken which have been described in the following section. After adapting all speed enhancement techniques, the number of hidden layers and the number of neurons were selected based on convergence criteria and performance. These aspects have been described in Section 4.8.

4.6 Learning

The most significant property of an artificial neural network is that it can learn from experience and becomes knowledgeable about the environment. Among all the learning algorithms, back propagation learning, more precisely described as the steepest gradient descent learning using back propagation of error is widely used in the learning of ANNs. The advantage of this algorithm is its simplicity of calculation for updating weights and thresholds. Hence, in this research back propagation algorithm has been utilized to train the proposed ANN. It is a supervised learning algorithm which requires

an external teacher which generates the desired output for the ANN. The ILFA has been used as a teacher to generate an output vector corresponding to an input vector, and these two vectors together termed as 'training patterns' have been used by the back propagation algorithm to train the proposed ANN. The input vector and the number of training patterns have been carefully selected so that they represent almost all possible states of the environment.

In classical pattern recognition, the number of training patterns should be 3-5 times higher than the number of features (inputs) used [27]. According to Lippmann [28], this number should be at least several times larger than the ratio of the number of synaptic weights in the network to the number of outputs.

According to the first suggestion, minimum number of training patterns required for an effective training of the network is 270 (54 x 5) using the upper bound. Referring to the second suggestion, this number would be greater than the previous one. With 54 inputs, 29 hidden neurons and 4 outputs, training patterns should be few times larger than 797.5 {(54*55+55*4)/4}. If we consider a multiplication of 3 times, the number becomes 2392. Although the higher the training samples the better knowledge and performance of the network, the performance of the network will tend to saturate as the number is increased beyond certain value and at the same time it will take more time to learn. However, we have selected 2600 training patterns, a number greater than both suggestions so that the trained ANN can give better performance with the test patterns.

4.6.1 Derivation of weight update formula

During learning (training), the free parameters of an ANN e.g. synaptic weights and thresholds are adjusted so that actual outputs of the network become closer to the desired outputs for the given training patterns. In a back propagation algorithm, the error (difference between actual output of the network and desired output) is propagated backwards to update the weights. To derive the weight update formula, let us consider the signal flows in the neural network shown in Figure 4.6.

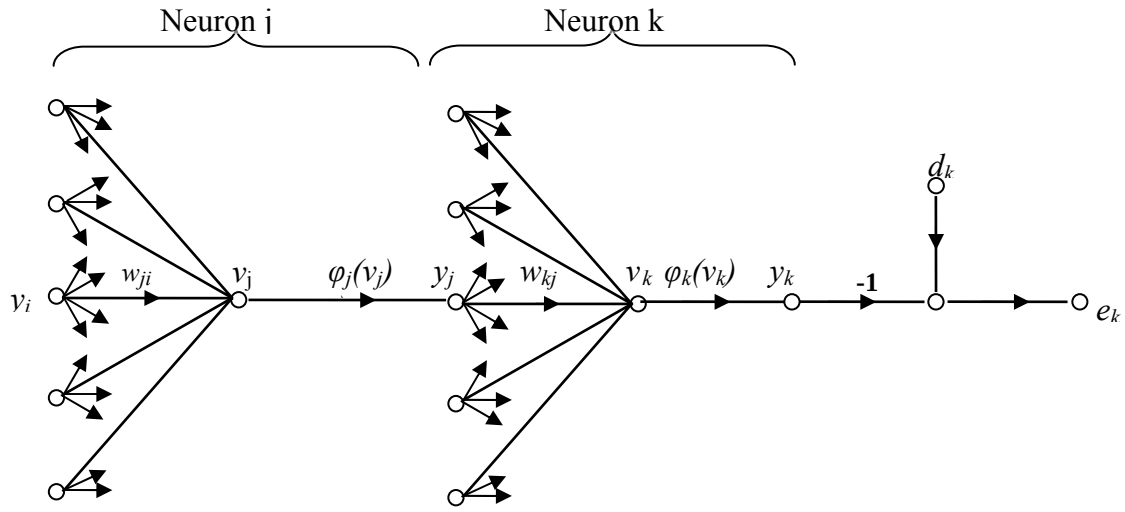

Fig. 4.6: Signal flow diagram inside neural network.

Weight update for layer k (w_{kj})

The error signal at output layer k can be define as

$$e_k = d_k - y_k \qquad \ldots \quad \ldots \quad \ldots \quad \ldots \quad (4.1)$$

The instantaneous sum of squared errors of the network can be written as

$$E = \frac{1}{2}\sum_{k=1}^{p} e_k^2 \qquad \ldots \quad \ldots \quad \ldots \quad \ldots \quad (4.2)$$

where, p is the total number of neurons at output layer. According to the signal flow diagram shown in Figure 4.6, the net internal activity v_k at any neuron in level k can be defined as

$$v_k = \sum_{j=1}^{n} w_{kj} \times y_j + \theta_k \qquad \ldots \quad \ldots \quad \ldots \quad \ldots \quad (4.3)$$

where, n is the total number of input to the neuron at level k and θ_k is threshold for that neuron, which is independent of input from previous layer. After somatic operation at level k, the output of y_k is

$$y_k = \varphi(v_k) \qquad \ldots \quad \ldots \quad \ldots \quad \ldots \quad (4.4)$$

where $\varphi(.)$ is the activation function of the neuron at level k.

Back propagation algorithm is implemented using gradient descent algorithm. Therefore, applied update of weight Δwkj is proportional to instantaneous gradient $\partial E / \partial dw_{kj}$. According to the chain rule this gradient can be written as

$$\frac{\partial E}{\partial w_{kj}} = \frac{\partial E}{\partial e_k}\frac{\partial e_k}{\partial y_k}\frac{\partial y_k}{\partial v_k}\frac{\partial v_k}{\partial w_{kj}} \quad \ldots \quad \ldots \quad \ldots \quad (4.5)$$

Differentiating Equation (4.2) with respect to e_k, we get

$$\frac{\partial E}{\partial e_k} = e_k \quad \ldots \quad \ldots \quad \ldots \quad \ldots \quad \ldots \quad (4.6)$$

Differentiating both sides of Equation (4.1) with respect to y_k, we get

$$\frac{\partial e_k}{\partial y_k} = -1 \quad \ldots \quad \ldots \quad \ldots \quad \ldots \quad \ldots \quad (4.7)$$

Differentiating Equation (4.4) with respect to v_k,

$$\frac{\partial y_k}{\partial v_k} = \varphi'_k (v_k) \quad \ldots \quad \ldots \quad \ldots \quad \ldots \quad (4.8)$$

Differentiating Equation (4.3) with respect to w_{kj},

$$\frac{\partial v_k}{\partial w_{kj}} = y_j \quad \ldots \quad \ldots \quad \ldots \quad \ldots \quad (4.9)$$

Using equations (4.6) to (4.9), Equation (4.5) can be written as

$$\frac{\partial E}{\partial w_{kj}} = -e_k * \varphi'(v_k) * y_j \quad \ldots \quad \ldots \quad \ldots \quad (4.10)$$

Using *error-correction learning rule* or *delta rule* (also known as *Widrow-Hoff* rule) [24], correction to weight Δw_{kj} is

$$\Delta w_{kj} = -\eta \frac{\partial E}{\partial w_{kj}} \quad \ldots \quad \ldots \quad \ldots \quad (4.11)$$

where η is a constant called learning rate constant. Equation (4.11) can be rewritten as

$$\Delta w_{kj} = \eta * \delta_k * y_j \quad \ldots \quad \ldots \quad \ldots \quad \ldots \quad (4.12)$$

where δ_k is called local gradient which is defined by

$$\delta_k = -\frac{\partial E}{\partial e_k}\frac{\partial e_k}{\partial y_k}\frac{\partial y_k}{\partial v_k}$$

$$= e_k * \varphi'_k *(v_k) \quad \ldots \quad \ldots \quad \ldots \quad \ldots \quad (4.13)$$

A hyperbolic tangent function was used as an activation function. Therefore, the output at layer k is defined by

$$y_k = a * \tanh(b * v_k) \quad \ldots \quad \ldots \quad \ldots \quad \ldots \quad (4.14)$$

Differentiating Equation (4.14) and utilizing Equation (4.13), the local gradient δ_k can be defined by

$$\delta_k = a * b * e_k * \sec h^2(b * v_k) \quad \ldots \quad \ldots \quad \ldots \quad \ldots \quad (4.15)$$

Weight correction (Δw_{kj}) = {learning rate(η)} . {local gradient (δ_k)} . {input signal of the neuron (y_j)}

Weight update for layer j (w_{ji})

For hidden neurons, there is no specified target output and therefore the weight correction for layer *j* (w_{ji}) is different from that of the output layer. Error signal for a hidden neuron would have to be determined recursively in terms of the error signals of all the neurons to which that hidden neuron is directly connected. According to Equation (4.13), we may redefine local gradient for hidden neuron j as

$$\delta_j = \frac{\partial E}{\partial v_j}$$

$$= \frac{\partial E}{\partial y_j}\frac{\partial y_j}{\partial v_j} \quad \ldots \quad \ldots \quad \ldots \quad \ldots \quad (4.16)$$

Now, we define output of neuron *j* as

$$y_j = \varphi(v_j) \quad \ldots \quad \ldots \quad \ldots \quad \ldots \quad (4.17)$$

Differentiating Equation (4.17) we get

$$\frac{\partial y_j}{\partial v_j} = \varphi'(v_j) \quad \ldots \quad \ldots \quad \ldots \quad \ldots \quad (4.18)$$

From Equations (4.16) and (4.18), we get

$$\delta_j = -\frac{\partial E}{\partial y_j}\varphi'(v_j) \quad \ldots \quad \ldots \quad \ldots \quad \ldots \quad (4.19)$$

Differentiating equation (4.2) with respect to y_j, we get

$$\frac{\partial E}{\partial y_j} = \sum_k \frac{\partial E}{\partial e_k}\frac{\partial e_k}{\partial y_j}$$

$$= \sum_k e_k \frac{\partial e_k}{\partial y_j}$$

$$= \sum_k e_k \frac{\partial e_k}{\partial v_k}\frac{\partial v_k}{\partial y_j} \quad \ldots \quad \ldots \quad \ldots \quad \ldots \quad (4.20)$$

We know that error e_k is:

$$e_k = d_k - y_k$$

$$= d_k - \varphi(v_k) \quad \ldots \quad \ldots \quad \ldots \quad \ldots \quad (4.21)$$

Differentiating Equation (4.21), we get

$$\frac{\partial e_k}{\partial v_k} = -\varphi'(v_k) \quad \ldots \quad \ldots \quad \ldots \quad \ldots \quad (4.22)$$

Also, according to signal flow diagram shown in Figure 4.6

$$v_k = \sum_{j=1}^{q} w_{kj} * y_j$$

where q is the number of input applied to neuron k. Differentiating with respect to y_j, we get

$$\frac{\partial v_k}{\partial y_j} = w_{kj} \quad \ldots \quad \ldots \quad \ldots \quad \ldots \quad (4.23)$$

Using Equations (4.22) and (4.23) in Equation (4.20), we get

$$\frac{\partial E}{\partial y_j} = -\sum e_k * \varphi'(v_k) * w_{kj} \quad \ldots \quad \ldots \quad \ldots \quad \ldots \quad (4.24)$$

From Equations (4.19) and (4.24), we can define local gradient δ_j as

$$\delta_j = \varphi'(v_j)\sum_k e_k * \varphi'(v_k) * w_{kj} \quad \ldots \quad \ldots \quad \ldots \quad \ldots \quad (4.25)$$

Using Equation (4.13) in Equation (4.25), we get

$$\delta_j = \varphi'(v_j)\sum_k \delta_k * w_{kj} \quad \ldots \quad \ldots \quad \ldots \quad \ldots \quad (4.26)$$

Since we have used hyperbolic tangent function as an activation function, we can write

$$\varphi(v_j) = a * \tanh(b * v_j)$$

Differentiating w.r.t v_j,

$$\varphi'(v_j) = a * b * \sec h^2(b * v_j) \quad \ldots \quad \ldots \quad \ldots \quad (4.27)$$

Therefore, local gradient for hidden layer *j* is:

$$\delta_j = a * b * \sec h^2(b * v_j)\sum_k \delta_k * w_{kj}$$

Weight correction for w_{ji} is:

$$\Delta w_{ji} = -\eta \frac{\partial E}{\partial w_{ji}}$$

$$= -\eta \frac{\partial E}{\partial v_j}\frac{\partial v_j}{\partial w_{ji}} \quad \ldots \quad \ldots \quad \ldots \quad \ldots \quad (4.28)$$

Now, according to Figure 4.6, v_j is:

$$v_j = \sum_{i=1}^{n} w_{ji} * yi\,,$$

Differentiating w.r.t w_{ji}, we get

$$\frac{\partial v_j}{\partial wji} = y_i \quad \ldots \quad \ldots \quad \ldots \quad \ldots \quad (4.29)$$

Using Equations (4.16) and (4.29) in Equation (4.28), we get

$$\Delta w_{ji} = \eta * \delta_j * y_i \quad \ldots \quad \ldots \quad \ldots \quad \ldots \quad (4.30)$$

Weight correction (Δw_{ji}) = {learning rate(η)}. {local gradient (δ_j)}. {input signal of the neuron (y_i)}

A problem of back propagation algorithm is that it can trap at a local minima. However, some methods have been developed to overcome this problem. The algorithm can overcome a local minimum if a momentum (a factor multiplied by previous change in

weight) is included in the weight update formula [26]. The weight update formula with a momentum is shown in Equation (4.31). Figures 4.7 and 4.8 show the effect of adding a momentum factor.

$$\Delta w_{ji}(n) = \eta \delta_j(n)\, y_i(n) + \alpha\, \Delta w_{ji}(n-1) \quad \ldots \quad \ldots \quad \ldots \quad (4.31)$$

where α is called momentum factor and n represents iteration number.

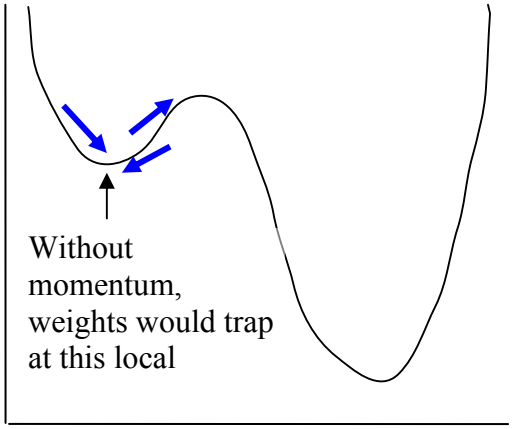

Fig. 4.7: Weight update without momentum

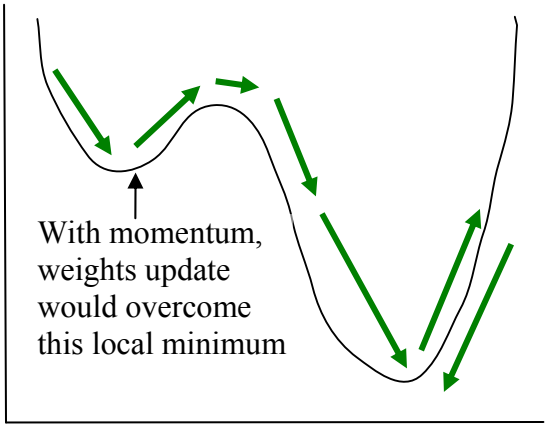

Fig. 4.8: Weight update with momentum

4.7 Enhancement of Convergence Speed

Back propagation algorithms are very popular for their simple mathematical calculations but at the same time well criticized for their slow rate of convergence. There has been a lot of successful research [23, 30-38] to enhance the convergence speed of back propagation algorithms. The approaches that have been used in this research to enhance the convergence speed are described in the following sections.

4.7.1 Initialization of weights

One of the approaches to speed up the training rate of a back propagation algorithm is to estimate the optimal initial weights. Several approaches to estimate the initial weights for a neural network have been reported in literature [23, 30, 33, 36, 37]. In Reference [23] the initial weights have been estimated in the following manner.

The weighted sum of the inputs to the jth hidden neuron can be represented by

$$a_j = w_{j0} + \sum_{i=1}^{N} w_{ji}.x_i \quad \ldots \quad \ldots \quad \ldots \quad \ldots \quad \ldots \quad (4.32)$$

where, w_{j0} is the threshold for jth hidden neuron, x_i are the inputs and w_{ji} are the initial weights which are randomly distributed (uniform distribution) between $-w_{max}$ to w_{max}. This approach ensures that the outputs of the hidden layers are in the active region while dynamic range of the activation function is fully utilized. The active region is assumed to be where the derivative of the activation function is one-twentieth of its maximum value [23].

The initial weights are optimized by keeping them in the active region. The activation function used here is

$$f(x) = a.\tanh(b.x),$$

where a=0.51 and b=0.61. With these values, the maximum value of the derivative is 0.3111 at x=0.0 and its one-twentieth is at x=6.05. Therefore,

$$|a_j| \leq 6.05$$

If $|a_j| \geq 6.05$, the neuron enters in the saturation region where the derivative of the activation function is very small.

In order to ensure the outputs of the hidden neurons are within the active region, the distance between the hyperplanes *P(-6.05)* and *P(6.05)* should be greater than or equal to the maximum possible distance between two points in the input space. The maximum possible distance D_{in} between two points of the input space is given by following equation [23]

$$D_{in} = \sqrt{\sum_{i=1}^{N} (\max(i) - \min(i))^2}$$

and the distance between hyperplanes *P(-6.05)* and *P(6.05)*is given by

$$d_{in} = \frac{12.1}{\sqrt{\sum_{i=1}^{N} w_{ji}^2}}$$

If D_{in} is set equal to d_{in} then,

$$\sqrt{\sum_{i=1}^{N} w_{ji}^2} = \frac{12.1}{D_{in}}$$

The length of the weight vector is approximated by

$$\sqrt{\sum_{i=1}^{N} w_{ji}^2} = \sqrt{N \times E(W^2)}$$

where, $E(W^2)$ is the second moment of the weights between input and hidden layer, which is given by,

$$E(W^2) = \frac{w_{\max}^2}{3}$$

Therefore,

$$w_{\max} = \frac{12.1}{D_{in}} \sqrt{\frac{3}{N}}$$

So, optimum initial weights will be random number between $-w_{max}$ to w_{max}.

Now, center of the input space is given by

$$C^{in} = \left(\frac{\max(x_1) + \min(x_1)}{2}, \frac{\max(x_2) + \min(x_2)}{2}, \ldots, \frac{\max(x_N) + \min(x_N)}{2} \right)^T$$

Therefore, threshold values for active region is given by,

$$w_{j0} = -\sum_{i=1}^{N} C^{in} \, w_{ji} \qquad \ldots \quad \ldots \quad \ldots \quad \ldots \quad \ldots \qquad (4.33)$$

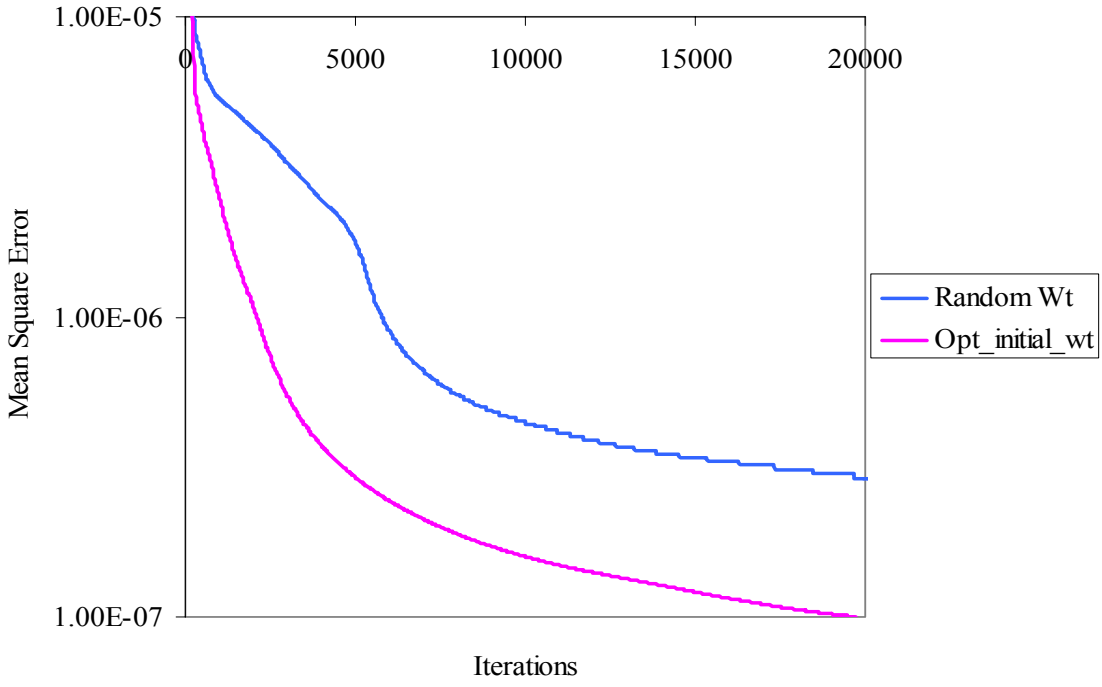

Fig. 4.9: Effect of weight initialization on convergence.

4.7.2 Adapting different learning rate for each weight direction

One of the main reasons for slow convergence of a back propagation algorithm lies in the fact that the corrections to synaptic weights becomes very small when error tends to be very small i.e. error surface becomes almost flat. This slow convergence in the flat directions and oscillations in the steep directions can be avoided by using a different learning rate for each direction in weight space [38]. However, attempts to find a proper learning rate for each weight usually results in a trade-off between the convergence speed and the stability of the training algorithm. In this research, to enhance convergence speed, different learning rates were used in different directions of weight space and they were made adaptive by delta-delta learning rule [24] using the following recursion formula:

$$\Delta\eta_{ji}(n+1) = \gamma \frac{\partial E(n)}{\partial W_{ji}(n)} \frac{\partial E(n-1)}{\partial W_{ji}(n-1)} \qquad \ldots \quad \ldots \quad \ldots \quad \ldots \qquad (4.34)$$

where η is learning rate, γ is a positive constant which determines step size, E is error and W_{ji} is synaptic weight connecting neuron i to neuron j. Figure 4.10 shows the effect of adaptive learning rate on the convergence of the training of the ANN.

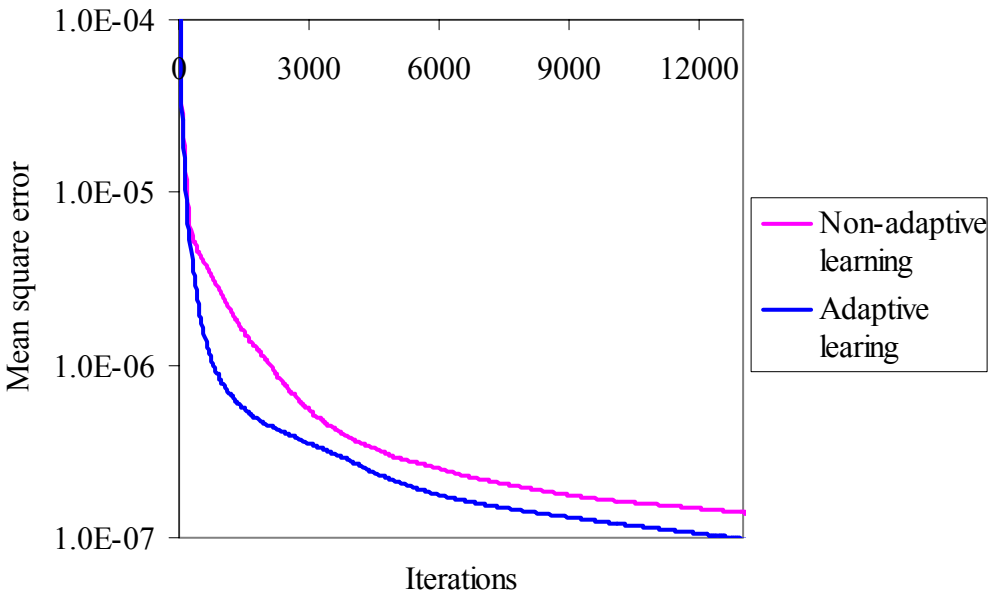

Fig.4.10 Effect of adaptive learning rate.

4.7.3 Adapting threshold values

Although threshold values are normally kept constant (usually -1.0), adapting these values with respect to error can enhance convergence speed. Threshold values have been made adaptive with the following formula [39]:

$$\theta_k^{n+1} = \theta_k^{n} + \eta_k^{n} \frac{\partial E(n)}{\partial \theta_k(n)} + \alpha(\theta_k^{n} - \theta_k^{n-1}) \quad \ldots \quad \ldots \quad \ldots \quad (4.35)$$

where θ_k is the threshold for layer k and α is the momentum factor and n represents iteration. Figure 4.11 shows that learning converges faster if thresholds are made adaptive using Equation (4.35).

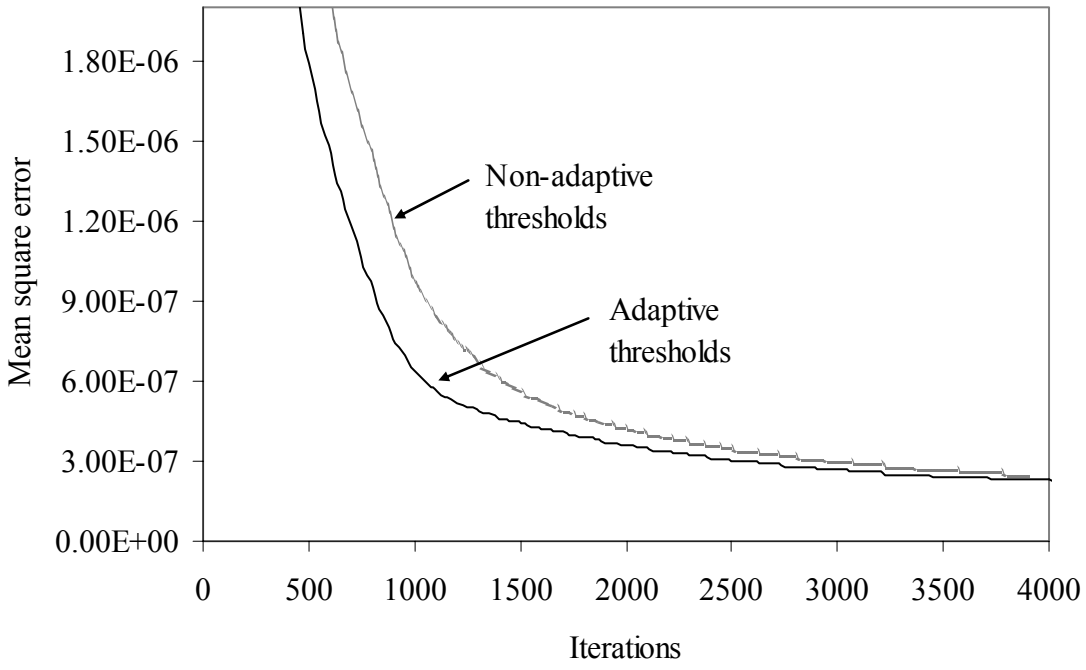

Fig.4.11 Effect of adaptive thresholds

4.7.4 Use of dual activation functions

The loss attributed to a transaction can be positive or negative (in case of counter flow). This aspect can be handled by the use of a hyperbolic tangent function. It was also observed that the reactive part of transmission loss is 3 to 5 times that of the real part. In this research two activation functions, therefore, were used in the output layer for two different types of outputs to keep the output neurons in the active region for both real and reactive outputs. It was observed that the use of dual activation functions not only

increases the convergence speed but some times it helps to reach higher level of convergence accuracy which cannot be obtained by a single activation function. Figure 4.12 shows the range of the outputs and the activation functions used in this research. Figure 4.13 shows the convergence characteristics for single and dual activation functions.

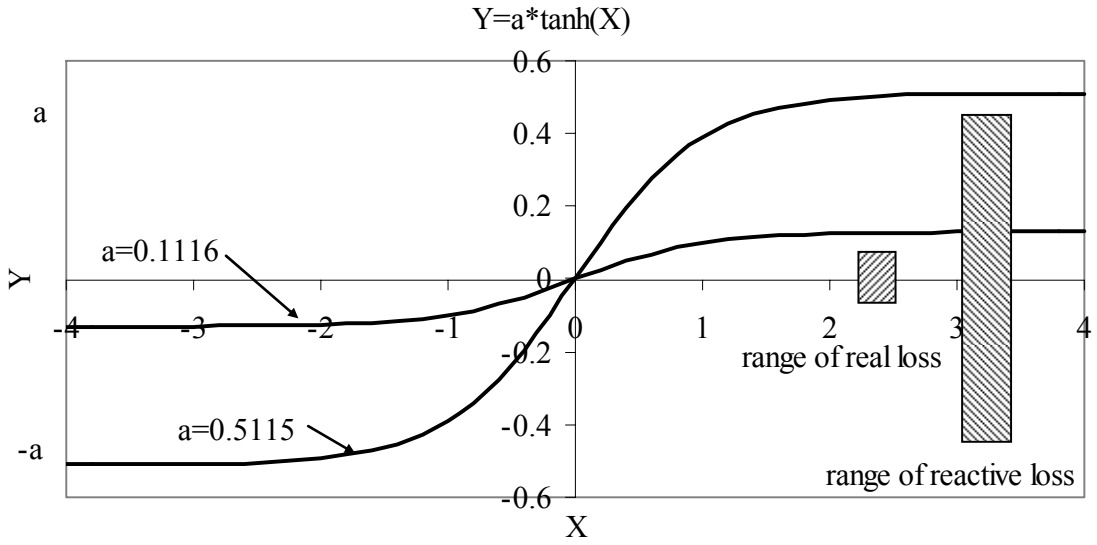

Fig. 4.12: Activation functions and output ranges

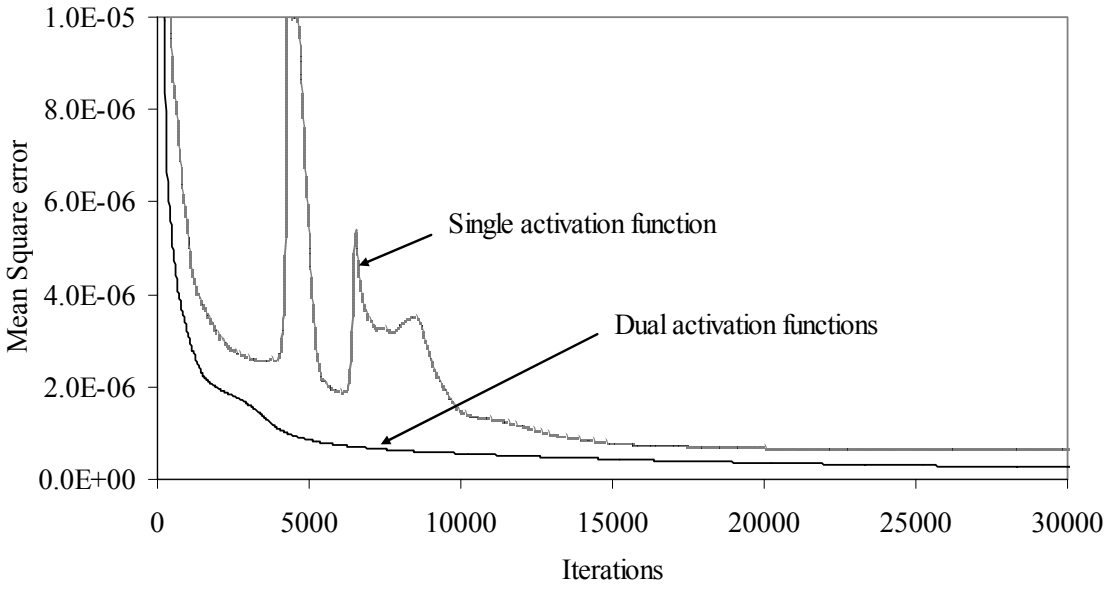

Fig.4.13: Convergence characteristics for single and dual activation function

4.8 Optimum Hidden Neurons

In the previous section we observed that proper initialization of synaptic weights and the thresholds, adapting different learning rate for each weight direction, adapting thresholds and the use of dual activation functions in output layer increased the convergence speed in the back propagation learning. With all these learning enhancement techniques, different neural network architectures were studied for the purpose of transmission loss allocation in the test system. It was found that increasing the number of neurons beyond 45, neither improves convergence characteristics nor gives better performance with the test patterns. Similarly, the optimum number of neurons with two hidden layers was obtained. Figure 4.14 shows the convergence characteristics with respect to the number of iterations for different number of hidden neurons in a single layer. Figure 4.15 shows the convergence characteristics of the neural network with one and two hidden layers. Fig. 4.16 shows the required number of iterations to attain an MSE of 1.2×10^{-7}. Figure 4.17 shows the time required to attain the same level of accuracy (MSE=1.2×10^{-7}) for different number of hidden neurons. Figure 4.18 shows the mean of the square errors (MSE) of the test patterns for different numbers of hidden layers and neurons.

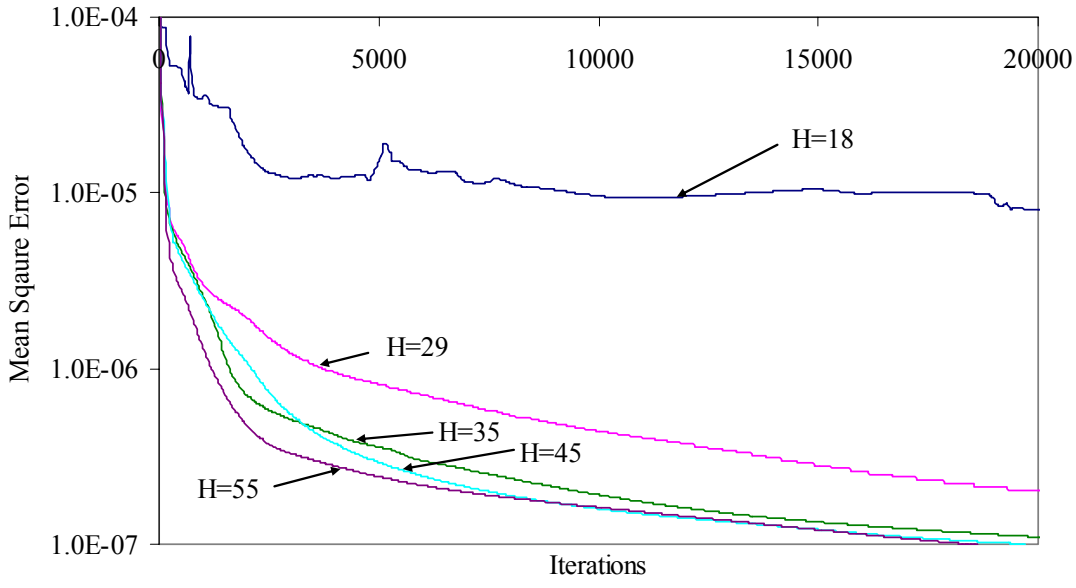

Fig. 4.14: Convergence characteristics for different numbers of hidden neurons in a single hidden layer feedforward network

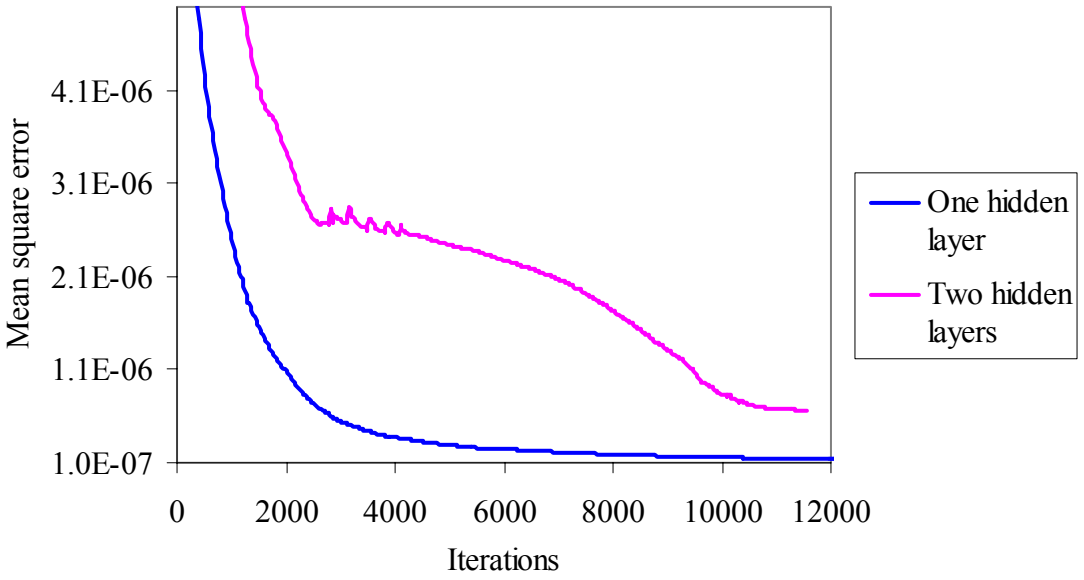

Fig. 4.15: Convergence characteristics of proposed neural networks with one and two hidden layers

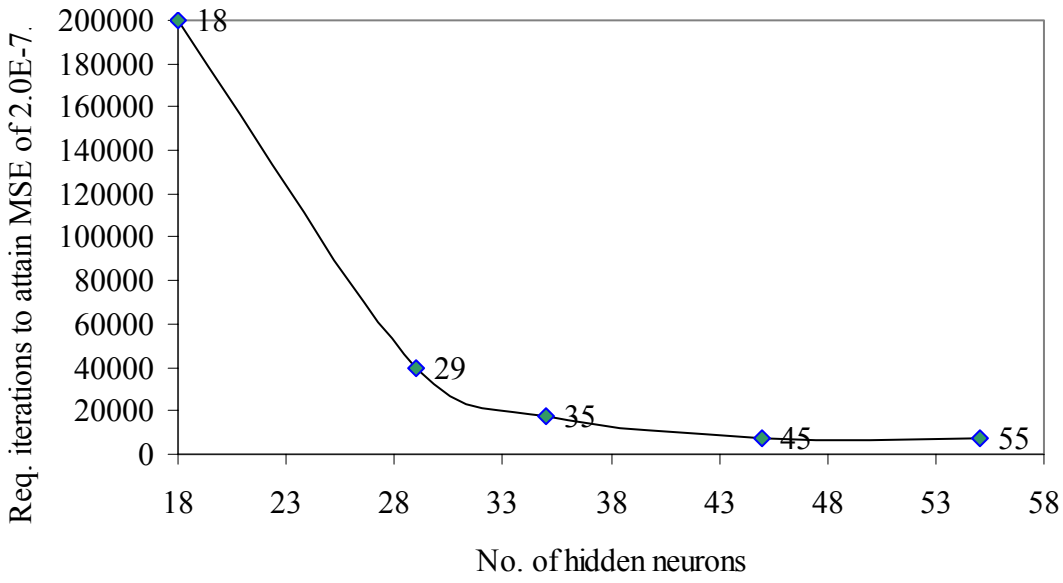

Fig. 4.16: The required number of iterations to attain a particular accuracy level (for MSE =1.2×10^{-7}) .

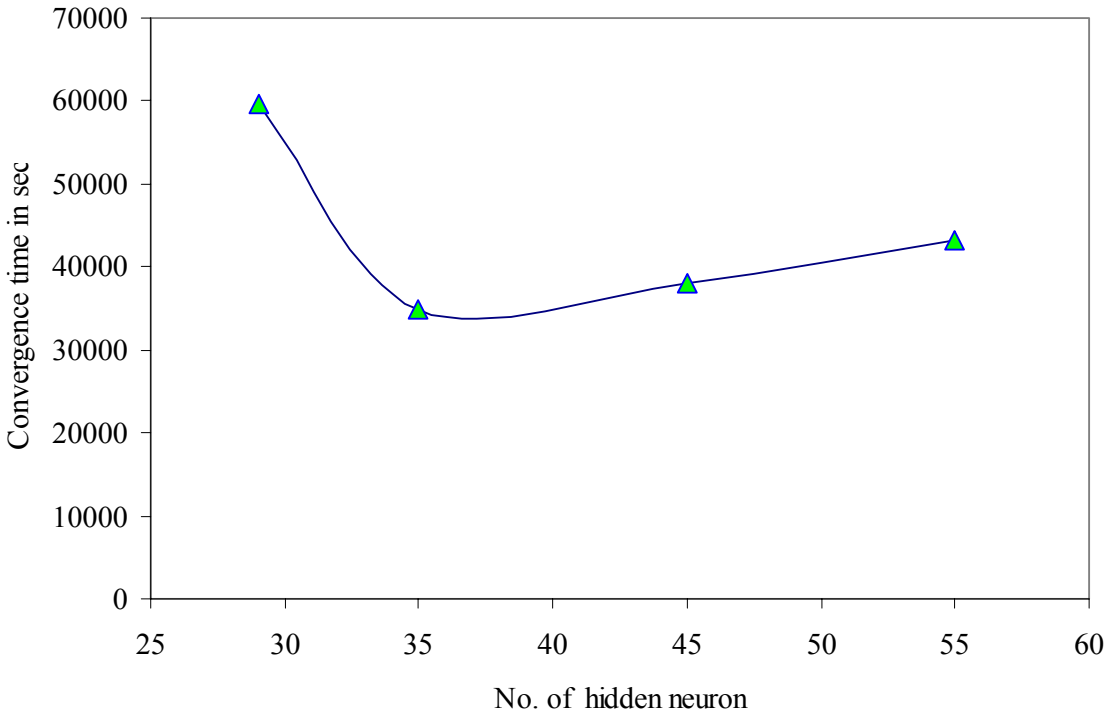

Fig. 4.17: The time required to attain same accuracy level.

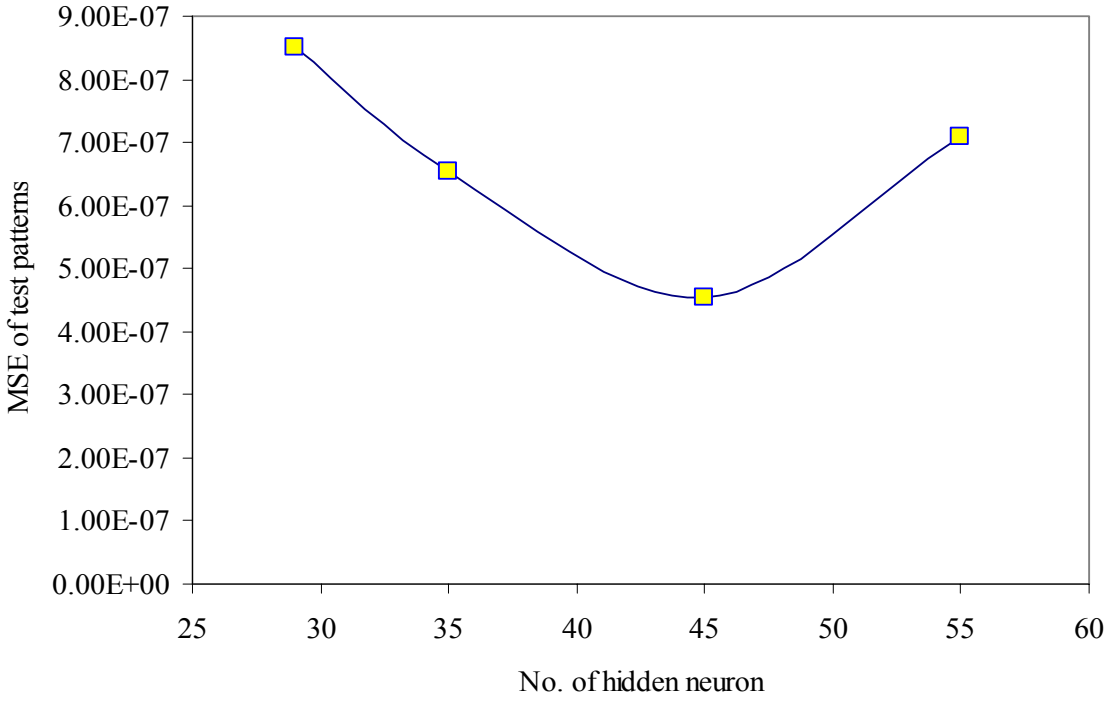

Fig.4.18: MSE of test patterns for different ANN architecture

Among all network architectures considered, it was observed that the network with a single hidden-layer with 45 hidden neurons provided the best result in terms of speed of convergence and accuracy.

4.9 Results

The proposed network was trained in 19701 iterations. Amplitudes of activation functions were 0.1116 and 0.5115 for real and reactive loss allocations respectively. A value of 0.61 was used for 'b' for both the activation functions. Learning rate (η) was chosen to be 0.85, momentum factor α was 0.48, step size γ for adaptive learning was 0.85. Mean square error (MSE) was used to check convergence accuracy. A value of 5.0E-08 was chosen for MSE to determine convergence of training. The trained network was tested with 838 test patterns. Test patterns were derived by varying all 54 inputs to simulate 24 hour load patterns on weekdays and weekends. Results obtained from the ANN and ILFA show that ANN can allocate losses with good accuracy. Only a few of these results are shown here. Figures 4.19 & 4.20 show the real and reactive loss allocations respectively for an off-peak hour. Figures 4.21 & 4.22 show the real and reactive loss allocations respectively for a peak hour. It can be noticed that the results obtained from the ANN agree very closely with those obtained using the ILFA.

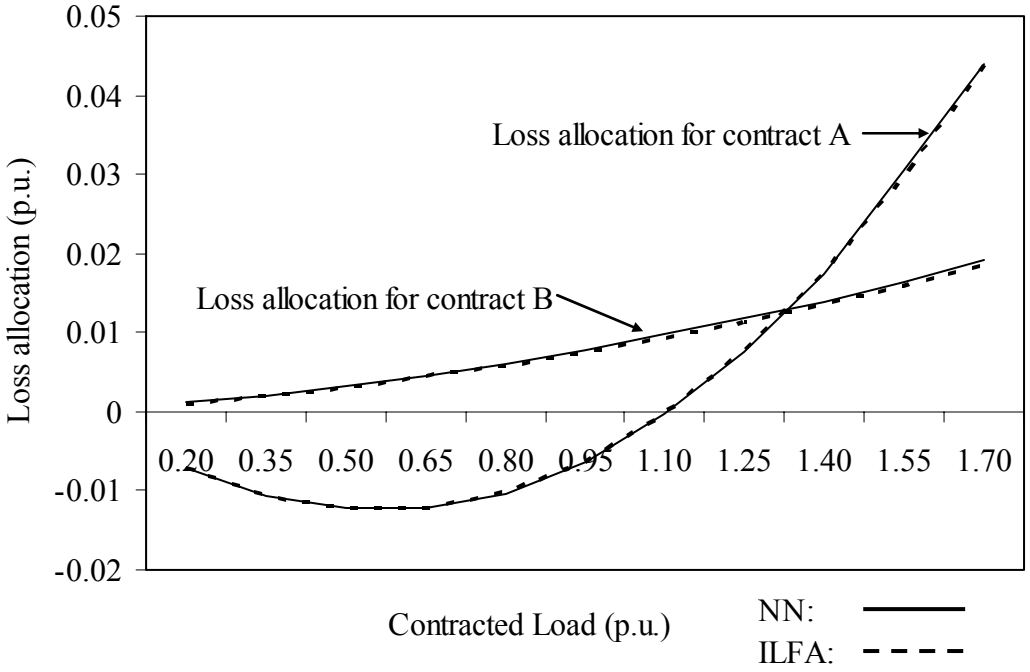

Fig. 4.19: Real loss allocations for off-peak hour on weekend

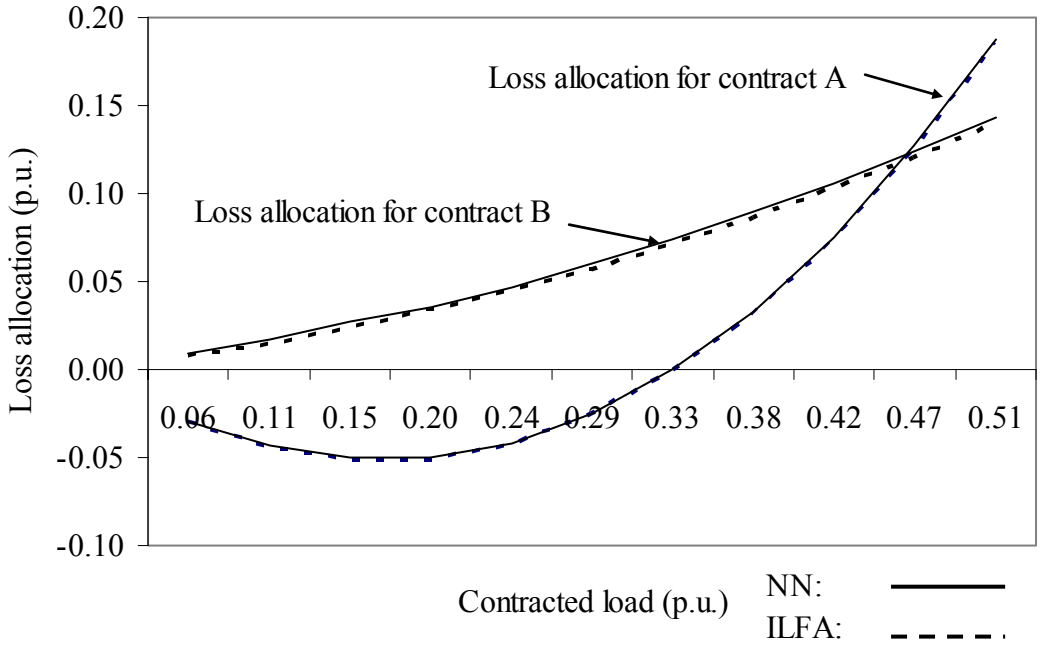

Fig. 4.20: Reactive loss allocations for off-peak hour on weekends

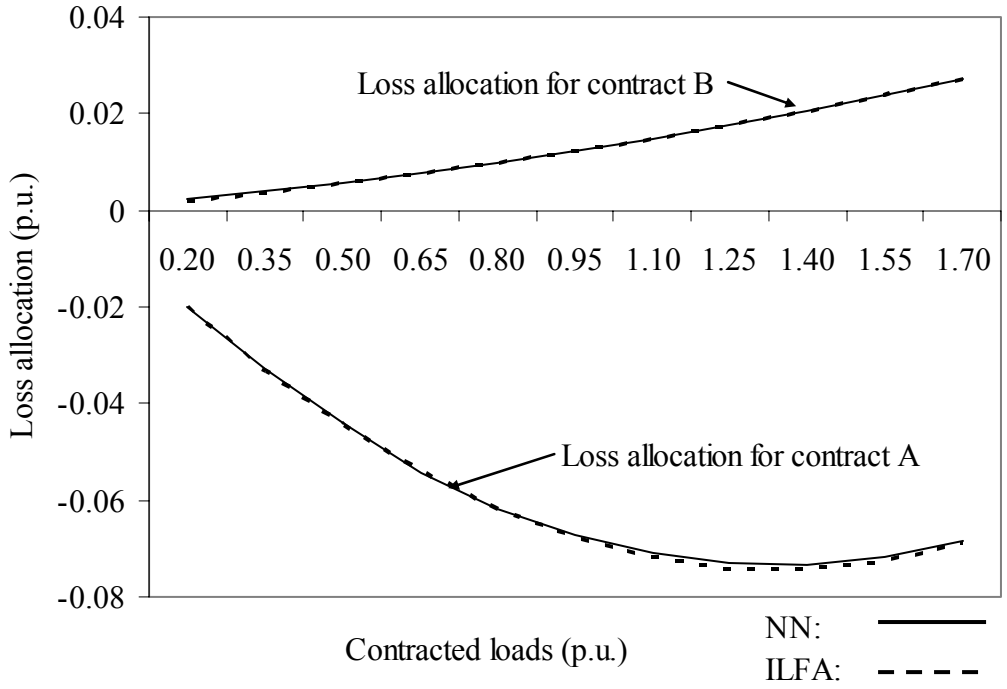

Fig. 4.21: Real loss allocations for peak hour on weekdays

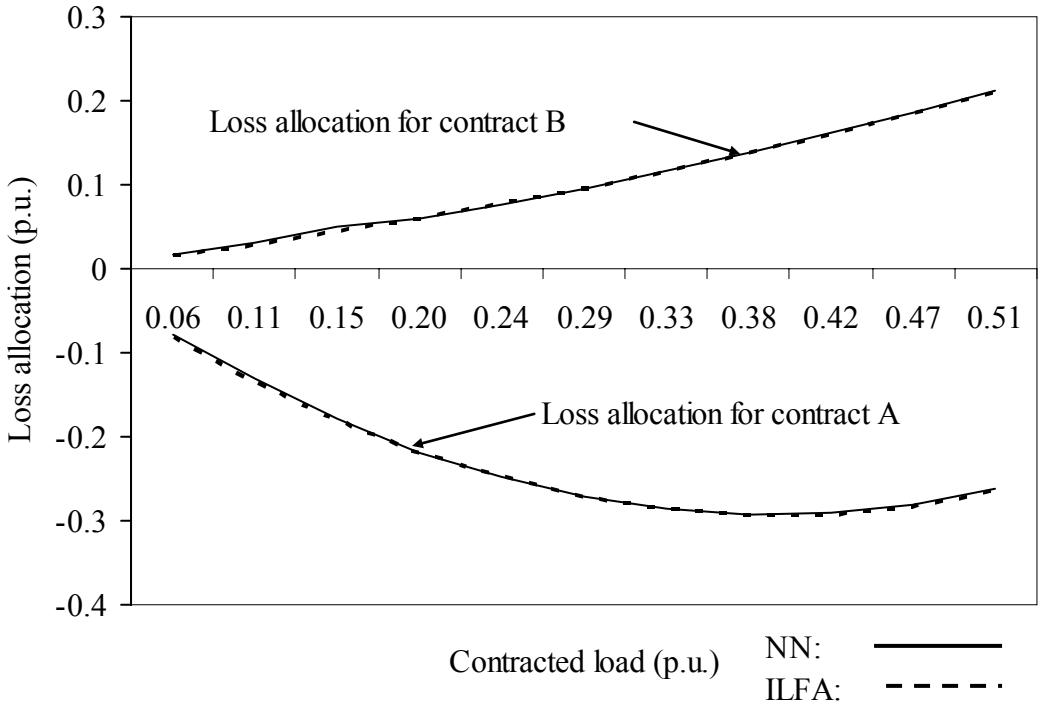

Fig. 4.22: Reactive loss allocations for peak hour on weekdays

4.10 Summary

An ANN was developed and utilized to assess transmission loss allocation for bilateral contracts. The results obtained from the proposed ANN were then compared with those obtained using the ILFA. The IEEE 24-bus reliability test system with two bilateral contacts was utilized to generate loss allocations. The test system was considered to operate in a pool structure that had a typical 24 hour load variations from 1116.6 MW and 207.1 MVAR to 2494 MW and 505.7 MVAR. Loss allocations for bilateral contracts were studied with variable load demand from 20 MW to 185 MW. The proposed network was trained with little difficulty and a method was developed for faster training of the network. The trained ANN was tested with 838 test patterns where different input vectors were considered. The results obtained from the ILFA and the trained ANN were compared graphically. It was observed that the trained ANN can allocate losses to bilateral contracts with very good accuracy.

CHAPTER 5: LOSS ALLOCATION WITH A LINE FAILURE

5.1 Limitations of Previously Proposed Network

Although artificial neural network solutions are extremely fast and straightforward even for complex problems, it has limitations too. For example, the trained neural network described in previous chapter can allocate losses for bilateral contracts in milliseconds but cannot work if the configuration of power transmission network changes. For any change in the transmission network new training patterns have be generated and the neural network has to be retrained. Although a transmission network does not change frequently, its configuration changes when a transmission line becomes unavailable. A transmission line can be unavailable due to maintenance or failure. Bilateral transactions may continue even after a line failure if the failure doesn't threaten system security and does not overload other lines. Therefore, it is desirable that a loss allocation method should be capable of handling unavailability of transmission lines. The retraining due to line failures can be bypassed if the status of transmission lines are used as additional inputs to the ANN. An artificial neural network will be presented in this chapter that will work without requiring retraining when transmission line becomes unavailable.

5.2 Transmission Line Outage

Today's power system networks are more secured than ever before and better protected against fault. At the same time, to secure the whole power network, more protective relays are used which in turn increase the tripping of transmission lines for various faults especially during bad weather or lightning. Moreover, a transmission line can be unavailable due to the failure of an equipment associated with transmission line e.g. transformer, breaker, relays. 4049 transmission line trips had happened in Japan from 1990 to 2000 [40]. In Alberta, transmission lines tripped 757 times from 1997 to 2001 [41]. Transmission lines and equipments associated with it are also taken out of service

for scheduled maintenance. The duration of transmission unavailability could be significant enough to affect the loss allocation and, therefore, should not be neglected.

5.3 Inclusion of Transmission Line Outages In Loss Allocation

Since unavailability of a transmission line changes transmission loss allocation, status of transmission lines (available / unavailable) have been used as inputs to the proposed neural network to make loss allocation responsive to line unavailability. With the inclusion of line status, the proposed neural network will be able to allocate losses to all parties accurately even during a transmission line outage. Unlike other inputs e.g. loads, generations and bus voltages which are directly used in p.u., each line is given a binary status, '0' if available and '1' if failed. Inclusion of transmission line status increases the size of the input vector and eventually increases the size of neural network. Therefore, instead of using the status of all transmission lines, the status of a selected number of transmission lines have been included in the input vector. A selection criteria to include transmission line status into the input vector has been developed and discussed in Section 5.5

5.4 Test System

The IEEE 24-bus reliability test system was utilized to provide numerical examples on loss allocation with line failures. Two bilateral contracts have been assumed to exist in the test system. Contract A exists between Generator A at Bus 7 and Load A at Bus 9. Contract B exists between Generator B at Bus 23 and Load B at Bus 19. Figure 4.2 shows the IEEE 24 bus reliability test system. Line numbers are marked in the figure. A Synchronous condenser was placed at Bus 6 to increase voltage stability during bilateral transactions.

The test system has 24 buses, 38 lines, 10 generation stations and 15 load buses. The system has a peak load of 2494 MW. 24 hour real and reactive loads are shown in Figure 4.3 & 4.4 and generations are shown in Figure 4.4. Line parameters are described in Table 2.1 in Chapter 2.

5.5 Selection And Grouping of Line Status to Be Used As Inputs

The inclusion of line status, however, creates another problem. The number of inputs related to line status could be very high in a large system. This could increase the training time of the ANN tremendously. The number of inputs can be kept low by selecting specific transmission lines in the following manner:

a) Status of those lines are ignored whose unavailability make the bilateral transactions impossible. In our test system, Generator A cannot deliver any power to the contracted Load A if Line 11 is unavailable. Therefore, status of Line 11 is not taken as an input to the neural network.

b) Status of those lines are ignored whose failures would prompt ISO to suspend the bilateral transactions for reason of system security and transmission congestion. Load flow studies have performed on the test system to ascertain these transmission lines whose operations are critical for the bilateral transactions. Load flow studies showed that any one failure of Lines 23, 27 or 24 during bilateral transactions would make system voltage unstable. In such a case, ISO would have to interrupt the bilateral transactions. Status of these lines, therefore, were not considered in the proposed ANN.

c) Loss allocation does not change significantly for failure of every transmission line. Loss allocation studies have shown that unavailability of certain transmission lines have significant effect on loss allocation while the failure of other lines do not change loss allocation a lot. Figure 5.1 & Figure 5.2 show that in many cases loss allocation curves remain in the vicinity of the no-line-failure-curve. So the status of these lines can be ignored to reduce the number of inputs. Figure 5.1 shows that unavailability of any one of the Lines 2, 6, 8, 9, 10, 18, 19, 21, 22, 23, 24, 25, 28, 29, 30, 31, 32, 36 or 38 does not change loss allocation significantly. On the other hand Figure 5.1 shows that unavailability of any one of the Lines 3, 4, 5, 6, 8, 9, 10, 12, 13, 14, 19, 20, 22, 24, 25, 28, 30, 31, 32 or 38 does have relatively significant effect on loss allocation. Therefore, the status of Lines 1, 2, 3, 4, 5, 7, 12, 13, 14, 15, 17, 27, 18, 21, 29, and 36 have

been used as inputs while ignoring the status of the Lines 6, 8, 9, 19, 20, 24, 25, 26, 28, 30, 31, 32 and 38.

d) The number of inputs could be further lowered by ignoring the status of these lines whose failure rates are significantly less than those of the others lines.

e) Loss allocation studies have shown that unavailability of certain lines has indistinguishable effect on loss allocation. For example, Figure 5.1 shows that unavailability of any of Lines 1, 7, 14, 27 has same effect on loss allocation for Contract A. Similarly Figure 5.2 shows that for unavailability of either Lines 7 or 27 the loss allocation for Contract B is the same. Therefore, combining these two phenomena, we can group the status of Lines 7 and 27 together as one input.

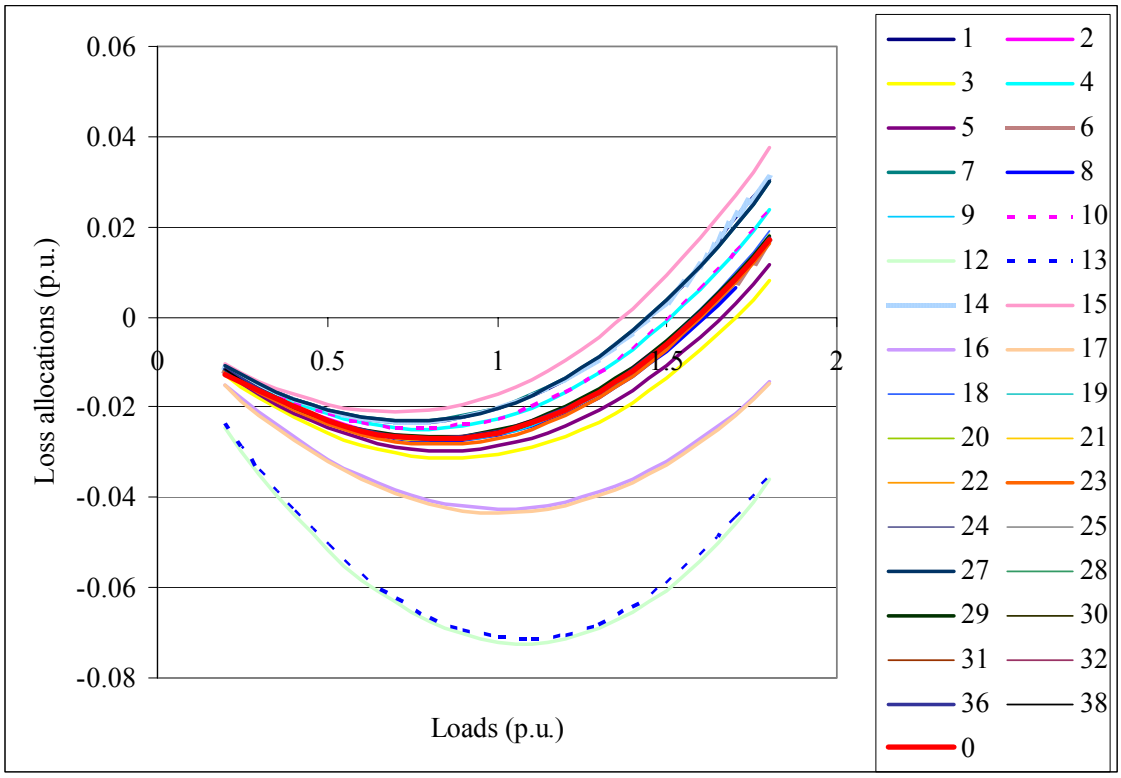

Fig. 5.1: Real loss allocations for Contract A for unavailability of different lines

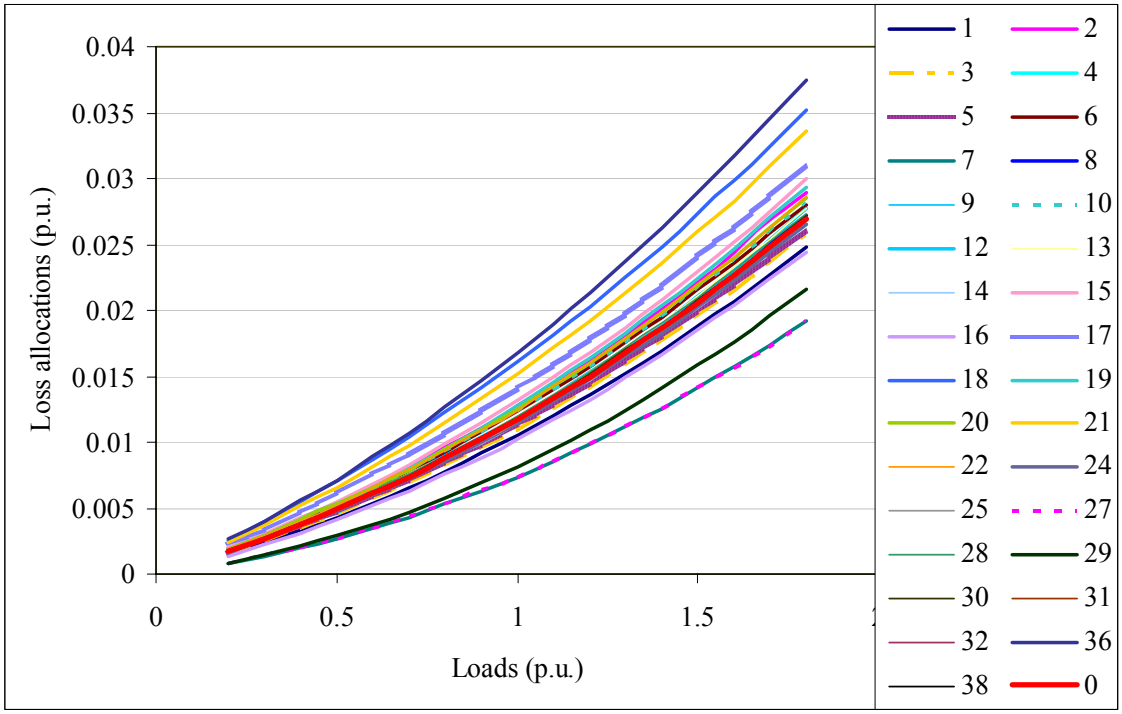

Fig.5.2: Real loss allocations for Contract B for unavailability of different lines.

Based on above criteria the status of certain transmission lines have been selected as input to the neural network. Several load flow studies were performed to ascertain which transmission lines would fall into the selected group. Only single level contingencies were considered. This was done due to the fact that the probability of concurrent failure of two or more transmission lines in a system is generally very insignificant. Load flow studies also showed that bus voltages at some buses would go very near to unstable region if any one the line of 2, 3 o 7 fails. However, the voltages would still be in the acceptable region and, therefore, bilateral transactions may proceed. Based on the load flow studies it was, therefore, concluded that the status of Lines 1, 2, 3, 4, 5, 7, 12, 13, 14, 15, 17, 18, 21, 29 & 36 should be added to the ANN to represent unavailability of transmission lines.

5.6 Proposed Neural Network Architecture

A multilayer feedforward neural network has been proposed for loss allocation for bilateral contracts. The proposed network can assess transmission losses even during the unavailability of some selected transmission lines. The inputs to the network were

selected carefully so that the proposed network represents all possible practical situations including unavailability of a transmission line due to line failure or line maintenance. Most independent system variables e.g. loads, generations, bus voltages were used as inputs to this neural network which in turn makes the loss allocation process responsive to practical situations. Desired outputs of the network were real loss and reactive loss for contracts A & B. The inputs and outputs of the network are described in Table 5.1

Table:5.1: Description of inputs and outputs of ANN

Layer	Neurons	Description
Inputs	I_1-I_2	Real load for Contracts A & B (p.u.)
	I_3-I_4	Reactive load for contracts A & B (p.u.)
	I_5-I_{19}	Real loads on buses (p.u.)
	I_{20}-I_{34}	Reactive loads on buses (p.u.)
	I_{35}-I_{44}	Generations on buses (p.u.)
	I_{45}-I_{54}	Bus voltages (p.u.)
	I_{55}-I_{69}	Line status of selected lines
Output	O_1-O_2	Real loss for Contracts A & B (p.u.) respectively
	O_3-O_4	Reactive loss for contracts A & B (p.u.) respectively

To find the most suitable architecture for loss allocation, the number of hidden layers and the number of neurons in them had to be optimized. The optimal number of hidden neurons depends on: (i) the number of input and output variables, (ii) the number of training records, (iii) the amount of noise in the output variables, (iv) the complexity of the relationship between input and output variables, and (v) the type of transfer functions. Since there is no 'rule of thumb' to determine the optimal number of hidden neurons [42], we approached this problem by repeatedly training neural networks with different numbers of hidden neurons and identifying the optimal number of hidden

neurons from those that yielded the best convergence characteristics and lowest mean square error for the test patterns. However, for single hidden layer, the optimum number of hidden neurons lies between n to 2n, where n is the number of inputs [43]. With several trials it was found that the network with 89 hidden neurons has the best performance. Figure 5.3 shows convergence characteristics for different number of hidden neurons.

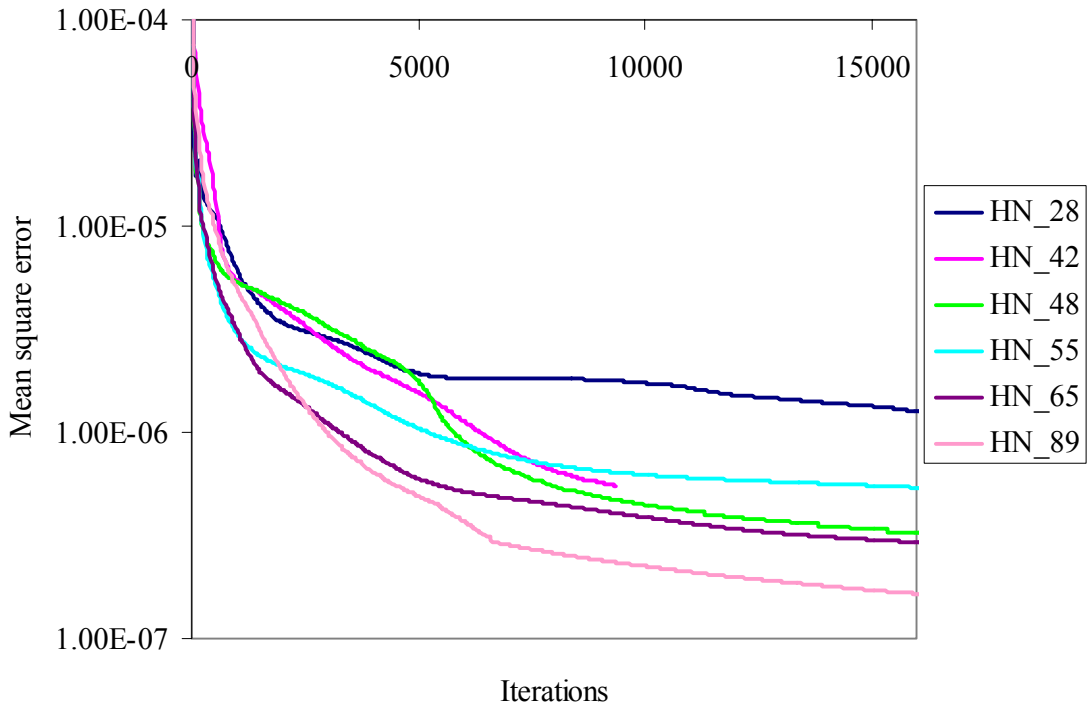

Fig. 5.3: Convergence characteristics for different number of hidden neurons.

Therefore, the proposed artificial neural network is a feed forward neural network which consists of three layers; an input layer, a hidden layer and an output layer. There are 69 inputs and 4 outputs as described in Table 5.1 and 89 hidden neurons in a single hidden layer.

5.7 Training

The proposed network was trained with a supervised learning algorithm. Among all supervised learning methods, back propagation algorithm is widely used for its simplicity. Although Quasi-Newton method has fast convergence characteristics, it

requires calculation of Hessian matrix for each iteration which becomes a complex task for large neural network. Therefore, back propagation algorithm was utilized to train the proposed network. *Incremental Load Flow Approach* (ILFA) had been used as a teacher to train the proposed network. Using this method, 5187 training patterns and 1840 test patterns were generated with all possible variation of inputs. 24 hour load patterns for weekdays and weekends were considered for generation of training and testing patterns. Bus voltages were varied from 1.01 to 1.05 p.u. and ±5% voltage tolerance were considered for all buses. Contracted loads were varied from 20 MW to 185 MW for both contracts. Training was conducted on a personal computer (Intel Pentium 4, 3.0 GHz) with Windows XP platform. Visual FORTRAN software was utilized for the training and testing of the network.

To enhance convergence speed, all the techniques discussed in Section 4.7 had been utilized in this case as well. However, due to the inclusion of transmission line status, non-linearity of training patterns increased as can be observed in Figure 5.1 & 5.2. It can be observed that the unavailability of a transmission line which makes only a small change in the input pattern, makes a significant change in the output. To make the network more dependent on transmission status, the number '5' was used instead of '1' as input to represent the unavailability of a line. The availability of transmission line was denoted by '0' as before. This gave a faster convergence which is shown in Figure 5.4. Other values for line status were tried but the use of number '5' to denote failure of line gave consistently better convergence.

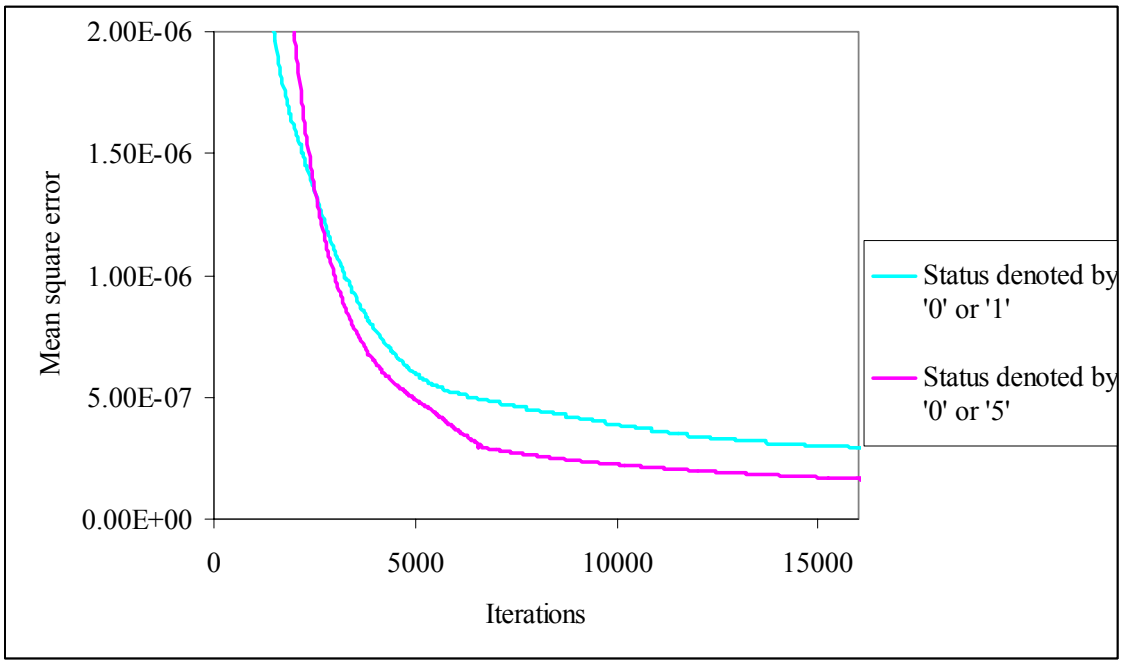

Fig. 5.4: Convergence characteristics for change in line status inputs.

Since the sum of the square of errors (SSE) changes with a change in the number of training patterns, the mean square error (MSE) was used to check the convergence of training. A value of 0.8 $x10^{-8}$ was chosen for MSE. The initial learning rate (η) was chosen as 0.85, momentum factor α was chosen as 0.48 and the step size γ for adaptive learning was chosen as 0.85. A value of 0.61 was chosen for 'b' for the activation function. Two amplitudes, 0.13 and 0.51 were used for the activation functions. 0.13 was utilized for the real loss allocation and 0.51 was utilized for the corresponding reactive loss allocation.

5.8 Results

The trained network was tested with 1840 test patterns. Test patterns were generated with all possible variations in inputs. 24 hour load variation for weekdays and weekends were considered and the bus voltages were varied from 1.01 p.u. to 1.04 p.u. Contracted loads were varied from 20 MW to 185 MW for each contract. Unavailability of selected lines was considered. Loss allocations for all test patterns were obtained by both ILFA method and the trained neural network. Comparison of some loss allocations are shown in Figures 5.5 to 5.16

Figure 5.5 and 5.6 show real and reactive loss allocations respectively for the peak hour with no line failure. The system load at the peak hour is 2494 MW. The loads for Contracts A and B were varied from 20 MW to 185 MW simultaneously.

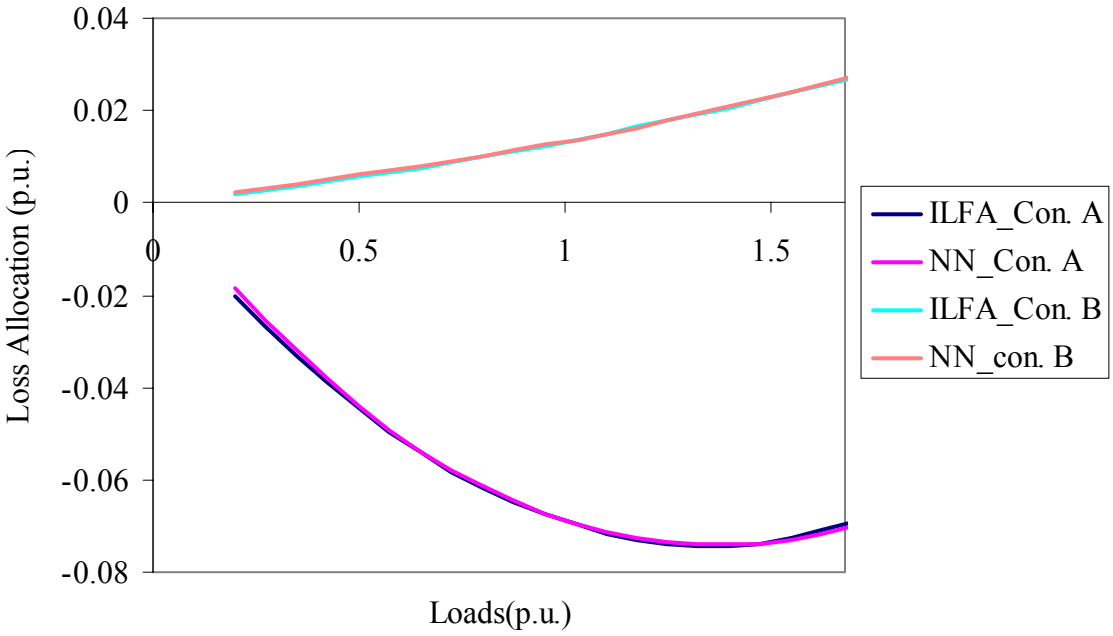

Fig. 5.5: Real loss allocation for a peak hour when all lines are available.

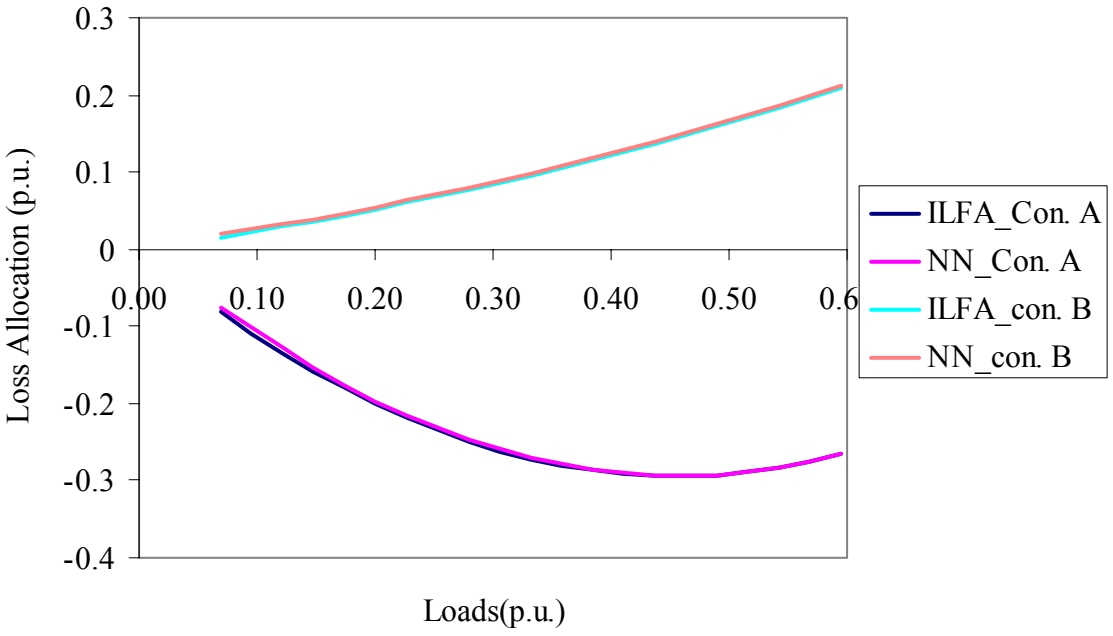

Fig. 5.6: Reactive loss allocation for a peak hour when all lines are available.

Figures 5.7 and 5.8 show real and reactive loss allocation for an off-peak hour when all lines are available. The system load at this hour was 1166 MW and 207.1 MVAR.

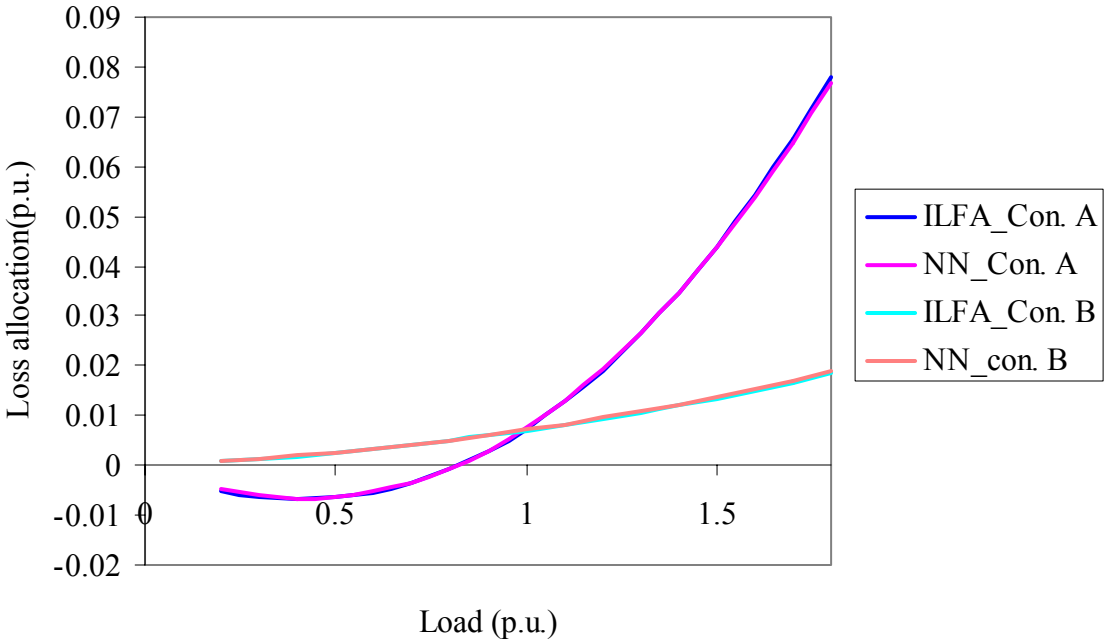

Fig. 5.7: Real loss allocation for an off-peak hour when all lines are available.

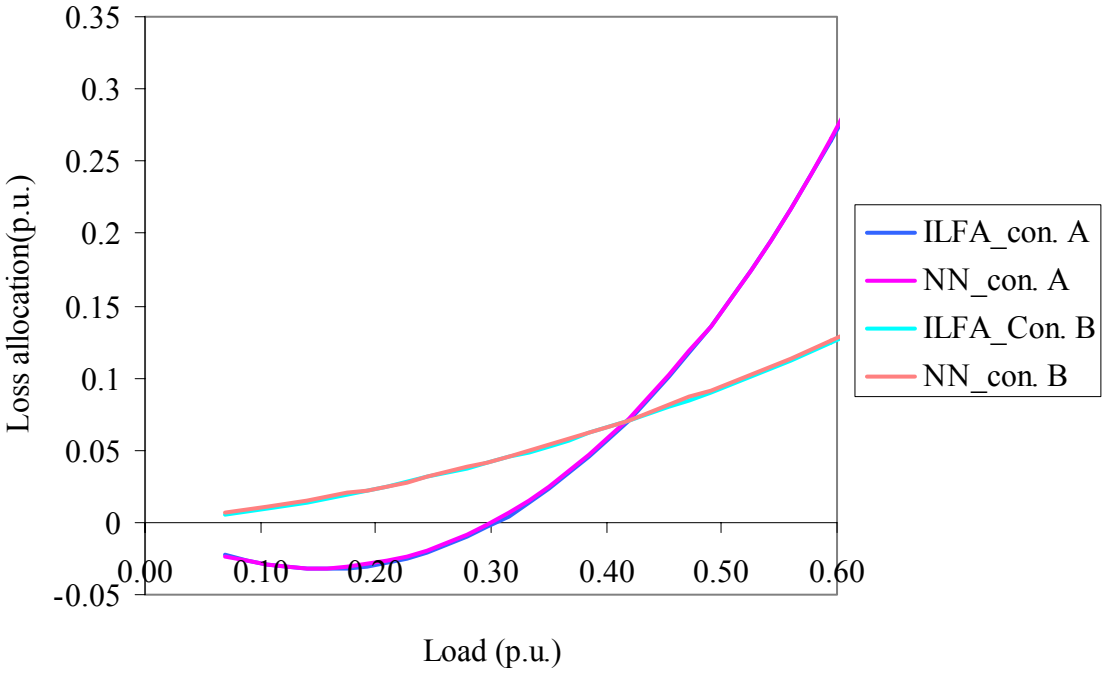

Fig. 5.8: Reactive loss allocation for an off-peak hour when all lines are available.

Figures 5.9 and 5.10 show real and reactive loss allocations respectively during the failure of Line# 1 when the system load was 2494 MW and 505.7 MVAR.

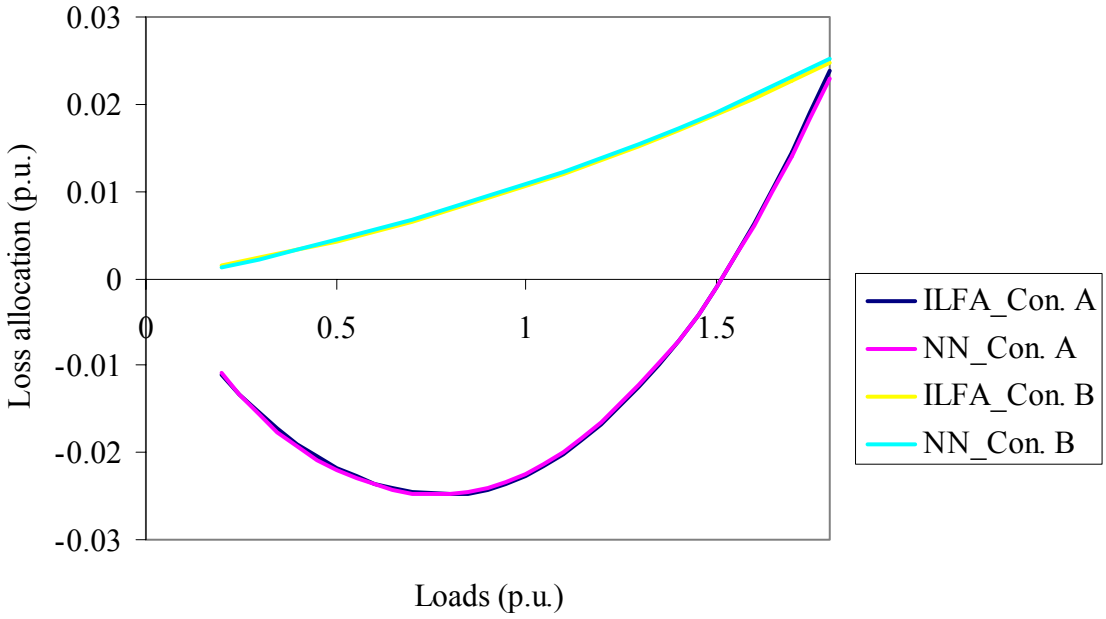

Fig. 5.9: Real loss allocation for a peak hour during failure of Line # 1.

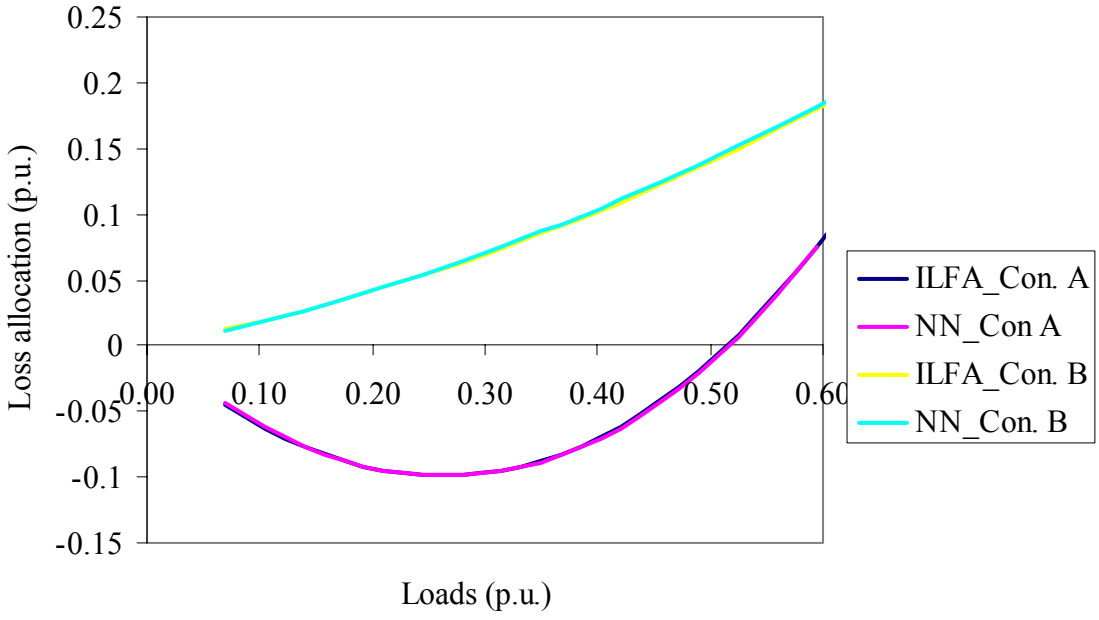

Fig. 5.10: Reactive loss allocation for a peak hour during failure of Line # 1.

Figures 5.11 & 5.12 show real and reactive loss allocations during the failure of Line# 4 when the system load was 2494MW and 505.7 MVAR.

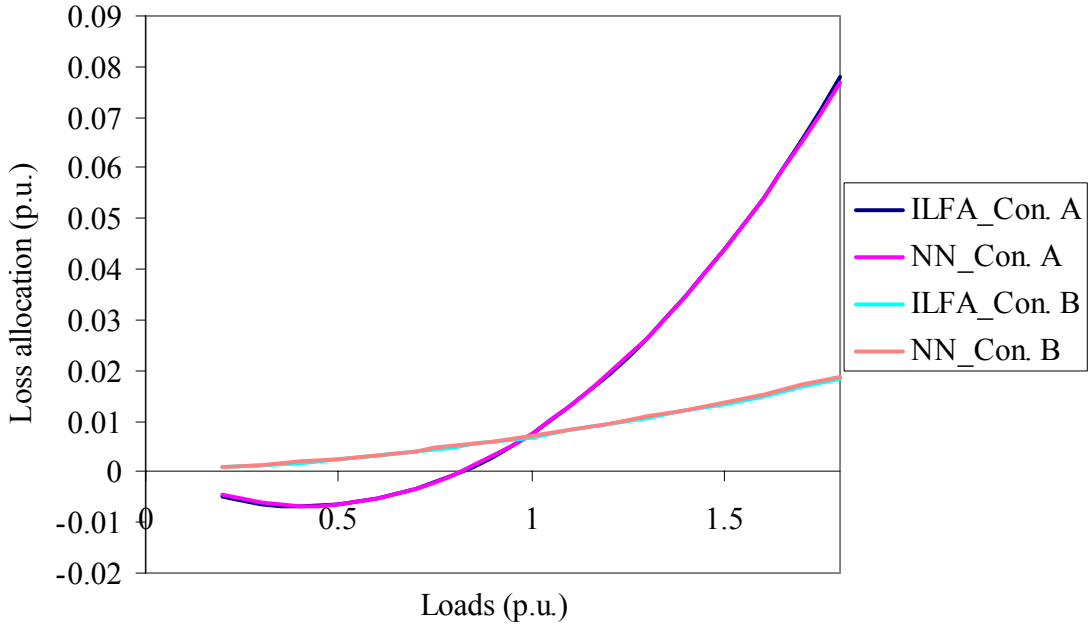

Fig. 5.11: Real loss allocation during failure of Line# 4

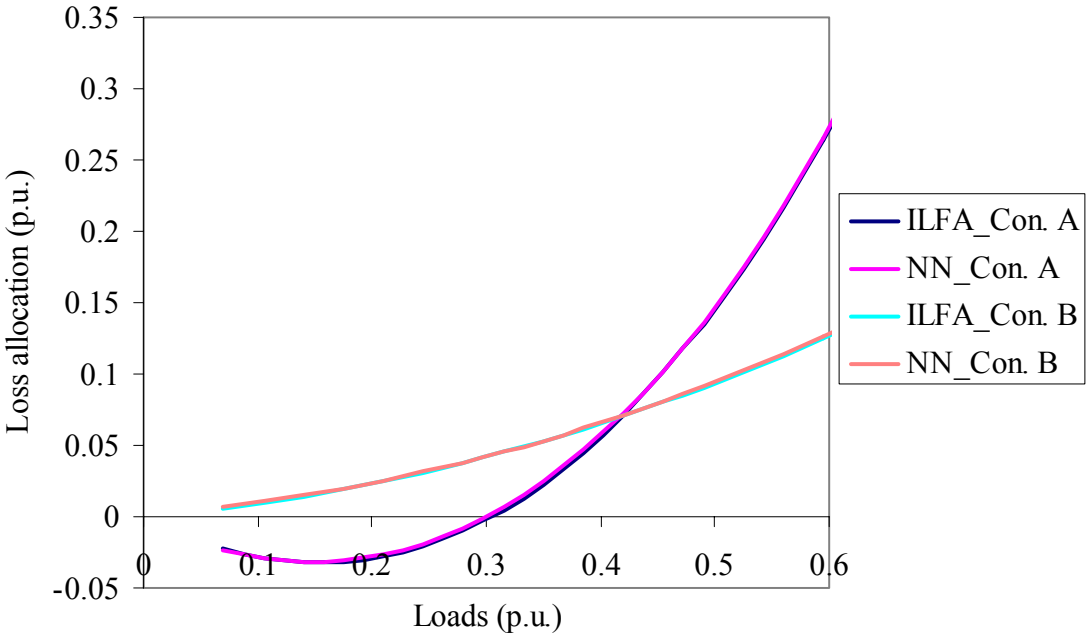

Fig. 5.12: Reactive loss allocation during failure of Line # 4

Figures 5.13 & 5.14 show real and reactive loss allocations respectively for an off-peak hour when Line# 2 was unavailable. The system load at this hour was 1221 MW and 226.6 MVAR.

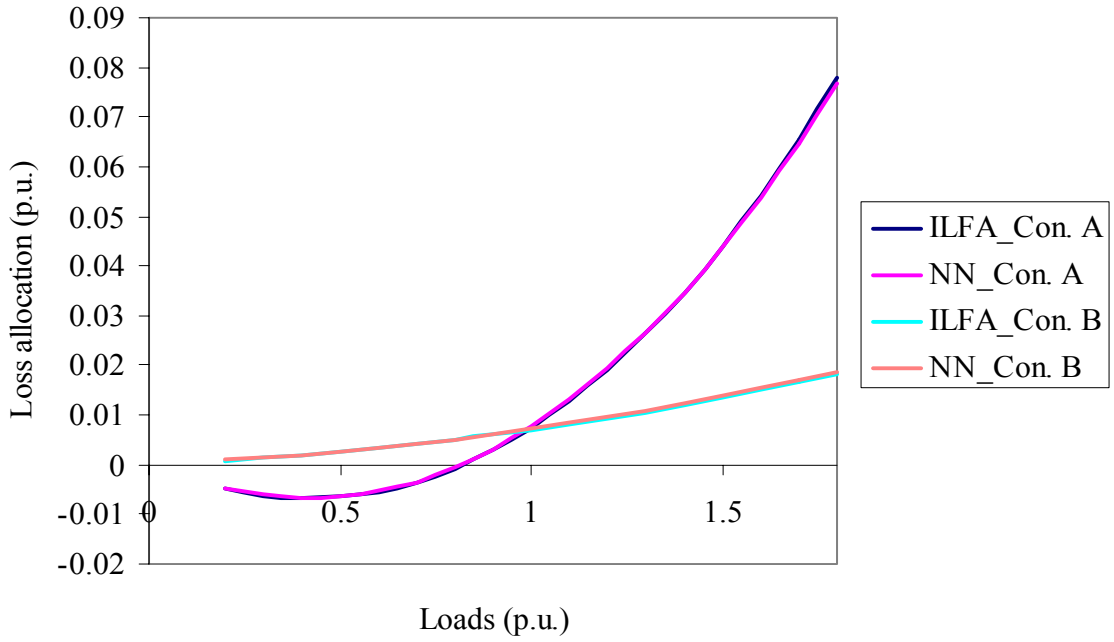

Fig. 5.13: Real loss allocation for off-peak hour during failure of Line # 2

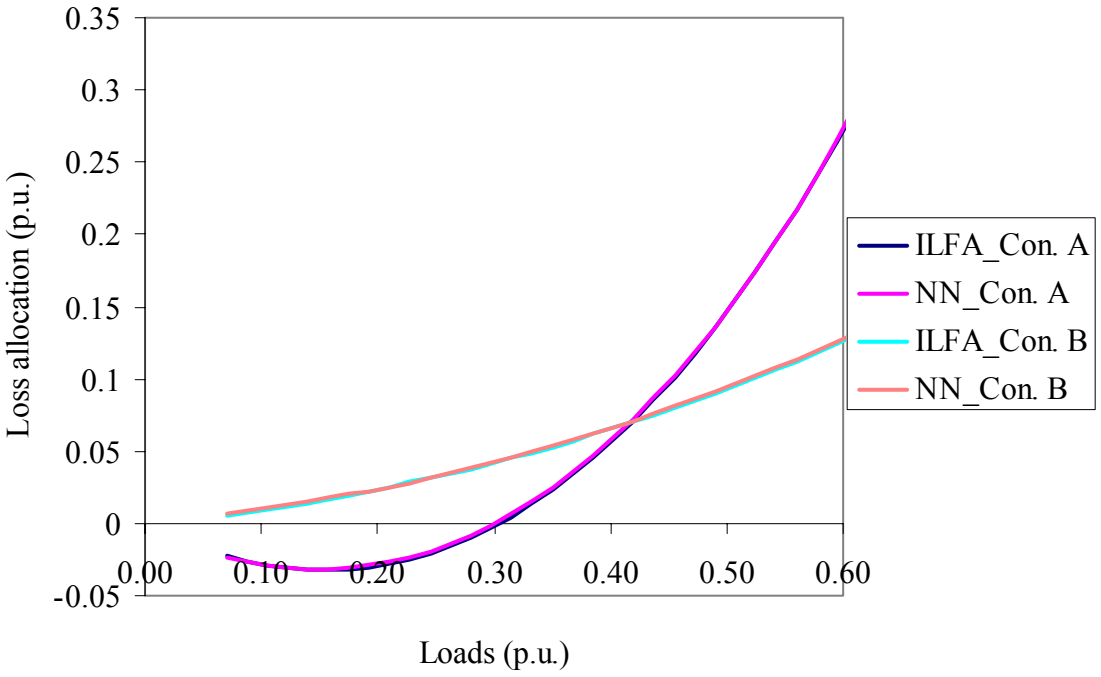

Fig.5.14: Reactive loss allocation for off peak hour during failure of Line # 2

Figures 5.15 & 5.16 show real and reactive loss allocations respectively during the failure of Line # 7 when the system load was 2420 MW and 420.9 MVAR.

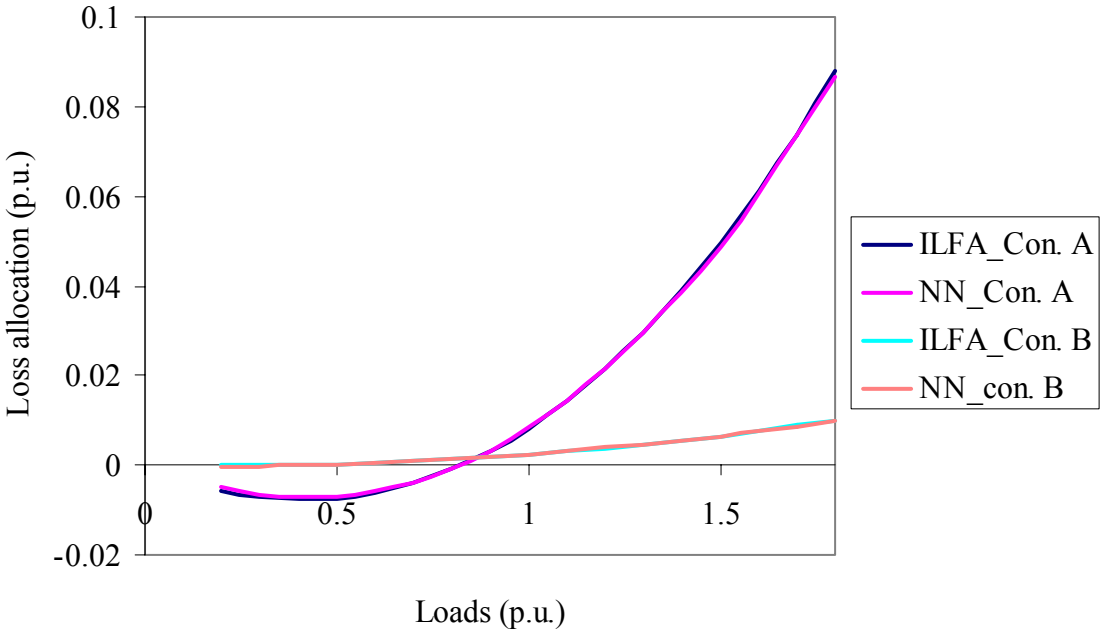

Fig.5.15: Real loss allocation during failure of Line # 7

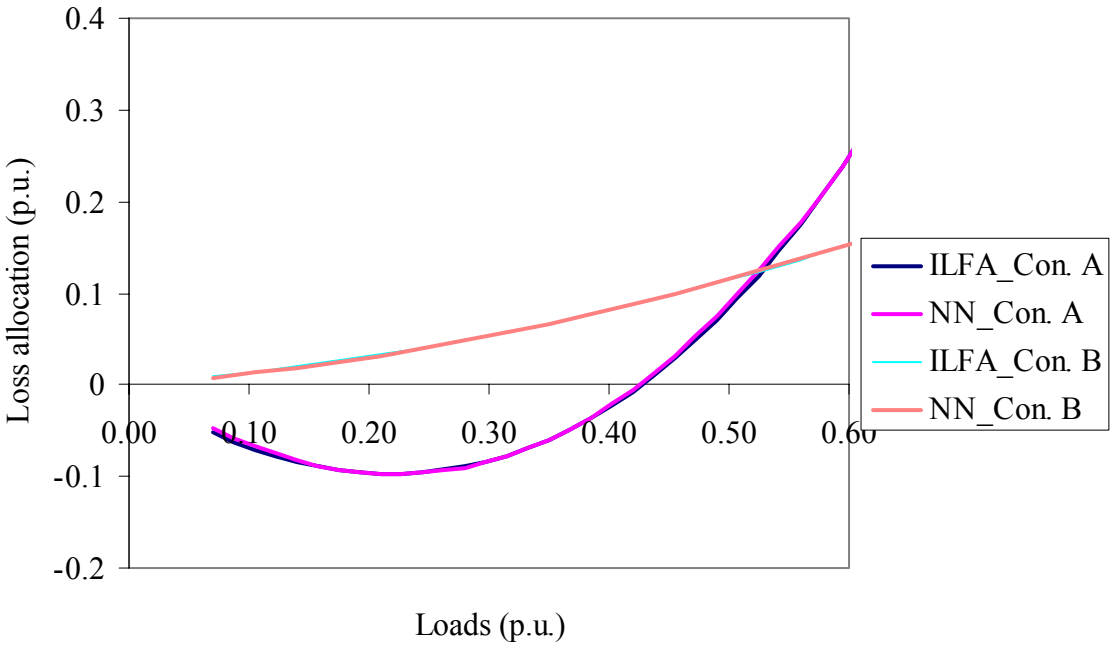

Fig.5.16: Reactive loss allocation during failure of Line # 7

It was noticed in Figures 5.5 to 5.16 that the results obtained by the trained ANN are in good agreement with the results obtained using the ILFA even during the failure of a transmission line.

5.9 Summary

In the previous chapter it was shown that the proposed ANN can allocate transmission losses for bilateral contracts in a deregulated power system. The ANN however, does not work if there is any change in the power system network due to the unavailability of a transmission line. In this chapter a modified ANN was presented that work even during the unavailability of a transmission line. To accomplish this, the status of the transmission lines had been used as inputs to the ANN.

Transmission loss allocations were computed by utilizing the ILFA and the proposed ANN. Two bilateral contracts were considered for the IEEE 24-bus reliability test system that consists of 10 generator buses, 15 load buses and 38 transmission lines. The status of selected transmission lines were utilized as inputs to the proposed ANN. The system operates as a pool with typical 24 hour load variations from 116.6 MW and 207.1 MVAR to 2494 MW and 505.7 MVAR. Loss allocations for bilateral contracts were assessed with variable load demand from 20 MW to 185 MW. Transmission losses were allocated to two bilateral contracts for 1840 test patterns utilizing both the ILFA and the trained ANN. Results obtained from both methods were compared graphically in Figures 5.5 to 5.16. It can be easily inferred from those figures that the trained ANN could allocate losses to bilateral contracts with very good accuracy.

CHAPTER 6: LOSS ALLOCATION IN A POOL DISPATCH

6.1 Introduction

Deregulation has brought many different market configurations in the electricity business. Transaction of electric energy may take many forms, like bilateral contracts, power exchange or power pool. Power pool is the most common form of market due to its simple structure. Generating utilities or IPPs and customers both bid for selling and buying power at the power pool. In some power pool, ISO or RMO allocates transmission loss to both buyer (load) and supplier (generator) in a previously agreed upon procedure. In other jurisdictions, the system operator allocates the losses to supplier (generator) only. In both cases, allocation of transmission loss is a complex task due to the fact that transmission loss is a non-linear and non-separable entity.

However, in the absence of a closed form solution for this problem, different electric utilities use different methods for loss allocation in a pool dispatch. Alberta Electric System Operator (AESO) uses *marginal loss approach* [44], Brazilian System Operator (ONS) uses *linear approximation of line losses* [45] and power pool of Mainland Spain and England use *pro rata technique* [6]. Some other methods are: (i) proportional sharing; (ii) incremental loss coefficient; (iii) z-bus allocation; (iv) average loss calculation method; (v) location-specific pricing; (vi) opportunity cost pricing.

Electrical energy cannot be stored directly and mass storage in other forms like chemical form (dc battery), potential energy (pump hydro generation) or compressed gas form involves enormous amount of money and requires huge generation capacity to reproduce electricity from stored energy. Due to this fact electrical energy has to be consumed as it is produced and therefore all decisions related to the production of electricity have to be made instantly. If a generator has to produce contracted load and corresponding transmission loss, it has to know its share of transmission loss at every instant. Unfortunately most of the methods of loss allocation mentioned above involve

complex mathematical operations and require huge computation time. In this chapter, an Artificial Neural Network (ANN) is proposed that can be used as a tool that can assess loss allocation in a power pool. The proposed ANN has been illustrated with numerical example and its results have been compared with parent method of loss allocation. In this chapter *Z-bus allocation* method has been selected as a teacher for the ANN. The ANN was trained and tested with the IEEE 14-bus test system.

6.2 Z-bus allocation

The goal of any loss allocation method is to take a solved power flow and systematically distribute the system transmission losses to all participating generators and loads. Z-bus allocation uses bus impedance matrix and injected bus current and allocate the system losses to all the buses. If a bus contains both generator and load, then the loss allocated to that bus is divided among the generator and the load using *pro rata* technique. Z-bus allocation is concerned with net real power injection at buses and total real power loss of the system.

Let P_{loss} = total system loss (real)

n = total number of buses

L_k = real loss allocated to Bus k

$$P_{loss} = \sum_{k=1}^{n} L_k \qquad \ldots \quad \ldots \quad \ldots \quad \ldots \quad (6.1)$$

To calculate L_k according to Z-bus allocation method, let us consider the network admittance matrix,

$$Y = G + jB \qquad \ldots \quad \ldots \quad \ldots \quad \ldots \quad (6.2)$$

Inverting Equation (6.2) we get Z-bus matrix as follows:

$$Z = Y^{-1} = R + jX \qquad \ldots \quad \ldots \quad \ldots \quad \ldots \quad (6.3)$$

Since total system loss is the sum of power injections at all buses, P_{loss} can be found as:

$$P_{loss} + jQ_{loss} = \sum_{k=1}^{n} V_k I_k^{*} \qquad \ldots \quad \ldots \quad \ldots \quad \ldots \quad (6.4)$$

where Q_{loss}= reactive component of the system loss

Therefore the real part of the system loss is

$$P_{loss} = \Re\left\{\sum_{k=1}^{n} V_k I_k^*\right\} \quad \ldots \quad \ldots \quad \ldots \quad \ldots \quad (6.5)$$

$$\text{Or } P_{loss} = \Re\left\{\sum_{k=1}^{n} I_k^*\left(\sum_{j=1}^{n} Z_{kj} I_j\right)\right\} \quad \ldots \quad \ldots \quad \ldots \quad \ldots \quad (6.6)$$

$$\text{Or } P_{loss} = \Re\left\{\sum_{k=1}^{n} I_k^*\left(\sum_{j=1}^{n} R_{kj} I_j\right)\right\} + \Re\left\{\sum_{k=1}^{n} I_k^*\left(\sum_{j=1}^{n} jX_{kj} I_j\right)\right\} \quad \ldots \quad \ldots \quad (6.7)$$

Since matrix X is symmetric, the 2nd term of Equation (6.7) becomes zero. So,

$$P_{loss} = \Re\left\{\sum_{k=1}^{n} I_k^*\left(\sum_{j=1}^{n} R_{kj} I_j\right)\right\} \quad \ldots \quad \ldots \quad \ldots \quad (6.8)$$

From Equations (6.1) and (6.8), L_k can be expressed as

$$L_k = \Re\left\{I_k^*\left(\sum_{j=1}^{n} R_{kj} I_j\right)\right\} \quad \ldots \quad \ldots \quad \ldots \quad (6.9)$$

If both demand, $P_{dk,}$ and generation, $P_{gk,}$ exist in the same Bus, k, then loss component L_k is further divided among the two using Pro Rata technique.

$$\text{Let } \gamma_k = \frac{P_{gk}}{P_{gk} - P_{dk}} \quad \ldots \quad \ldots \quad \ldots \quad (6.10)$$

Generator's share of loss component L_k is $\gamma_k L_k$ and load's share is $(1-\gamma_k)L_k$

6.3 Test system

The IEEE 14-bus network shown in Figure 6.1 was utilized as a test system to illustrate numerical example on Z-bus allocation. The system has loads on 13 buses, generations on 2 buses and synchronous condenser on 3 buses. Line data for the system are shown in Table 6.1. Two cases were considered for the system. First, the system was studied with load and generation data as shown in Table 6.2 which was taken from Reference [7] and later the system was studied with typical 24 hour load patterns for weekdays and weekends.

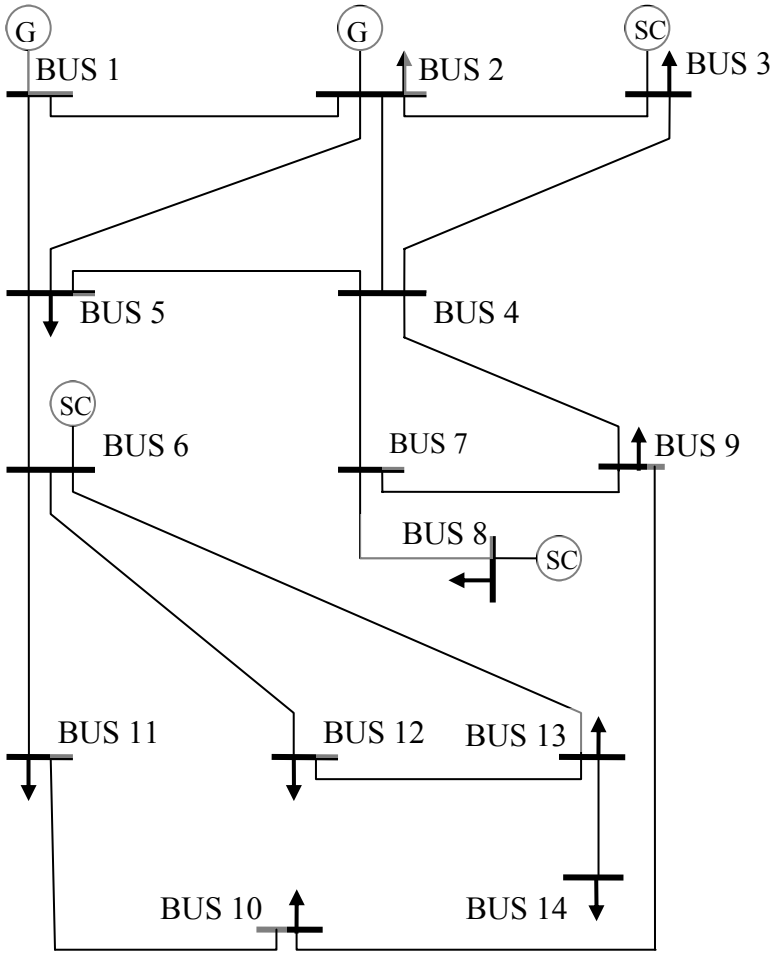

Fig. 6.1: The IEEE 14-bus network

Table 6.1: Line parameter for the 14-bus IEEE network

Line No.	From bus	To bus	R (p.u)	X (p.u.)	B (p.u.)
1	1	2	0.0194	0.0592	0.0528
2	1	5	0.0540	0.2230	0.0528
3	2	3	0.0470	0.1980	0.0438
4	2	4	0.0581	0.1763	0.0374
5	2	5	0.0570	0.1739	0.0340
6	3	4	0.0670	0.1710	0.0346
7	5	4	0.0134	0.0421	0.0128
8	4	7	0.0001	0.2091	0
9	4	9	0.0001	0.5562	0
10	5	6	0.0001	0.2520	0
11	6	11	0.0950	0.1989	0
12	6	12	0.1229	0.2558	0
13	6	13	0.0662	0.1303	0
14	7	8	0.0001	0.1762	0
15	7	9	0.0001	0.1100	0
16	9	10	0.0318	0.0845	0
17	9	14	0.1271	0.2704	0
18	10	11	0.0820	0.1921	0
19	12	13	0.2209	0.1999	0
20	13	14	0.1709	0.3480	0

Table 6.2: Load and generation data for the 14-bus IEEE system [3]

Bus no.	Generation	Load	
	Real (p.u.)	Real (p.u.)	Reactive (p.u.)
1	2.236	0.000	0.000
2	0.040	0.217	0.127
3	0.000	0.942	0.190
4	0.000	0.478	0.039
5	0.000	0.076	0.018
6	0.000	0.112	0.075
7	0.000	0.000	0.000
8	0.000	0.010	0.000
9	0.000	0.295	0.166
10	0.000	0.090	0.058
11	0.000	0.035	0.018
12	0.000	0.061	0.016
13	0.000	0.135	0.058
14	0.000	0.149	0.050

The data for a typical 24-hour load variation were taken from California ISO [10]. The system load was varied from 149.4 MW and 43.2 MVAR to 303.3 MW and 90.6 MVAR. 24-hour real and reactive loads on different buses of the system for weekdays are shown in Figures 6.2 and 6.3. Base quantities were 138 KV and 100 MVA. Bus voltage magnitudes of voltage control buses for the first case were (in p.u.): V_1=1.060, V_2=1.045, V_3=1.010, V_6=1.070, V_8=1.090. In the second case, voltage magnitudes of all voltage control buses were varied from 1.020 p.u. to 1.080 p.u.

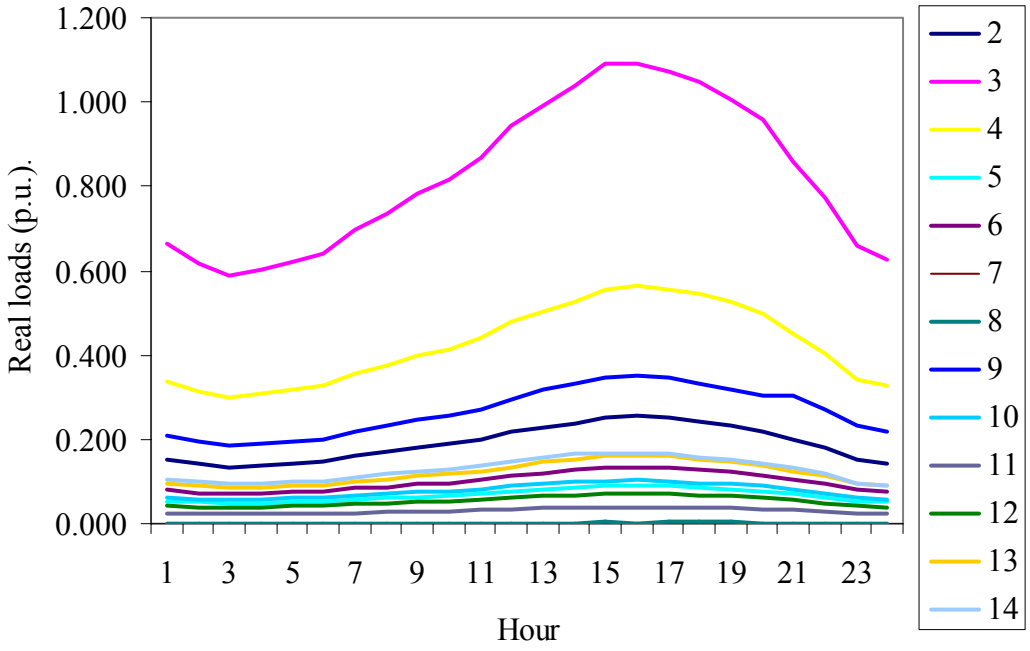

Fig.6.2: 24 hour real loads on different buses for the test system on weekdays

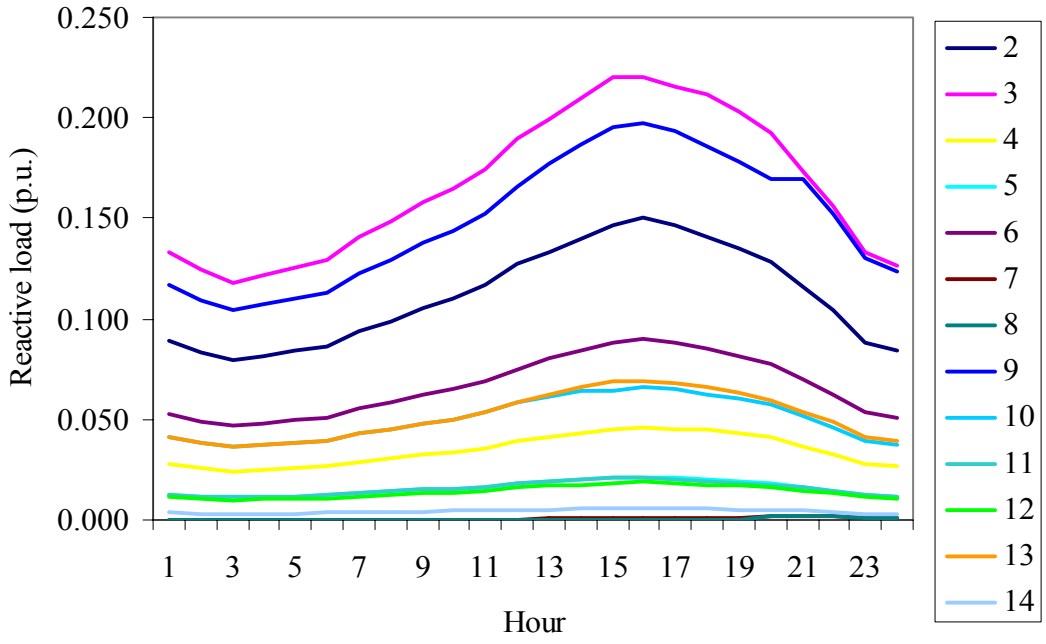

Fig.6.3: 24 hour total reactive loads on different buses for the test system on weekdays

6.4 Proposed Artificial Neural Network

A feed forward neural network was developed to allocate transmission losses to generators and loads for the test system in the context of a deregulated pool dispatch. The proposed network was trained with training patterns obtained using Z-bus allocation technique. The architecture of a neural network is partly fixed by its inputs and outputs and partly by the number of hidden layers and the number of neurons in it. Since the test system described in Section 6.3 has 14 buses, and we are only concern with the real parts of losses, the proposed ANN has 14 outputs corresponding to the real losses for 14 buses. Almost all system variables of the test system were utilized as input to the neural network to make the ANN responsive to all practical situations. All real and reactive loads and real generations at all buses and voltage magnitudes of the voltage control buses were used as inputs to the neural network. Other than the operational variables of the test system, transmission line status (whether line is available or failed) was also used as inputs to the ANN. To keep the size of the ANN manageable, only status of those transmission lines were selected that fall into the category described in Section 5.5. To do this selection, load flow analyses and loss allocation using Z-bus method were performed for each transmission line contingency. Status of some transmission lines were ignored if their unavailability makes the bus voltage unstable. Transmission Line #1 falls into this category. Status of some transmission lines were also ignored whose failures have insignificant impact on loss allocation. Unavailability of transmission Lines 5, 9, 11, 12, 16, 17, 18, 19 were ignored for this reason. Two more transmission line (Lines14, 20) status were not considered as inputs due to the fact that some loads could not be supplied without those lines. Therefore, the status of the remaining transmission Lines 2, 3, 4, 6, 7, 8, 10, 13 and 15 were used as inputs to the network. The proposed neural network has 42 inputs and 14 outputs which are described in Table 6.3.

Table 6.3: Description of inputs and outputs of ANN for loss allocation for pool dispatch

Layer	Neurons	Description
Input	I_1-I_2	Real power generation (p.u.)
	I_3-I_7	Bus voltage magnitude (p.u)
	I_8-I_{20}	Real loads (p.u.)
	I_{21}-I_{33}	Reactive load (p.u.)
	I_{34}-I_{42}	Status of transmission lines
Output	O_1-O_{14}	Real loss allocation for buses

A single layer of hidden neuron was considered due to its simplicity of weights and threshold updates. Since there is no 'rule of thumb' to determine the optimal number of hidden neurons [34], this task was approached by repeatedly training the neural network with different number of hidden neurons and identifying the optimal number of hidden neurons from the one that yielded the best convergence characteristics and lowest mean square error for the test patterns. However, for a single hidden layer, the optimum number of hidden neurons lies between *n* to *2n*, where n is the number of inputs [43]. With several trials it was found that the network with 67 hidden neurons has the best performance. Figure 6.4 shows convergence characteristics for different number of hidden neurons. Hyperbolic tangent functions were used as activation functions for hidden and output layers. A hyperbolic tangent function can be easily matched the output by simply changing its amplitudes.

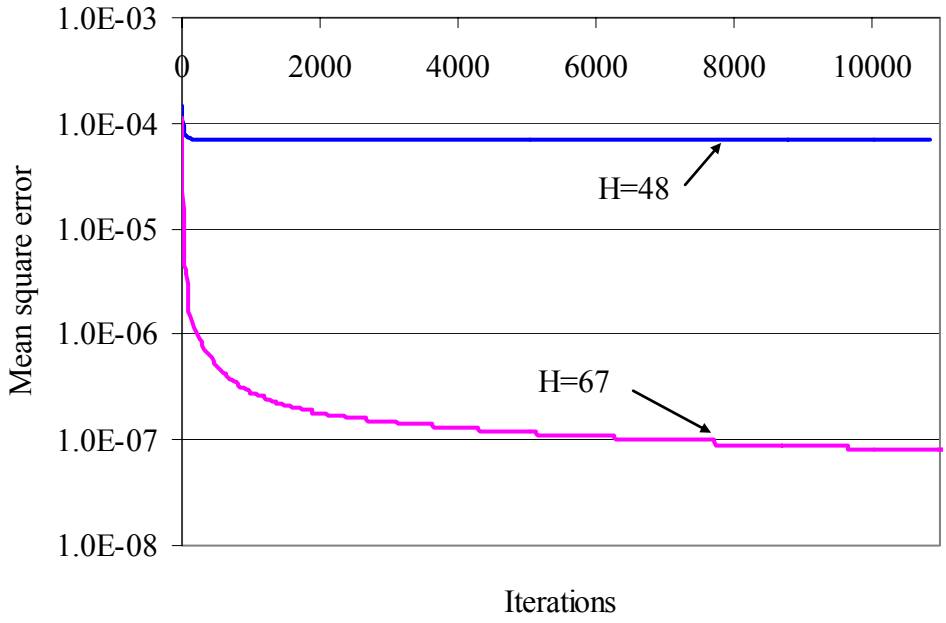

Fig. 6.4: Convergence characteristics with different number of hidden neurons.

6.5 Learning and Testing of ANN

The proposed ANN was trained with steepest descent supervised learning algorithm while the Z-bus allocation method was used as a teacher. Because of its simplicity of weight updates, back propagation was utilized to train the network. 2800 training and 506 testing patterns were generated utilizing Z-bus allocation for the training and testing of the ANN. In order to generate test patterns, load and generation at all busses were varied according to the 24 hour load patterns on weekdays and weekend, and the voltage magnitudes at the voltage control buses were varied from 1.03 to 1.09.

During the training it was observed that with a single activation function, learning does not converge to a good accuracy level. It was also observed that the loss allocation for Bus 1 is about 3500 times than that of Bus 7, about 312 times that of Bus 8, and about 89 times that of Bus 5 & 11. Therefore, with a single activation function, adjustment of weights to match target outputs became difficult. Therefore, the outputs were categorized in 9 different levels according to their maximum values. Accordingly nine activation functions were used in the output layer. The amplitudes of these 9 activation functions were 0.25 for Output 1 (for Bus 1), 0.16 for Output 3, 0.06 for Output 6, 0.025

for Output 4 & 9, 0.012 for Output 13 & 14, 0.006 for Output 2, 10 &12, 0.0028 for Output 5 & 11, 0.0008 for Output 8 and 0.00007 for Output 7. Although in Reference [7] the load in Bus 7 was considered zero, a small amount of real load was considered in some hours in a 24-hour load pattern. Therefore, very small amount of loss was allocated to this bus. Using nine activation functions in the output layer, the MSE converged to 3.5 x 10^{-8} in 46026 iterations. Figure 6.5 shows convergence characteristics with single and nine activation functions.

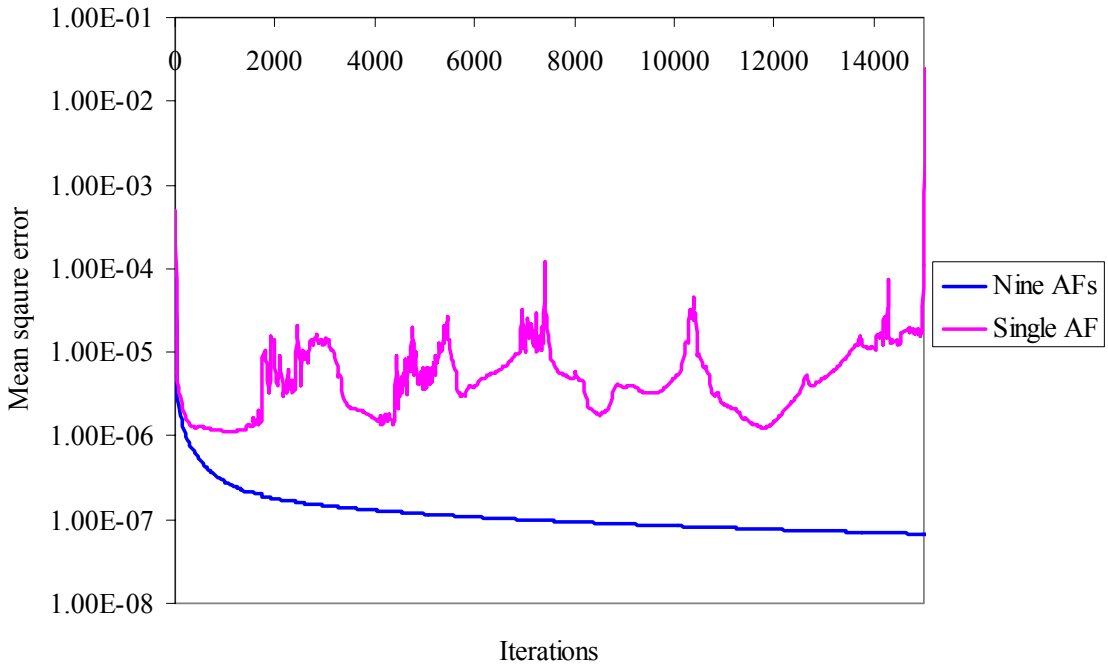

Fig. 6.5: Convergence with single and nine activation functions

A value of 0.61 was used for 'b' in all activation functions used in the hidden and the output layers. 0.25 was chosen as the amplitudes for the activation function used in the hidden layer. A value of $3.5x10^{-8}$ was used as a target for MSE to check for the convergence. Other selected parameters for the neural network were: initial learning rate (η) = 0.85, momentum factor (α) = 0.48 and step size (γ) = 0.85.

Outputs of test patterns obtained from the trained ANN and Z-bus allocation method were compared. Unavailability of lines was simulated to check the performance of the trained ANN during the failure of a line. Table 6.4 shows loss allocation for the given

data in Reference [7]. Columns 2 and 3 of Table 6.4 show the loss allocation obtained from Z-bus allocation and the trained ANN respectively for all 14 buses when all lines were available.

Table 6.4: Loss allocation for given data in Reference [7]

Bus No.	Z-bus loss allocation (p.u)	Neural network loss allocation (p.u.)
1	0.0771	0.0772
2	0.0014	0.0017
3	0.0284	0.0275
4	0.0087	0.0086
5	0.0007	0.0008
6	0.0041	0.0040
7	0.0000	0.0000
8	-0.0004	-0.0002
9	0.0057	0.0058
10	0.0019	0.0020
11	0.0006	0.0006
12	0.0010	0.0011
13	0.0027	0.0028
14	0.0047	0.0043

From Table 6.4, it can be easily noticed that loss allocation for Buses 1, 3, 4, & 9 are much greater compared to other buses. Therefore, these buses were chosen to compare loss allocation between Z-bus and the proposed ANN at different hours of the day with different configuration of the network due to the unavailability of transmission lines. Figure 6.6 shows loss allocation by Z-bus and the ANN for selected buses (Buses 1, 3, 4, 9) when all transmission lines were available.

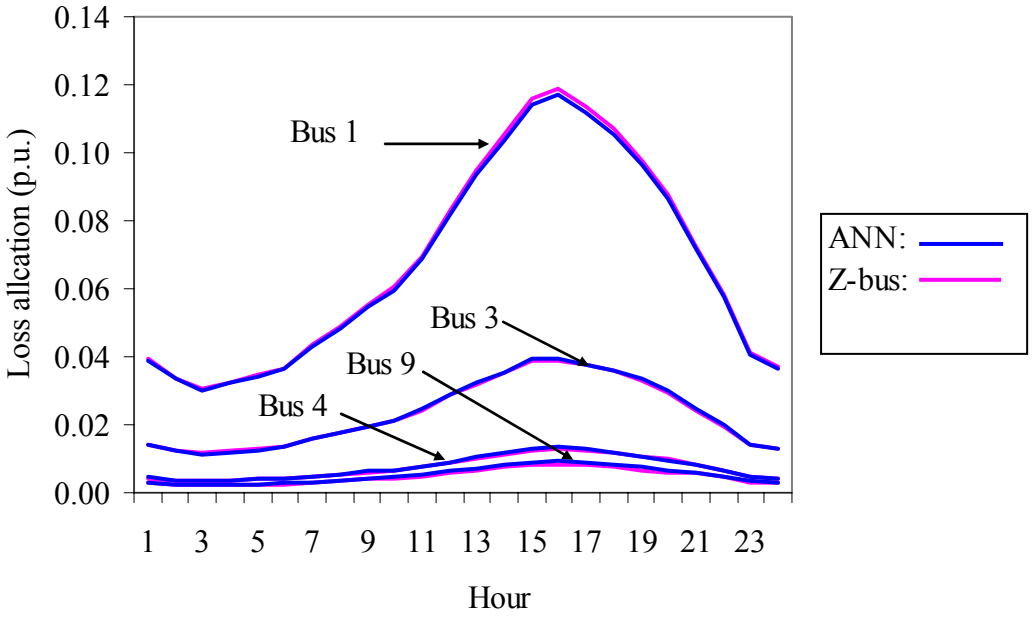

Fig. 6.6: Loss allocations for Buses 1, 3, 4, 9 when all lines are available

Figures 6.6-6.10 show loss allocations during the unavailability of different transmission lines.

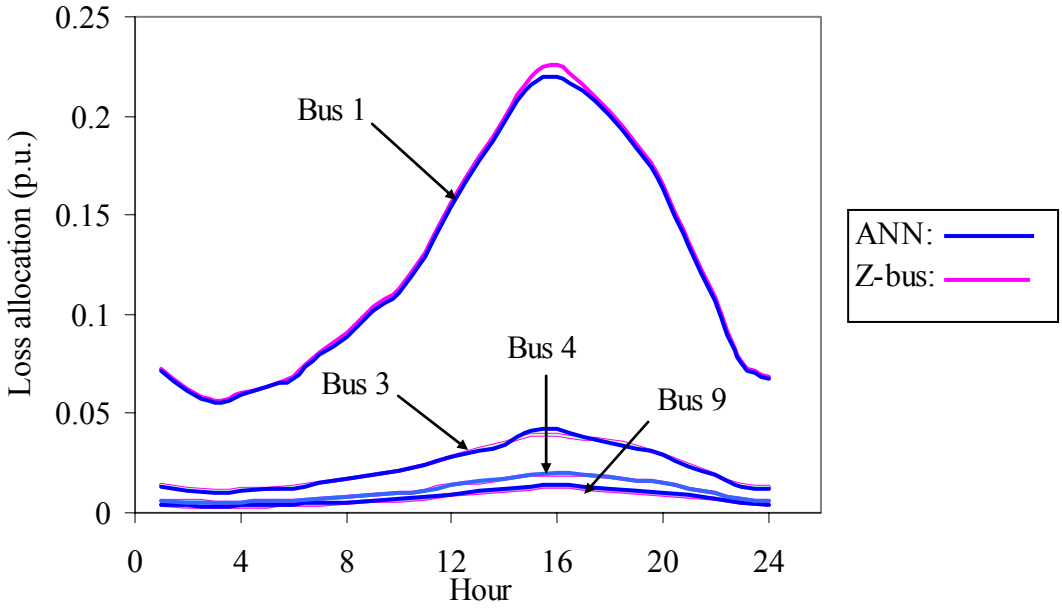

Fig. 6.7: Loss allocations for Buses 1, 3, 4 & 9 during the failure of Line 2

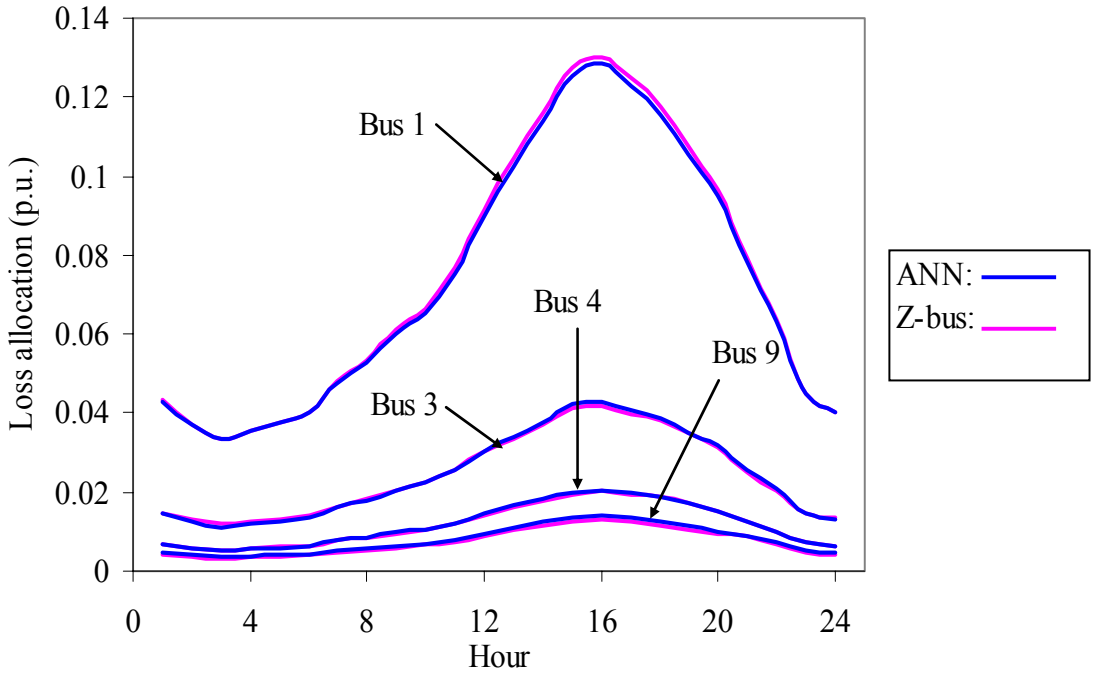

Fig. 6.8: Loss allocations for Buses 1, 3, 4 & 9 during the failure of Line 4

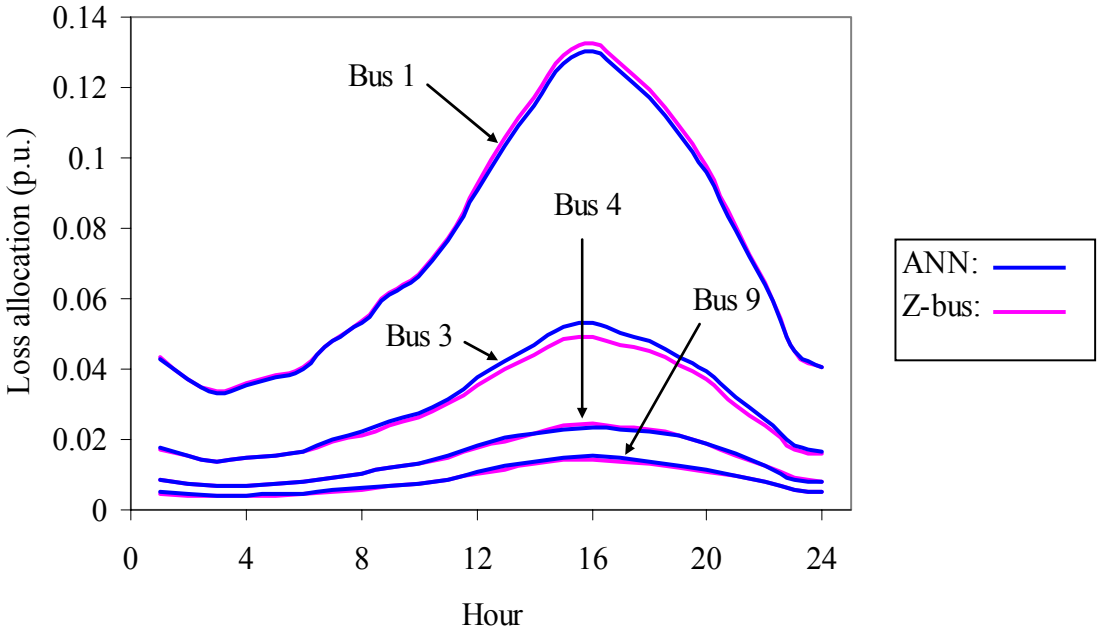

Fig. 6.9: Loss allocations during the failure of Line 7

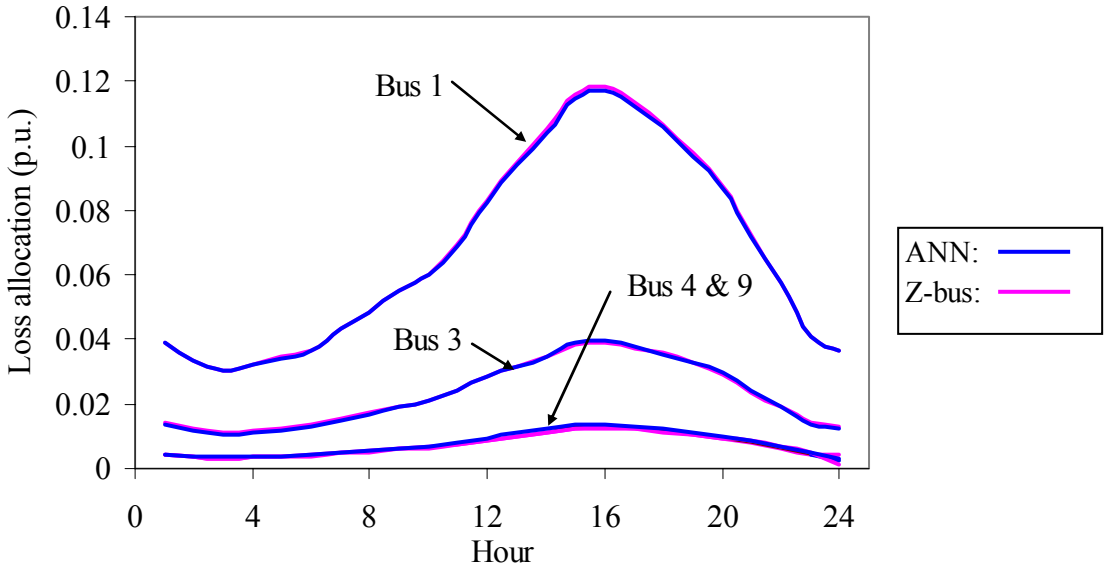

Fig. 6.10: Loss allocations during failure of Line 8

From Table 6.4 and Figures 6.6-6.10, it is evident that Bus 1 is responsible for more than 55% of the transmission loss. Therefore, loss allocation for Bus 1 obtained by both Z-bus and the proposed ANN were investigated for all possible line failures and the results are shown in Figure 6.11.

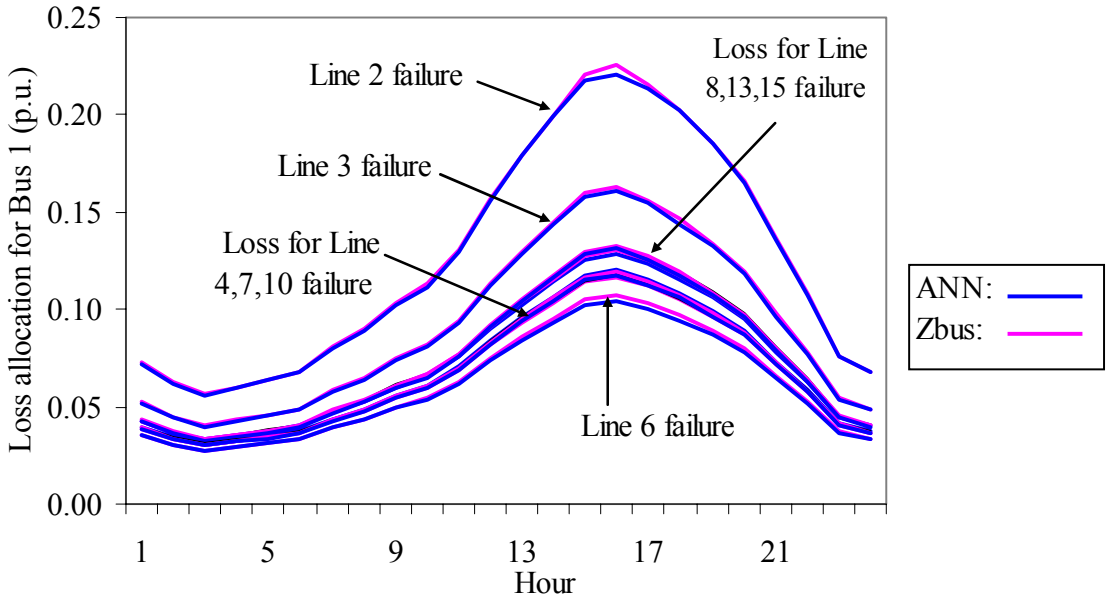

Fig.6.11: Loss allocation for Bus 1 for different line failures

Table 6.4 shows that proposed neural network can be utilized to allocate losses in a pool dispatch as well. Figures 6.6-6.11 show that the proposed ANN is very accurate in loss allocation under different loading conditions even when a transmission line is unavailable.

6.6 Summary

In Chapters 4 & 5, it was shown that artificial neural network can be utilized to allocate transmission losses to bilateral contracts in a deregulated power system. In this chapter transmission loss allocation in the context of a pool dispatch was presented. An ANN was developed, trained and tested to allocate losses to generators and loads in a pool dispatch. The IEEE 14-bus system was considered as test system to provide numerical examples. First, Z-bus allocation was utilized to allocate real part of the transmission loss to generators and loads. Using Z-bus allocation as a teacher, an ANN was developed and trained to do the same job. The ANN was developed in such a way that it can allocate transmission loss even during the unavailability of a transmission line. The proposed ANN was tested with 506 test patterns which were developed considering all possible variation of the independent variables of the test system. Loss allocations for the test patterns were computed by both Z-bus and the trained ANN and results were compared. Results obtained from both methods show that proposed ANN can allocate transmission losses to generators and loads with good accuracy. All selected transmission lines were made unavailable one at a time to check whether the proposed ANN can work during the failure or shut down of line. Study showed that the trained ANN can work without any modification during the failure of transmission line. Although Z-bus allocation was utilized to generate training and testing patterns and the loss allocation computed by the trained ANN matched very closely to those obtained by Z-bus allocation, any other allocation procedure agreed upon by all stack holders can be utilized for this purpose and the proposed ANN can be trained accordingly.

CHAPTER 7: CONCLUSIONS

7.1 Conclusions

A new transmission loss allocation tool based on artificial neural networks has been developed. The proposed artificial neural networks can simulate transmission loss allocation determined by Incremental Load Flow Approach (ILFA) and Z-bus allocation techniques. For loss allocations to bilateral contracts, the ILFA was used as a teacher to train the proposed neural network. The developed ANN was tested with the 24-bus IEEE reliability test system with two bilateral contracts. Results obtained from the ILFA and the proposed ANN was compared for various loading conditions. It was found that the proposed ANN can allocate transmission loss to bilateral contracts with good accuracy. The ANN was designed to handle loss allocation even under single transmission contingency provided the contingency does not threaten voltage stability during the bilateral transaction. The proposed ANN can be trained with little difficulty for large power system network. The trained ANN can provide solution in a quick manner. The proposed ANN can yield negative loss allocation to reward generators or loads that cause counter flow in the network. Although the ILFA was utilized to generate training data, any other method of loss allocation can be utilized for that purpose.

A major disadvantage of a neural network is that it is depended on the architecture of a power system network. Its configuration would change whenever a transmission line becomes unavailable due to maintenance or line failure. As a consequence, the ANN has to be retrained. To avoid retraining, an ANN was developed to handle the unavailability of a transmission line. To accomplish this objective, transmission line status (available /unavailable) was added to the input vector of the neural network. With the inclusion of line status, the developed ANN was able to allocate losses to all parties accurately even during a transmission line outage. Unlike other inputs e.g. loads, generations, bus voltages which are directly used in p.u., each line was given a binary status, ‘0’ if available and ‘1’ if failed. Inclusion of line status in the input vector,

however, created another problem. The number of inputs related to line status could be very high in a large system. This could increase the training time tremendously. Extensive loss allocation studies proved that only a few transmission line outages had significant impact on loss allocation. A selection criterion for line status input was developed to identify these lines and to keep the size of the neural network manageable. The status of a line was selected as input if its failure had significant impact on loss allocation but did not threaten system voltage stability nor made the bilateral transaction impossible. Only single level contingency was considered as the probability of two line failures at the same time is negligible. The proposed ANN was developed and tested with the IEEE 24-bus Reliability Test System. The results showed that the developed ANN can allocate real and reactive parts of transmission loss with good accuracy. The training and testing patterns were obtained using the ILFA method. The results obtained from the developed ANN were in good agreement with those obtained using the ILFA. Therefore, an ANN can be used to simulate the loss allocations obtained using the ILFA. The ANN provides results in fast and convenient manner with less mathematical complexity.

In a pool operation, the principle of transmission loss allocation is different than that of bilateral contracts. One of the main objectives of a pool operation is to minimize the operating cost. When the price of energy is set by market clearing price i.e. every suppliers get same price for per unit of energy they supply, the load scheduling is done in such a way that transmission loss is minimized. In a pool operation, transmission loss can be allocated to generators or to both the generators and consumers. In this research, the later topology was used for loss allocation. An artificial neural network was developed and trained to assess the share of loss for each generator and consumer. A feed forward architecture has been chosen for the ANN and the network was trained using back propagation algorithm with enhanced learning technique. Z-bus allocation method was used as a teacher. Since only real part of transmission loss is allocated by the Z-bus allocation method, the output of the developed ANN was designed to provide only real part of transmission loss as well. To make the ANN capable of handling transmission line outage, the status of selected transmission lines were included in the input vector of the ANN. The selection criteria developed in Section 5.5 were used to

keep the size of the ANN manageable. Enhanced learning techniques proved that the ANN could be trained with little difficulty. The developed ANN was tested with typical 24 hour load variation for weekdays and weekends considering transmission line outage on the IEEE 14-bus Reliability Test System. Results obtained from the Z-bus allocation method and the developed ANN showed that the ANN can allocate losses to generators and loads with very good accuracy. Although the Z-bus allocation method was used a teacher to train the neural networks any other allocation method can be used to train the ANN.

Neural networks are usually trained with a huge number of training patterns. It is, therefore, important to speed up the learning process of ANNs. In this research two techniques were developed to enhance convergence speed. In the first technique, multiple activation functions were used at the output layer which had increased the learning speed to a great extent. Multiple activation functions can be used in any ANN where the magnitudes of the output elements are greatly different from each others. This technique also eliminates the requirement of normalization and de-normalization of the outputs. The second technique was used to denote the status of the transmission lines. It was realized that only a little change in the input vector of the ANN due to a line failure had great impact on loss allocation. To incorporate this effect in the ANN, the line failure status was denoted by "5" instead of "1" whereas "no-line-failure" was denoted by "0". This had also improved the speed of convergence. This feature can be used in any ANN where some inputs have stronger co-relation with the outputs compared to other inputs. In addition to these techniques, some other previously reported enhanced learning techniques were also used. They are: proper initialization of synaptic weights and thresholds, adapting learning rate in each weight direction and adapting threshold values. With these techniques the developed ANNs were trained in few hours in FORTRAN platform on a personal computer.

The developed ANNs calculated shares of transmission loss in the order of a few milliseconds. For two bilateral contracts in the IEEE 24-bus systems, the proposed ANN provided loss allocation results in 543 μsec in a 3GHz Pentium IV personal computer. The ILFA took 2.25 sec for the same loss allocation. For a pool operation in

the IEEE 14-bus network, the proposed ANN took 7.9 msec whereas Z-bus allocation took 40 msec to provide the loss allocation results. The proposed ANNs can be trained with other loss allocation procedures acceptable to the stakeholders. The required inputs for the ANN are the standard power system data which are readily available in any power system network. Data can be used directly in p.u. quantity and do not require any normalization. The outputs i.e. share of losses is expressed in p.u. quantity. The proposed artificial neural network approach can be used as an effective tool to allocate transmission loss on a real-time basis. An ANN can be used as a loss meter to calculate aggregate loss for a generator or a load. This feature can also be utilized to resolve the discrepancies between actual loss and recovered loss over a period of time. For example, Average Loss Factor method for loss allocation creates a discrepancy between actual transmission loss and recovered loss [46]. The short fall or excess recovered loss then can be distributed to the stakeholders. The discrepancy accumulated over a time period can be assessed with the help of the loss meter.

In this research the ILFA and Z-bus allocation procedures were used as teachers to train the neural networks but any other loss allocation method acceptable to the stakeholders can also be used to train the neural networks. The ANN based loss allocation method can be implemented in any power system with little difficulty.

7.2 Scope of Future Work

The developed neural networks were designed in such a way that it could handle some changes in power system structure. Changes in a power system structure may happen in many ways. In this research, the change in a power system structure was considered only due to the unavailability of a transmission line. A power system structure may also be changed when a new generation station is added, a new transmission line is built or a new bus is added to the existing system. Techniques can be developed to handle future expansions into an ANN structure to make it a universal structure.

Further research can be carried out to design and develop a hardware to implement ANN based transmission loss allocation. Utilizing this hardware a loss meter similar to a digital energy meter can be developed which will aggregate losses for generators or loads over a period of time.

REFERENCES

[1] URL: http://www.eei.org/industry_issues/industry_overview_and_statistics/history/.

[2] A.R. Bhuiya, "*A Study of Bilateral Contracts in a Deregulated Power System Network*", A Ph.D. thesis, Department of Electrical Engineering, University of Saskatchewan, January 2004.

[3] URL:http://www.thimo.com/.

[4] URL: http://www.nordpool.no/information/reports/Report-Nordic%20Market.pdf

[5] H.H. Happ, "*Cost of Wheeling Methodologies*", IEEE Transactions on Power System, Volume 9, No.1, February 1994, pp. 147-146.

[6] A. J. Conejo, J. M. Arroyo, N. Alguacil, and A. L. Guijarro, "*Transmission Loss Allocation: A Comparison of Different Practical Algorithms",* IEEE Transactions on Power Systems, Volume 17, No. 3, August 2002, pp.571-576.

[7] Antonio J. Conejo, Francisco D. Galiana, and Ivana Kockar, "*Z-Bus Loss Allocation",* IEEE Transactions On Power Systems, Volume 16, No. 1, February 2001, pp.105-110.

[8] R. Allan, D. Kirschen, G.Strbac, *"Contributions of Individual Generators to Loads and Flows", IEEE Transactions on Power Systems,* Volume12, No.1, February 1997, pp.52-60.

[9] J. Bialek "*Topological Generation and Load Distribution Factors for Supplemental Charge Allocation in Transmission Open Access*", IEEE Transactions on Power Systems, Volume12, No.3, Aug 1997, pp.1185-1193.

[10] J.W.M. Cheng, "*Studies of Bilateral Contracts with Respect to Steady-State Security in a Deregulated Environment*", IEEE Transactions on Power Systems, Volume13, No.3, August 1998, pp. 1020-1025.

[11] M.D. Anderson, J. Yang, "*Tracing the Flow of Power in Transmission Networks for Use-of-Transmission System charges and Congestion Management*", IEEE Power Engineering Society Winter Meeting, January 31-February 4, 1999, New York City, New York, USA, pp. 799-805.

[12] R.S. Fang, A.K. David, "*Optimal Dispatch Under Transmission Contracts*", IEEE Transactions on Power Systems, Volume14, No.3, May 1999, pp.732-737.

[13] A.G. Expósito, JMR Santos, TG Garcia and E.A.R Velsaco "*Fair Allocation of Transmission Power Losses"* IEEE Transactions on Power System, Volume11 No.1, February 2000, pp. 184-188.

[14] A.Bhuiya, N.Chowdhury, "*Allocation of Transmission loss in Deregulated Power System Network with Bilateral Contracts"*, 1999 Large Engineering Systems Conference on Power Engineering, Halifax, Nova Scotia, Canada, June 20-22,1999, pp. 220-229.

[15] Hadi Saadat, "*Power System Analysis*", McGraw-Hill, New York, 1999.

[16] M.E. El-Hawary, G.S. Christensen, "*Optimal Economic Operation of Electric Power Systems*", Academic Inc., New York, 1979.

[17] Robert H. Lasseter, Ronghai Wang, "*The Impact Of Generation Mix On Placement Of Static Var Compensators",* IEEE Transactions on Power Delivery, Volume 14, NO. **3,** July 1999, pp. 1018-1023.

[18] Santiago Raymón Y Cajal, "*The Structure and Connexions of Neurons*", Nobel Lecture, December 12, 1906 (URL: http://nobelprize.org/medicine/laureates/1906/cajal-lecture.html).

[19] URL:http://www.enchantedlearning.com/subjects/anatomy/brain/Neuron.shtml.

[20] URL: http://72.14.207.104/search?q=cache:AL2U_ThzqjcJ:coursemain.ee.ukzn.ac.za/enel4aih2/notes/Introduction.doc+Brain+takes+only+10-16+joules+per+operation+per+second&hl=en.

[21] URL: http://www.cs.stir.ac.uk/~lss/NNIntro/InvSlides.html.

[22] S. K. Redlapalli, "*Development of Neural Units with Higher-Order Synaptic Operations and their Applications to Logic Circuits and Control Problems*", An M. Sc. thesis, Department of Mechanical Engineering, University of Saskatchewan, 2004.

[23] Jim Y. F. Yam and Tommy W. S. Chow, "*Feed forward Coefficients Networks Training Speed Enhancement by Optimal Initialization of the Synaptic"* IEEE Transactions on Neural Networks, Volume 12, No.2, March 2001, pp.430-434.

[24] Simon Haykin, "*Neural Network*: *A Comprehensive Foundation",* 2nd Edition, IEEE Press, 1999.

[25] R. Haque, N. Chowdhury, "*An Artificial Neural Network Based Transmission Loss Allocation For Bilateral Contracts*" 18th Annual Canadian Conference on Electrical and Computer Engineering CCECE05, May 1-4, 2005, pp. 2197-2201.

[26] Phansalkar, V.V., Sastry, P.S., *"Analysis of the back-propagation algorithm with momentum",* IEEE Transactions on Neural Networks, Volume: 5, Issue: 3, May 1994, pp. 505 – 506.

[27] URL: http://www.dacs.dtic.mil/techs/neural/neural6.html.

[28] William S. Meisel, "*Computer Oriented Approaches to Pattern Recognition*", Academic Press Inc., New York, 1972.

[29] R.P. Lippman, "*An Introduction to Computing with Neural Nets*", IEEE ASSP Magazine, April 1987, pp. 4-22.

[30] G. Thimm and E. Fiesler, "*High-order and Multilayer Perceptron Initialization*," IEEE Transactions on Neural Networks, Volume 8, pp. 349–359, 1997.

[31] Ng, S.C.; Cheung, C.C.; Leung, S.H.; Luk, A **"***Fast Convergence For Backpropagation Network With Magnified Gradient Function*" Proceedings of the International Joint Conference on Neural Networks, 2003. Volume 3, 20-24 July 2003, pp.1903 – 1908.

[32] W. Jin Z.J. Li L.S. Wei H.Zhen "*The Improvements Of BP Neural Network Learning Algorithm"* 5th International Conference on Signal Processing Proceedings, 2000. WCCC-ICSP 2000, Publication Date: 21-25 August 2000 Volume: 3, pp. 1647 – 1649.

[33] H. Espinosa, F. Redondo; "*Multilayer Feedforward Weight Initialization*".;. Proceedings of IJCNN '01. International Joint Conference on Neural Networks, 2001, Volume 1, 15-19 July 2001, pp.166 – 170.

[34] Polycarpou, M.M.; Ioannou, P.A "*Learning And Convergence Analysis Of Neural-Type Structured Networks*", IEEE Transactions on Neural Networks, Volume 3, Issue 1, January 1992, pp.39 – 50.

[35] Keeni, K.; Nakayama, K.; Shimodaira, H.; "*A Training Scheme For Pattern Classification Using Multi-Layer Feed-Forward Neural Networks*" . ICCIMA '99. Third International Conference on Computational Intelligence and Multimedia Applications, 1999, 23-26 September 1999, pp.307 – 311.

[36] G. P. Drago and S. Ridella, "*Statistically Controlled Activation Weight Initialization (SCAWI)*," IEEE Transactions Neural Networks, Volume 3, pp. 627–631, 1992.

[37] L. F. A. Wessels and E. Barnard, *"Avoiding False Local Minima by Proper Initialization Of Connections*," IEEE Transactions on Neural Networks, Volume 3, pp. 899–905, 1992.

[38] M. Reidmiller, H. Braun, "*A Direct Adaptive Method for Faster BackPropagation Learning: The RPROP Algorithm*", Proceedings of the IEEE International Conference on Neural Networks 1993 (ICNN 93), 1993.

[39] S. Shahnawaz Ahmed, S.M. Rezaul Haque, M. Mutasim Billah and M. Sabbir Hoassin, "*Predicting Power System Voltage Profile Using A Neural network Trained With An Adaptive Learning Algorithm"*, International Journal of Power and Energy System, Volume 17, No.2, pp.78-86.

[40] URL: http://criepi.denken.or.jp/en/e_publication/pdf/den385.pdf.

[41] URL: http://www.aeso.ca/files/LineStation-Data-Web_2001.pdf.

[42] W.S. Sarle, "*Donoho-Johnstone Benchmarks: Neural Net Results"* 1999 fpt://ftp.sas.com/pub/neural/dojo/dojo.html.

[43] URL: http://dphs10.saclay.cea.fr/Spp/Experiences/OPAL/opalcern/nnrecipe.html#Archi.

[44] URL: http://www.aeso.ca/files/Loss_Factor_Calculation_Methodology.pdf.

[45] T.S.P Fernandez and K.C.D. Almeida "*Methodologies for Loss and Line Flow Allocation Under a Pool-Bilateral Market*" 14th PSCC Sevilla, 24-28th June 2002, Session 23, paper 2, pp. 1-7.

[46] A.Bhuiya, N.Chowdhury "Determination Of Loss Factors In A Deregulated System" 18th Annual Canadian Conference on Electrical and Computer Engineering CCECE05, May 1-4, 2005, pp. 547-551.

APPENDIX A

$$[F] = diag\begin{bmatrix} 0.3586 \\ 0.3947 \\ 0 \\ 0 \\ 0 \\ 0 \\ 1.4651 \\ 0 \\ 0 \\ 0 \\ 0 \\ 0 \\ 0.6001 \\ 0 \\ 1.5026 \\ 1.3484 \\ 0 \\ 0.2255 \\ 0 \\ 0 \\ 0.0040 \\ -0.0188 \\ 0.2147 \\ 0 \end{bmatrix} \qquad [Q_{G0}] = \begin{bmatrix} 0.2277 \\ -0.1609 \\ 0 \\ 0 \\ 0 \\ 0 \\ -0.3251 \\ 0 \\ 0 \\ 0 \\ 0 \\ 0 \\ -0.3655 \\ 0 \\ -0.4450 \\ -0.0899 \\ 0 \\ -1.2060 \\ 0 \\ 0 \\ 0.5919 \\ -0.0686 \\ -0.6206 \\ 0 \end{bmatrix}$$

Table A1: Real load in p.u. for weekdays (from hour 1 to 12)

Bus \Hr	1	2	3	4	5	6	7	8	9	10	11	12
1	0.610	0.568	0.541	0.557	0.575	0.592	0.644	0.678	0.721	0.751	0.799	0.868
2	0.543	0.505	0.481	0.496	0.511	0.527	0.572	0.603	0.641	0.668	0.710	0.772
3	1.007	0.937	0.892	0.920	0.948	0.977	1.062	1.118	1.190	1.239	1.318	1.433
4	0.418	0.389	0.367	0.378	0.390	0.402	0.437	0.460	0.489	0.509	0.542	0.589
5	0.397	0.369	0.352	0.363	0.374	0.385	0.419	0.441	0.469	0.489	0.520	0.565
6	0.761	0.708	0.674	0.695	0.716	0.738	0.803	0.845	0.899	0.936	0.996	1.083
7	0.699	0.650	0.619	0.639	0.658	0.679	0.738	0.776	0.826	0.860	0.915	0.995
8	0.962	0.899	0.856	0.883	0.901	0.928	1.009	1.062	1.130	1.177	1.252	1.361
10	1.091	1.015	0.966	0.996	1.027	1.059	1.151	1.211	1.289	1.342	1.428	1.552
13	1.482	1.379	1.313	1.354	1.396	1.439	1.564	1.646	1.751	1.824	1.941	2.109
14	1.095	1.019	0.961	0.991	1.022	1.053	1.145	1.205	1.282	1.335	1.421	1.544
15	1.754	1.632	1.554	1.602	1.652	1.703	1.851	1.969	2.095	2.182	2.321	2.523
16	0.559	0.520	0.496	0.511	0.527	0.543	0.590	0.621	0.661	0.688	0.732	0.796
18	1.876	1.742	1.659	1.701	1.754	1.808	1.965	2.069	2.201	2.292	2.439	2.651
20	0.716	0.666	0.634	0.654	0.674	0.695	0.755	0.795	0.846	0.881	0.937	1.019

Table A2: Real load in p.u. for weekdays (from hour 13 to 24)

Bus \Hr	13	14	15	16	17	18	19	20	21	22	23	24
1	0.965	1.016	1.069	1.080	1.058	1.016	0.980	0.931	0.838	0.754	0.641	0.609
2	0.858	0.903	0.951	0.970	0.941	0.903	0.858	0.815	0.734	0.660	0.561	0.533
3	1.592	1.676	1.764	1.800	1.746	1.676	1.592	1.513	1.361	1.225	1.042	0.989
4	0.654	0.689	0.725	0.740	0.718	0.689	0.655	0.622	0.560	0.504	0.428	0.407
5	0.628	0.661	0.696	0.710	0.689	0.661	0.628	0.597	0.537	0.483	0.411	0.390
6	1.203	1.266	1.333	1.360	1.319	1.266	1.203	1.143	1.029	0.926	0.787	0.748
7	1.106	1.164	1.225	1.250	1.200	1.550	1.473	1.399	1.259	1.133	0.963	0.915
8	1.512	1.592	1.676	1.710	1.659	1.592	1.513	1.437	1.293	1.164	0.989	0.940
10	1.725	1.815	1.911	1.950	1.892	1.816	1.775	1.686	1.518	1.366	1.161	1.103
13	2.344	2.467	2.597	2.650	2.500	2.400	2.280	2.166	1.993	1.774	1.454	1.382
14	1.716	1.806	1.901	1.940	1.882	1.900	1.805	1.715	1.543	1.389	1.181	1.122
15	2.804	2.951	3.107	3.170	3.075	2.952	2.850	2.708	2.437	2.193	1.864	1.771
16	0.884	0.931	0.980	1.000	0.970	0.931	0.885	0.840	0.756	0.681	0.579	0.550
18	2.945	3.100	3.263	3.330	3.230	3.101	2.946	2.799	2.519	2.267	1.927	1.830
20	1.132	1.192	1.254	1.280	1.242	1.192	1.132	1.076	0.968	0.871	0.741	0.704

Table A3: Reactive load in p.u. for weekdays (from hour 1 to hour 12)

Bus \Hr	1	2	3	4	5	6	7	8	9	10	11	12
1	0.124	0.116	0.110	0.114	0.117	0.121	0.131	0.138	0.147	0.153	0.163	0.177
2	0.112	0.104	0.099	0.102	0.105	0.109	0.118	0.124	0.132	0.138	0.146	0.159
3	0.207	0.193	0.183	0.189	0.195	0.201	0.218	0.230	0.245	0.255	0.271	0.295
4	0.085	0.079	0.074	0.077	0.079	0.081	0.089	0.093	0.099	0.103	0.110	0.119
5	0.078	0.073	0.069	0.072	0.074	0.076	0.083	0.087	0.093	0.096	0.103	0.111
6	0.152	0.142	0.135	0.139	0.143	0.148	0.161	0.169	0.180	0.187	0.199	0.217
7	0.140	0.130	0.124	0.128	0.132	0.136	0.148	0.155	0.165	0.172	0.183	0.199
8	0.197	0.184	0.175	0.181	0.184	0.190	0.207	0.217	0.231	0.241	0.256	0.279
10	0.224	0.208	0.198	0.204	0.211	0.217	0.236	0.248	0.264	0.275	0.293	0.318
13	0.302	0.281	0.268	0.276	0.284	0.293	0.319	0.335	0.357	0.372	0.395	0.430
14	0.220	0.205	0.193	0.199	0.205	0.212	0.230	0.242	0.258	0.268	0.286	0.310
15	0.354	0.329	0.314	0.323	0.334	0.344	0.374	0.398	0.423	0.441	0.469	0.509
16	0.112	0.104	0.099	0.102	0.105	0.109	0.118	0.124	0.132	0.138	0.146	0.159
18	0.383	0.356	0.339	0.347	0.358	0.369	0.401	0.422	0.449	0.468	0.498	0.541
20	0.145	0.135	0.129	0.133	0.137	0.141	0.153	0.162	0.172	0.179	0.190	0.207

Table A4: Reactive load in p.u. for weekdays (from hour 13 to 24)

Bus \Hr	13	14	15	16	17	18	19	20	21	22	23	24
1	0.197	0.207	0.218	0.220	0.216	0.207	0.197	0.187	0.168	0.151	0.129	0.122
2	0.177	0.186	0.196	0.200	0.194	0.186	0.177	0.168	0.151	0.136	0.116	0.110
3	0.327	0.344	0.363	0.370	0.359	0.345	0.327	0.311	0.280	0.252	0.214	0.203
4	0.133	0.140	0.147	0.150	0.146	0.140	0.133	0.126	0.113	0.102	0.087	0.082
5	0.124	0.130	0.137	0.140	0.136	0.130	0.124	0.118	0.106	0.095	0.081	0.077
6	0.241	0.253	0.267	0.272	0.264	0.253	0.241	0.229	0.206	0.185	0.157	0.150
7	0.221	0.233	0.245	0.250	0.243	0.233	0.221	0.210	0.189	0.170	0.145	0.137
8	0.310	0.326	0.343	0.350	0.340	0.326	0.310	0.294	0.265	0.238	0.203	0.192
10	0.354	0.372	0.392	0.400	0.388	0.372	0.354	0.336	0.303	0.272	0.231	0.220
13	0.478	0.503	0.529	0.540	0.524	0.503	0.478	0.454	0.418	0.372	0.305	0.289
14	0.345	0.363	0.382	0.390	0.378	0.363	0.345	0.328	0.295	0.265	0.226	0.214
15	0.566	0.596	0.627	0.640	0.621	0.596	0.566	0.538	0.484	0.436	0.370	0.352
16	0.177	0.186	0.196	0.200	0.194	0.186	0.177	0.168	0.151	0.136	0.116	0.110
18	0.601	0.633	0.666	0.680	0.660	0.633	0.602	0.571	0.514	0.463	0.393	0.374
20	0.230	0.242	0.255	0.260	0.252	0.242	0.230	0.219	0.197	0.177	0.150	0.143

Table A5: Real load in p.u. for weekends (from hour 1 to 12)

Bus \Hr	1	2	3	4	5	6	7	8	9	10	11	12
1	0.624	0.580	0.552	0.558	0.575	0.581	0.592	0.623	0.663	0.690	0.719	0.782
2	0.578	0.538	0.512	0.518	0.523	0.528	0.538	0.566	0.602	0.627	0.654	0.710
3	0.992	0.923	0.879	0.888	0.896	0.906	0.922	0.971	1.033	1.076	1.120	1.218
4	0.436	0.405	0.382	0.386	0.390	0.394	0.401	0.423	0.449	0.468	0.488	0.530
5	0.419	0.390	0.371	0.375	0.379	0.382	0.389	0.410	0.436	0.454	0.473	0.514
6	0.723	0.672	0.640	0.647	0.653	0.660	0.672	0.708	0.753	0.784	0.817	0.888
7	0.729	0.678	0.646	0.653	0.659	0.666	0.678	0.714	0.759	0.791	0.824	0.896
8	0.760	0.710	0.676	0.697	0.704	0.711	0.773	0.814	0.866	0.902	0.939	1.021
10	1.007	0.937	0.892	0.920	0.929	0.958	1.041	1.096	1.166	1.195	1.271	1.381
13	1.302	1.212	1.154	1.166	1.177	1.189	1.293	1.361	1.447	1.483	1.578	1.715
14	1.102	1.025	0.967	0.997	1.007	1.017	1.106	1.164	1.238	1.269	1.350	1.467
15	1.720	1.600	1.523	1.571	1.586	1.602	1.742	1.853	1.971	2.020	2.061	2.240
16	0.553	0.514	0.490	0.505	0.510	0.526	0.531	0.559	0.595	0.620	0.659	0.716
18	1.542	1.431	1.363	1.367	1.409	1.413	1.536	1.567	1.667	1.737	1.848	2.008
20	0.693	0.645	0.614	0.633	0.653	0.673	0.680	0.716	0.761	0.793	0.844	0.917

Table A6: Real load in p.u. for weekends (from hour 13 to 24)

Bus \Hr	13	14	15	16	17	18	19	20	21	22	23	24
1	0.868	0.914	0.962	0.972	0.953	0.914	0.980	0.956	0.908	0.817	0.694	0.660
2	0.789	0.831	0.875	0.892	0.866	0.831	0.789	0.770	0.731	0.658	0.559	0.531
3	1.353	1.424	1.499	1.530	1.484	1.425	1.353	1.320	1.254	1.128	0.959	0.911
4	0.589	0.620	0.653	0.666	0.646	0.620	0.589	0.574	0.546	0.491	0.417	0.397
5	0.571	0.602	0.633	0.646	0.627	0.602	0.572	0.557	0.529	0.476	0.405	0.385
6	0.986	1.038	1.093	1.115	1.082	1.038	0.987	0.962	0.914	0.822	0.699	0.664
7	0.995	1.047	1.103	1.125	1.200	1.550	1.527	1.489	1.414	1.273	1.082	1.028
8	1.134	1.194	1.257	1.283	1.244	1.194	1.176	1.147	1.090	0.981	0.834	0.792
10	1.535	1.616	1.701	1.736	1.683	1.616	1.592	1.552	1.474	1.327	1.128	1.072
13	1.906	2.006	2.111	2.154	2.090	2.006	1.976	1.927	1.830	1.629	1.336	1.269
14	1.630	1.716	1.806	1.843	1.788	1.900	1.872	1.825	1.733	1.560	1.326	1.260
15	2.383	2.509	2.641	2.695	2.560	2.355	2.320	2.262	2.149	1.934	1.644	1.561
16	0.796	0.838	0.882	0.900	0.873	0.838	0.826	0.784	0.745	0.671	0.570	0.541
18	2.231	2.349	2.473	2.498	2.423	2.326	2.291	2.176	1.959	1.841	1.565	1.487
20	1.019	1.073	1.129	1.152	1.117	1.073	1.057	1.004	0.903	0.813	0.691	0.657

Table A7: Reactive load in p.u. for weekends (from hour 1 to 12)

Bus \Hr	1	2	3	4	5	6	7	8	9	10	11	12
1	0.118	0.110	0.105	0.108	0.111	0.115	0.125	0.131	0.140	0.145	0.155	0.168
2	0.105	0.098	0.093	0.096	0.099	0.102	0.111	0.117	0.124	0.129	0.138	0.150
3	0.195	0.181	0.172	0.178	0.183	0.189	0.205	0.216	0.230	0.239	0.255	0.277
4	0.080	0.074	0.070	0.072	0.074	0.077	0.083	0.088	0.093	0.097	0.103	0.112
5	0.076	0.071	0.067	0.069	0.072	0.074	0.080	0.084	0.090	0.093	0.099	0.108
6	0.148	0.137	0.131	0.135	0.139	0.143	0.156	0.164	0.174	0.182	0.193	0.210
7	0.136	0.126	0.120	0.124	0.128	0.132	0.143	0.151	0.160	0.167	0.178	0.193
8	0.191	0.178	0.170	0.175	0.179	0.184	0.200	0.211	0.224	0.234	0.249	0.270
10	0.217	0.202	0.192	0.198	0.204	0.211	0.229	0.241	0.256	0.267	0.284	0.309
13	0.293	0.273	0.260	0.268	0.276	0.284	0.309	0.325	0.346	0.361	0.384	0.417
14	0.214	0.199	0.187	0.193	0.199	0.205	0.223	0.235	0.250	0.260	0.277	0.301
15	0.347	0.323	0.308	0.317	0.327	0.337	0.366	0.390	0.415	0.432	0.459	0.499
16	0.110	0.102	0.097	0.100	0.103	0.106	0.116	0.122	0.130	0.135	0.144	0.156
18	0.364	0.338	0.322	0.330	0.340	0.351	0.381	0.401	0.427	0.445	0.473	0.514
20	0.140	0.130	0.124	0.128	0.131	0.136	0.147	0.155	0.165	0.172	0.183	0.199

Table A8: Reactive load in p.u. for weekends (from hour 13 to 24)

Bus \Hr	13	14	15	16	17	18	19	20	21	22	23	24
1	0.177	0.186	0.196	0.198	0.194	0.186	0.298	0.283	0.255	0.229	0.195	0.185
2	0.158	0.166	0.175	0.180	0.175	0.168	0.159	0.151	0.136	0.123	0.104	0.099
3	0.292	0.307	0.323	0.333	0.323	0.310	0.295	0.280	0.266	0.239	0.203	0.193
4	0.118	0.124	0.131	0.135	0.131	0.126	0.119	0.113	0.102	0.100	0.085	0.081
5	0.114	0.120	0.122	0.126	0.122	0.117	0.111	0.106	0.095	0.086	0.073	0.069
6	0.221	0.233	0.237	0.245	0.237	0.228	0.217	0.206	0.185	0.167	0.142	0.135
7	0.203	0.214	0.218	0.225	0.218	0.210	0.199	0.189	0.170	0.153	0.130	0.124
8	0.284	0.299	0.306	0.315	0.306	0.299	0.284	0.270	0.243	0.231	0.196	0.187
10	0.325	0.342	0.349	0.360	0.349	0.342	0.325	0.309	0.278	0.250	0.213	0.202
13	0.439	0.462	0.471	0.486	0.471	0.462	0.439	0.417	0.384	0.379	0.311	0.296
14	0.317	0.334	0.340	0.351	0.340	0.334	0.317	0.301	0.271	0.244	0.207	0.197
15	0.520	0.548	0.559	0.576	0.559	0.548	0.520	0.494	0.445	0.400	0.380	0.361
16	0.163	0.171	0.175	0.180	0.175	0.171	0.163	0.154	0.139	0.125	0.106	0.101
18	0.536	0.564	0.594	0.612	0.594	0.582	0.553	0.525	0.520	0.468	0.398	0.378
20	0.207	0.218	0.229	0.234	0.227	0.222	0.211	0.201	0.181	0.163	0.138	0.131

Table A9: Initial load flow solution by Newton-Raphson Method

Bus No.	Voltage Mag	Angle Degree	--- Load --- MW	Mvar	--- Generation --- MW	Mvar	Injected Mvar
1	1.030	0.000	1.080	0.220	1.593	0.799	0.000
2	1.030	-0.002	0.970	0.200	1.720	0.518	0.000
3	0.978	2.845	1.800	0.370	0.000	0.000	0.000
4	0.990	-0.988	0.740	0.150	0.000	0.000	0.000
5	0.994	-2.824	0.710	0.140	0.000	0.000	0.000
6	1.000	-5.699	1.360	0.267	0.000	0.000	0.720
7	1.020	-12.119	1.250	0.250	1.000	1.140	0.000
8	0.971	-10.413	1.710	0.350	0.000	0.000	0.000
9	0.993	2.390	0.000	0.000	0.000	0.000	0.000
10	0.987	-2.426	1.950	0.400	0.000	0.000	0.000
11	0.996	6.884	0.000	0.000	0.000	0.000	0.000
12	1.000	7.047	0.000	0.000	0.000	0.000	0.000
13	1.030	10.028	2.650	0.540	3.940	1.999	0.000
14	0.996	10.436	1.940	0.390	0.000	0.000	0.000
15	1.030	18.477	3.170	0.640	1.550	1.884	0.000
16	1.030	17.759	1.000	0.200	1.550	2.000	0.000
17	1.022	22.303	0.000	0.000	0.000	0.000	0.000
18	1.020	23.740	3.330	0.680	4.000	0.304	0.000
19	1.023	16.570	0.000	0.000	0.000	0.000	0.000
20	1.018	15.538	1.280	0.260	0.000	0.000	0.000
21	1.030	24.461	0.000	0.000	4.000	0.608	0.000
22	1.030	30.375	0.000	0.000	3.000	-0.125	0.000
23	1.020	15.717	0.000	0.000	3.100	0.045	0.000
24	0.995	12.763	0.000	0.000	0.000	0.000	0.000
Total			24.940	4.340	25.453	8.563	
		Line Flow and Losses					
Total loss					0.513	4.223	

Table A10: Load flow solution for economical load dispatch

Bus No.	Voltage Mag	Angle Degree	--- Load --- MW	Mvar	--- Generation --- MW	Mvar	Injected Mvar
1	1.030	0.000	1.080	0.220	4.018	0.331	0.000
2	1.030	-1.261	0.970	0.200	0.483	0.761	0.000
3	0.981	-3.136	1.800	0.370	0.000	0.000	0.000
4	0.991	-3.971	0.740	0.150	0.000	0.000	0.000
5	0.993	-4.494	0.710	0.140	0.000	0.000	0.000
6	1.000	-8.640	1.360	0.267	0.000	0.000	0.720
7	1.020	-15.959	1.250	0.250	1.007	1.124	0.000
8	0.972	-14.293	1.710	0.350	0.000	0.000	0.000
9	0.995	-2.050	0.000	0.000	0.000	0.000	0.000
10	0.987	-5.911	1.950	0.400	0.000	0.000	0.000
11	1.000	1.653	0.000	0.000	0.000	0.000	0.000
12	1.001	2.994	0.000	0.000	0.000	0.000	0.000
13	1.030	6.642	2.650	0.540	5.327	1.736	0.000
14	1.001	2.344	1.940	0.390	0.000	0.000	0.000
15	1.030	7.059	3.170	0.640	1.439	1.552	0.000
16	1.030	7.060	1.000	0.200	0.797	1.674	0.000
17	1.024	9.573	0.000	0.000	0.000	0.000	0.000
18	1.020	10.705	3.330	0.680	3.904	-0.417	0.000
19	1.023	8.050	0.000	0.000	0.000	0.000	0.000
20	1.018	8.908	1.280	0.260	0.000	0.000	0.000
21	1.030	11.214	0.000	0.000	3.813	0.423	0.000
22	1.030	11.577	0.000	0.000	0.451	0.011	0.000
23	1.020	10.121	0.000	0.000	4.066	-0.137	0.000
24	1.003	3.340	0.000	0.000	0.000	0.000	0.000
Total			24.940	4.340	25.304	7.057	
			Line Flow and Losses				
Total loss					0.364	2.717	

APPENDIX B

All terms except P_L and K_{LO} in this appendix are matrices.

Standard transmission loss formula derived in Chapter 2 is

$$\begin{aligned}P_L &= P_G{}^T A_p P_G - P_D{}^T A_p P_G - P_G{}^T A_p P_D + P_D{}^T A_p P_D - P_G{}^T B_p Q_G + P_D{}^T B_p Q_G \\ &\quad + P_G{}^T B_p Q_D - P_D B_p Q_D + Q_G{}^T B_p P_G - Q_D{}^T B_p P_G - Q_G B_p P_D + Q_D{}^T B_p P_D \\ &\quad + Q_G{}^T A_p Q_G - Q_D{}^T A_p Q_G - Q_G{}^T A_p Q_D + Q_D{}^T A_p Q_D \\ &= \begin{bmatrix} P_G^T & Q_G^T \end{bmatrix} \begin{bmatrix} Ap & -Bp \\ Bp & Ap \end{bmatrix} \begin{bmatrix} P_G \\ Q_G \end{bmatrix} + \begin{bmatrix} P_D^T & Q_D^T \end{bmatrix} \begin{bmatrix} Ap & -Bp \\ Bp & Ap \end{bmatrix} \begin{bmatrix} P_D \\ Q_D \end{bmatrix} \\ &\quad - P_D^T A_p P_G - P_D^T A_p{}^T + P_D^T B_p Q_G + Q_D^T B_p{}^T - Q_D^T B_p P_G - P_D^T B_p T Q_G - Q_D^T A_p Q_G - Q_D^T A_p{}^T Q_G \end{aligned} \quad \ldots \quad \ldots \quad \ldots \quad \text{(B1}$$

Since $A_p = A_p{}^T \quad and \quad B_p = -B_p{}^T$, Equation (B1) can be written as

$$\begin{aligned}P_L &= \begin{bmatrix} P_G{}^T & Q_G{}^T \end{bmatrix} \begin{bmatrix} A_p & -B_p \\ B_p & A_p \end{bmatrix} \begin{bmatrix} P_G \\ Q_G \end{bmatrix} + \begin{bmatrix} P_D{}^T & Q_D{}^T \end{bmatrix} \begin{bmatrix} A_p & -B_p \\ B_p & A_p \end{bmatrix} \begin{bmatrix} P_D \\ Q_D \end{bmatrix} \\ &\quad + 2\begin{bmatrix} -P_D{}^T A_p - Q_D{}^T B_p & P_D{}^T B_p - Q_D{}^T A_p \end{bmatrix} \begin{bmatrix} P_G \\ Q_G \end{bmatrix} \end{aligned} \quad \ldots \quad \ldots \quad \text{(B2}$$

The first term of Equation (B2 is

$$\begin{aligned}&\begin{bmatrix} P_G{}^T & Q_G{}^T \end{bmatrix} \begin{bmatrix} A_p & -B_p \\ B_p & A_p \end{bmatrix} \begin{bmatrix} P_G \\ Q_G \end{bmatrix} \\ &= P_G{}^T A_p P_G - P_G{}^T B_p Q_G + Q_G{}^T B_p P_G + Q_G{}^T A_p Q_G \\ &= P_G{}^T A_p P_G - P_G{}^T B_p (Q_{G0} + FP_G) + (Q_{G0} + FP_G)^T B_p P_G + (Q_{G0} + FP_G)^T A_p (Q_{G0} + FP_G) \\ &= P_G{}^T A_p P_G - P_G{}^T B_p Q_{G0} - P_G{}^T B_p F P_G + Q_{G0}^T B_p P_G + P_G{}^T F^T B_p P_G + Q_{G0}^T A_p Q_{G0} \\ &\quad + Q_{G0}^T A_p F P_G + P_G{}^T F^T A_p Q_{G0} + P_G{}^T F^T A_p F P_G \end{aligned} \quad \ldots \quad \ldots \quad \ldots \quad (B2)$$

3rd term of Equation (B1) is

$$\begin{aligned}&= 2\begin{bmatrix} -P_D{}^T A_p - Q_D{}^T B_p & P_D{}^T B_p - Q_D{}^T A_p \end{bmatrix} \begin{bmatrix} P_G \\ Q_G \end{bmatrix} \\ &= \begin{bmatrix} E_p & E_q \end{bmatrix} \begin{bmatrix} P_G \\ Q_G \end{bmatrix} = E_p P_G + E_q Q_G \end{aligned}$$

where,

$$E_p = 2\left(-P_D{}^T A_p - Q_D{}^T B_p\right) \text{ and}$$

$$E_q = 2\left(P_D{}^T B_p - Q_D{}^T A_p\right)$$

Therefore, the 3rd term is

$$= E_p P_G + E_q Q_G = E_p P_G + E_q\left(Q_{G0} + FP_G\right) \quad \ldots \quad \ldots \quad \text{(B3)}$$

Putting (B2) and (B3) in (B1),

$$P_L = P_G{}^T A_p P_G - P_G{}^T B_p Q_{G0} - P_G{}^T B_p F P_G + Q_{G0}^T B_p P_G + P_G{}^T F^T B_p P_G + Q_{G0}^T A_p Q_{G0}$$
$$+ Q_{G0}^T A_p F P_G + P_G{}^T F^T A_p Q_{G0} + P_G{}^T F^T A_p F P_G + E_p P_G + E_q Q_{G0} + E_q F P_G$$
$$+ \begin{bmatrix} P_D{}^T & Q_D{}^T \end{bmatrix} \begin{bmatrix} A_p & -B_p \\ B_p & A_p \end{bmatrix} \begin{bmatrix} P_D \\ Q_D \end{bmatrix}$$

$$= P_G{}^T \left(A_p - B_p F + F^T B_p + F^T A_p F\right) P_G + \left\{E_p + E_q F + 2Q_{G0}^T \left(A_p F + B_p\right)\right\} P_G$$
$$+ \begin{bmatrix} P_D{}^T & Q_D{}^T \end{bmatrix} \begin{bmatrix} A_p & -B_p \\ B_p & A_p \end{bmatrix} \begin{bmatrix} P_D \\ Q_D \end{bmatrix} + Q_{Go}^T A_p Q_{G0} + E_q Q_{G0}$$

or,

$$P_L = P_G{}^T B_L P_G + B_{L0}^T P_G + K_{L0} \quad \ldots \quad \ldots \quad \ldots \quad \text{(B4)}$$

where,

$$B_L = A_p - B_p F + F^T B_p + F^T A_p F$$

$$B_{L0}^T = E_p + E_q F + 2Q_{G0}^T (A_p F + B_p)$$

$$K_{L0} = \begin{bmatrix} P_D^T & Q_D^T \end{bmatrix} \begin{bmatrix} A_p & -B_p \\ B_p & A_p \end{bmatrix} \begin{bmatrix} P_D \\ Q_D \end{bmatrix} + Q_{G0}^T A_p Q_{G0} + E_q Q_{G0}$$

The loss formula expressed in Equation (B4) is known as Kron's transmission loss formula.